U

TITLE		
AERODYNAMIC DATA FOR STRUCTURAL LOADS		
REPORT NO.	DATE	MODEL NO.
LR 9062	3-2-53	C-130
SUBMITTED UNDER (CONTRACT, SPEC., ETC.)		

Form 375-3

Lockheed

A Division of Lockheed Corporation
P O Box 551, Burbank California 91520 U S A

[redacted]

UNCLASSIFIED [redacted]

(u)

REPORT NO. 9062

DATED March 2, 1953

LOCKHEED AIRCRAFT CORPORATION

BURBANK, CALIFORNIA

COPY 20

TITLE

AERODYNAMIC DATA
For
STRUCTURAL LOADS

SUBMITTED UNDER

MODEL C-130 REFERENCE

PREPARED BY R. L. Dickinson GROUP Aerodynamics
R. L. Dickinson

CHECKED BY R.G. Cathaway APPROVED BY P. A. Colman
R.G. Cathaway P. A. Colman

NO. PAGES NO. PICTURES

NO. DRAWINGS

REVISIONS

DATE	REV. BY	PAGES AFFECTED	REMARKS

UNCLASSIFIED

[redacted]

TABLE OF CONTENTS

FIGURE INDEX

FIGURE INDEX (Cont'd.)

FIGURE INDEX (Cont'd.)

FIGURE INDEX (Cont'd.)

FIGURE INDEX (Cont'd.)

FIGURE INDEX (Cont'd.)

INTRODUCTION

This report presents the aerodynamic data necessary for a complete determination of the structural flight loads on the airplane. Included are the effects of compressibility, power and configuration changes such as pylon tanks on, ramp deflected, flaps extended, etc. Data specifically for this airplane are obtained from the results of extensive low- and high-speed wind tunnel tests conducted by Lockheed. Additional data as necessary are from NACA publications and other Lockheed investigations.

Many configurations were tested in the development of this airplane. Some were made necessary by the type of test to be run; others by design changes or by stability and/or control requirements. In each case, the data most applicable have been selected for presentation in this report.

GENERAL

The C-130 is primarily a military cargo airplane of conventional arrangement. It is powered by four propeller-driving Allison T-56 gas turbine engines. The airplane is a high-wing design with standard empennage. It incorporates hydraulically boosted primary controls, Lockheed-Fowler flaps for landing and take-off. Loading and unloading are accomplished by means of a ramp at the rear of the fuselage which can be opened for airdrops. Paratroops may be dropped from personnel doors at the rear of the fuselage and are protected from air blast by means of shields immediately forward of the doors. Main landing gear is contained in fairings on each side of the fuselage.

Basic data applicable to the airplane and describing its geometric characteristics are presented on the following pages. A dimensioned three-view drawing of the airplane is presented in Fig. 1. Physical parameters necessary to the purpose of this report are summarized in Table I, along with those items of performance which affect structural flight loads determination. In Fig. 2 are presented curves showing military and normal rated power available at all speeds for several altitudes. Fig. 3 presents curves which summarize design speeds at all altitudes in level flight and dive.

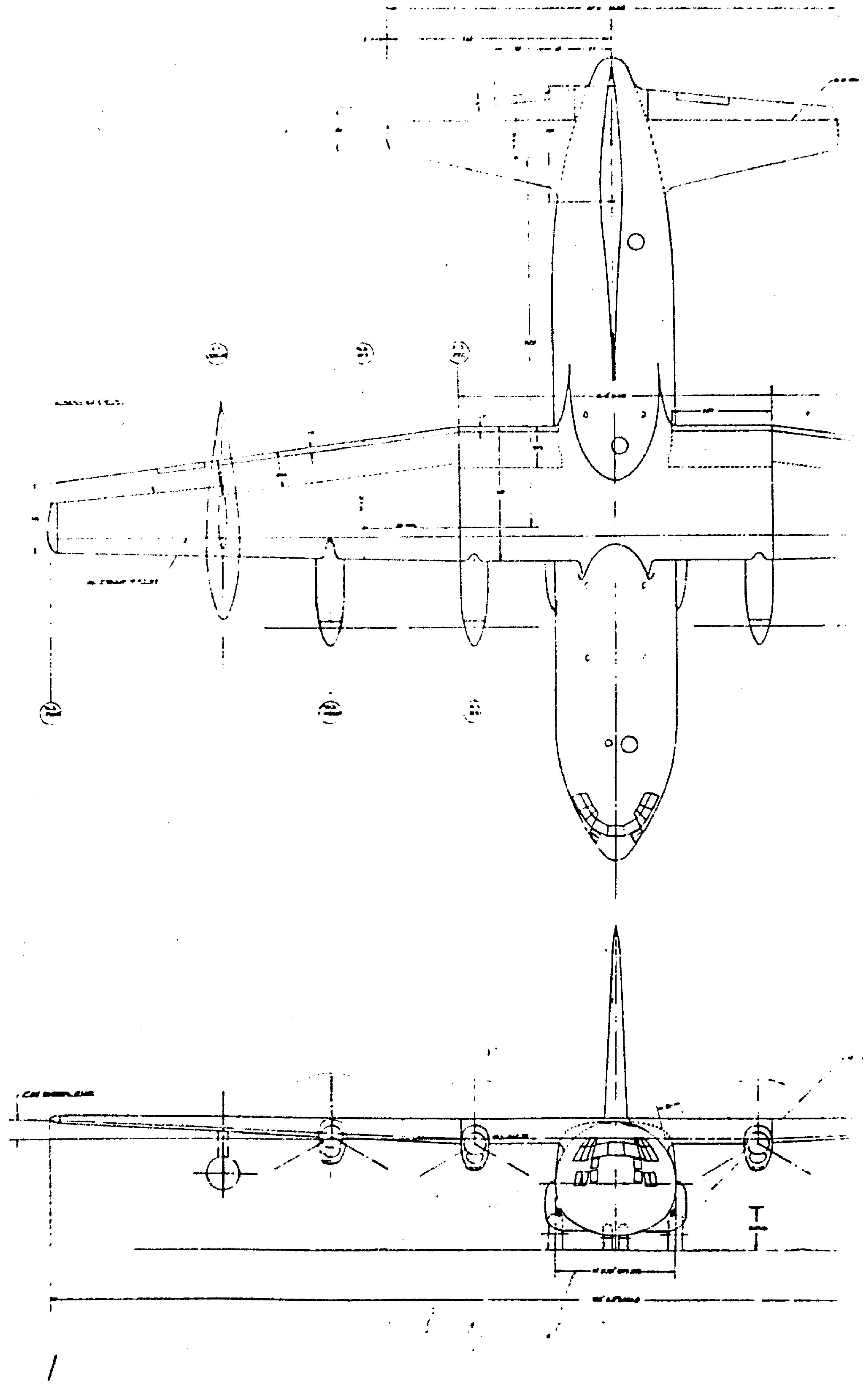

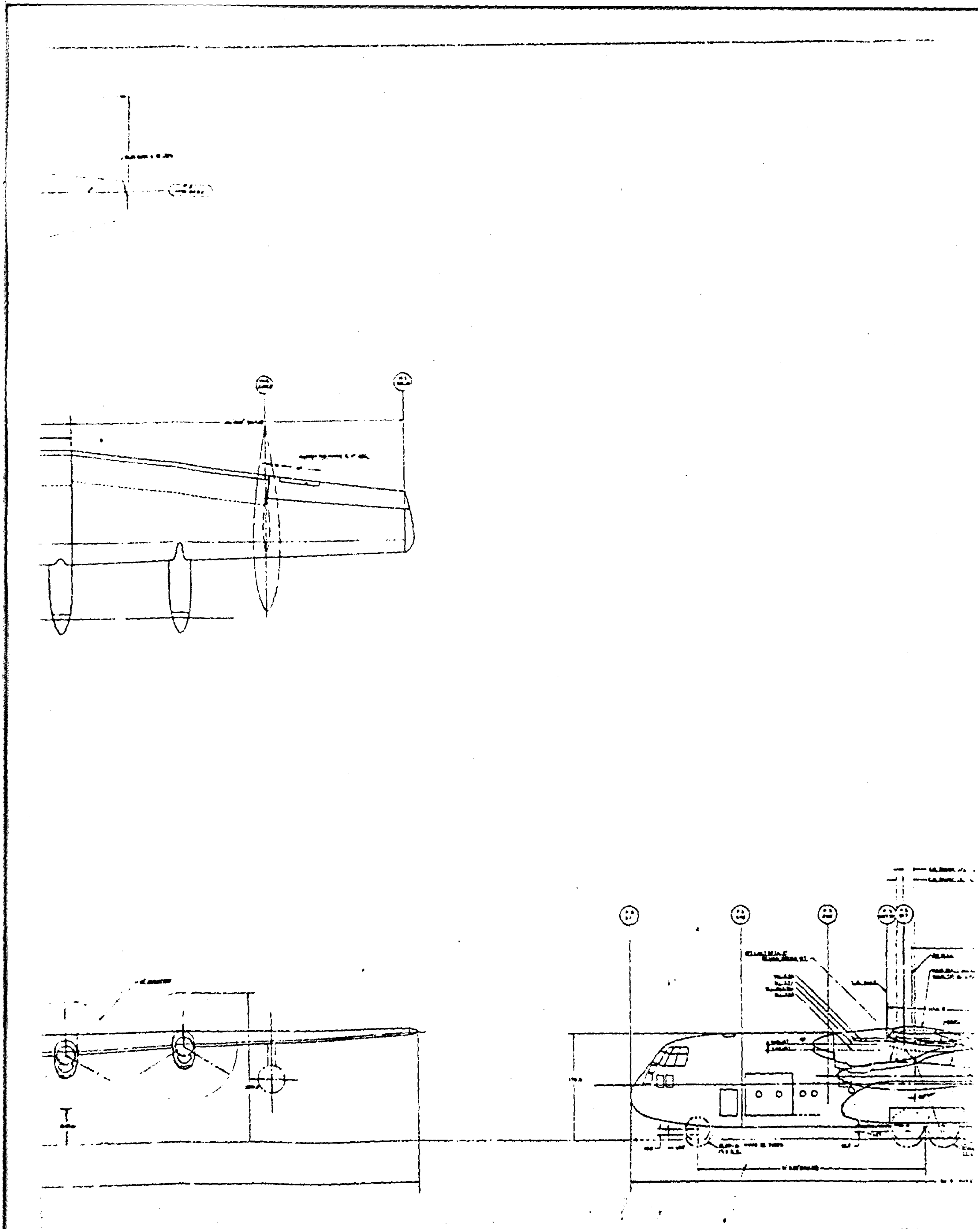

2

L R

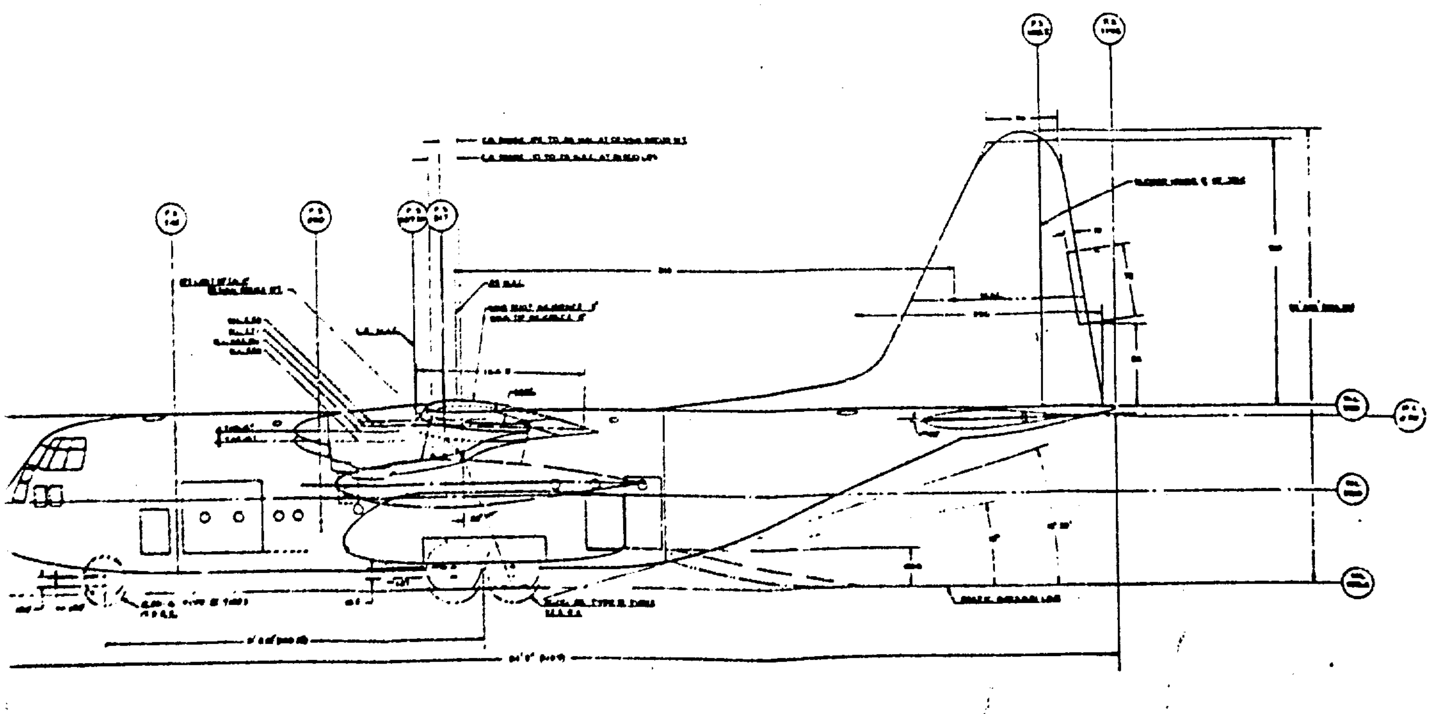

3,

LR 9062

[redacted]

FIG. 1

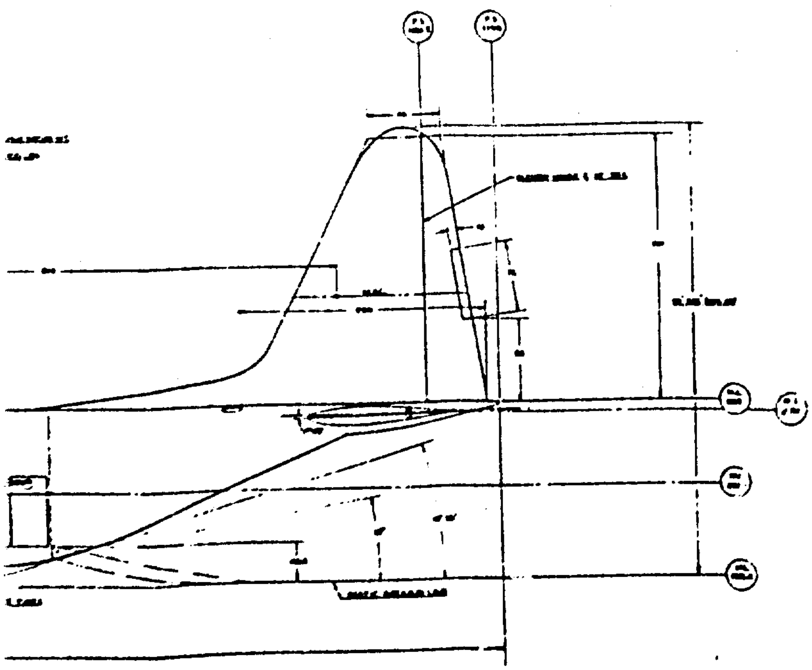

[redacted]

TABLE I

BASIC DATA

Wing	
Area, S	1744.6 sq.ft.
Span, b	132.6 ft.
Mean Aerodynamic Chord, $\bar{c}$	164.5 in.
Aspect Ratio, A	10.09
Taper Ratio, λ	.52
Dihedral, Γ (Outer Panel)	2.50°
Incidence	
Root, i_r	3.0°
Tip, i_t	0°
Geometric Twist	-3.0°
Airfoil Sections	
Root	NACA 64A-318
Tip	NACA 64A-412
Chords,	
Root to W.S. 220	192 in.
Tip (W.S. 792)	100 in.
Straight Element, 18% c	F.S. 517
Location of .25 $\bar{c}$	F.S. 528.51
Aileron (Each Side)	
Area, S_a	55.0 sq.ft.
Mean Chord, $\bar{c}_a$	33.5 in.
Deflection Limits, δ_a	+15°,-25°

Tab Area, S_{a_t}	2.9 sq.ft.
Tab Mean Chord, $\bar{c}_{a_t}$	6.5 in.
Tab Deflection Limits, δ_{a_t}	$\pm$ 20°
Wing Flaps (Each Side)	
Type	Lockheed-Fowler
Area, S_f	171.0 sq.ft.
Mean Chord	
Outboard Flap	49.5 in.
Center Section Flap	57.5 in.
Maximum Deflection, δ_F	36°
Horizontal Tail	
Area, S_t	495.6 sq.ft.
Span, b_t	52.7 ft.
Mean Chord, $\bar{c}_t$	122. in.
Aspect Ratio, A_t	5.59
Taper Ratio, λ_t	.374
Airfoil Section	Inverted NACA 23012
Chords	
Root (Sta. 0)	166 in.
Tip (Sta. 313)	62 in.
Straight Element, 70% chord	F.S. 1107.0
Location of .25 $\bar{c}_t$	F.S. 1052.1
Stabilizer incidence, i_s	-1.75°
Tail Length, l_t (.25 $\bar{c}$ to .25 $\bar{c}_t$)	523.6 in.
Tail Volume, $\bar{V}_t$	.903

Elevator

Area, S_e	114.9 sq.ft.
Mean Chord, $\bar{c}_e$	33.5 in.
Deflection Limits, δ_e	+15°,-40°
Tab Area, S_{e_t}	15.3 sq.ft.
Tab Mean Chord, $\bar{c}_{e_t}$	11.0 in.
Tab Deflection Limits, δ_{e_t}	±30°

Vertical Tail

Area, S_v	300.0 sq.ft.
Span, b_v	23.3 ft.
Aspect Ratio, A_v	1.81
Mean Chord, $\bar{c}_v$	177.8 in.
Taper Ratio, λ_v	.296
Airfoil Section	NACA 64 A-015
Chords	
Root	250. in.
Tip	74. in.
Straight Element, 75% Chord	F.S. 1128.5
Location of .25 $\bar{c}_v$	F.S. 1039.6
Tail Volume, $\bar{V}_v$	.0552

Rudder

Area, S_r	75.0 sq.ft.
Mean Chord, $\bar{c}_r$	44.5 in.
Deflection Limits, δ_r	±35.°
Tab Area, S_{r_t}	5.0 sq.ft.

Tab Mean Chord, $\bar{c}_{r_t}$	10.0 in.
Tab Deflection Limits, δ_{r_t} (for trim)	$\pm 25°$

Maximum Lift Coefficients

Clean Airplane	1.60
Take-off Flaps	2.00
Landing Flaps	2.60

Minimum Lift Coefficients

Clean Airplane	-1.0

Design Weights and Load Factors

YC-130

Design Gross Weight	110,500 lbs.
Max. Load Factors, $V \leq V_H$	+3.0,-1.0
Max. Load Factors at V_D	+2.5,-0.75
Max. Take-Off Weight	127,200 lbs.
Max. Load Factors	2.0
Design Landing Weight	99000#
Max. Alt. Land. Wt. (8 ft/sec. sink speed)	107500 lbs.

C-130A

Design Gross Weight	108,000 lbs.
Max. Load Factors, $V \leq V_H$	+3.0,-1.0
Max. Load Factors at V_D	+2.5,-0.75
Max. Take-Off Weight	124,200 lbs.
Max. Load Factors	2.0
Design Landing Weight	96000#
Max. Alt. Landing Wt. (8 ft/sec. sinking speed)	105,000 lbs.

Design Velocities (Sea Level)

YC-130

Landing Flap Extension	168 knots
Take-Off Flap Extension	183 "
Landing Gear Door Opening	168 "
Cargo Door Opening	130 "
Level Flight	290 "
Dive	348 "

C-130A

Landing Flap Extension	145 knots
Take-Off Flap Extension	183 "
Landing Gear Door Opening	168 "
Cargo Door Opening	130 "
Level Flight	287 "
Dive	345 "

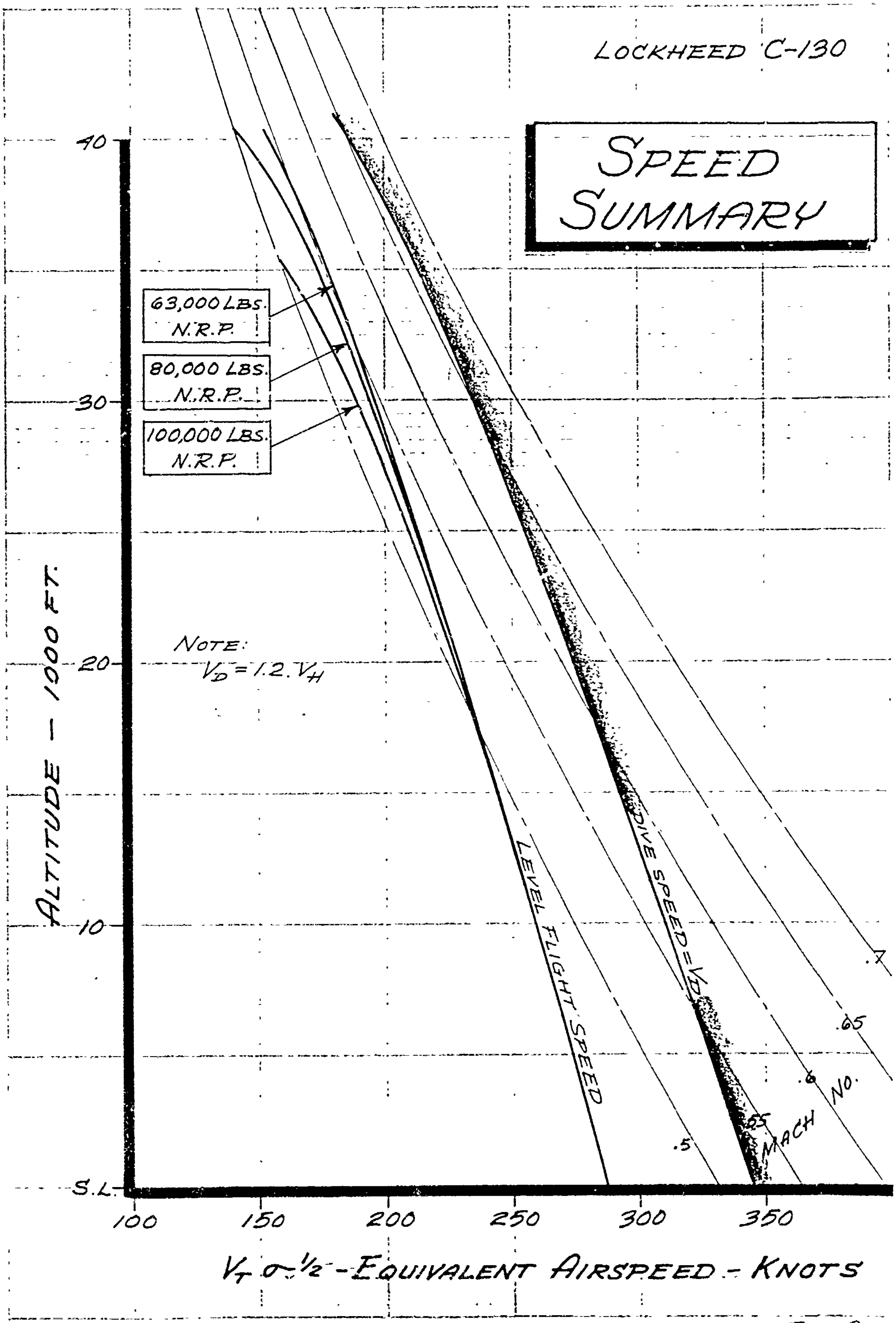
LOCKHEED C-130
SPEED SUMMARY
63,000 LBS. N.R.P.
80,000 LBS. N.R.P.
100,000 LBS. N.R.P.
NOTE: $V_D = 1.2 V_H$
LEVEL FLIGHT SPEED
DIVE SPEED = V_D
MACH NO.
.5
.55
.6
.65
.7
ALTITUDE - 1000 FT.
40
30
20
10
S.L.
100
150
200
250
300
350
$V_T \sigma^{1/2}$ - EQUIVALENT AIRSPEED - KNOTS

FIG. 2

LOCKHEED YC-130

MILITARY AND NORMAL RATED POWER AT SEVERAL ALTITUDES

FOUR ENGINES OPERATING

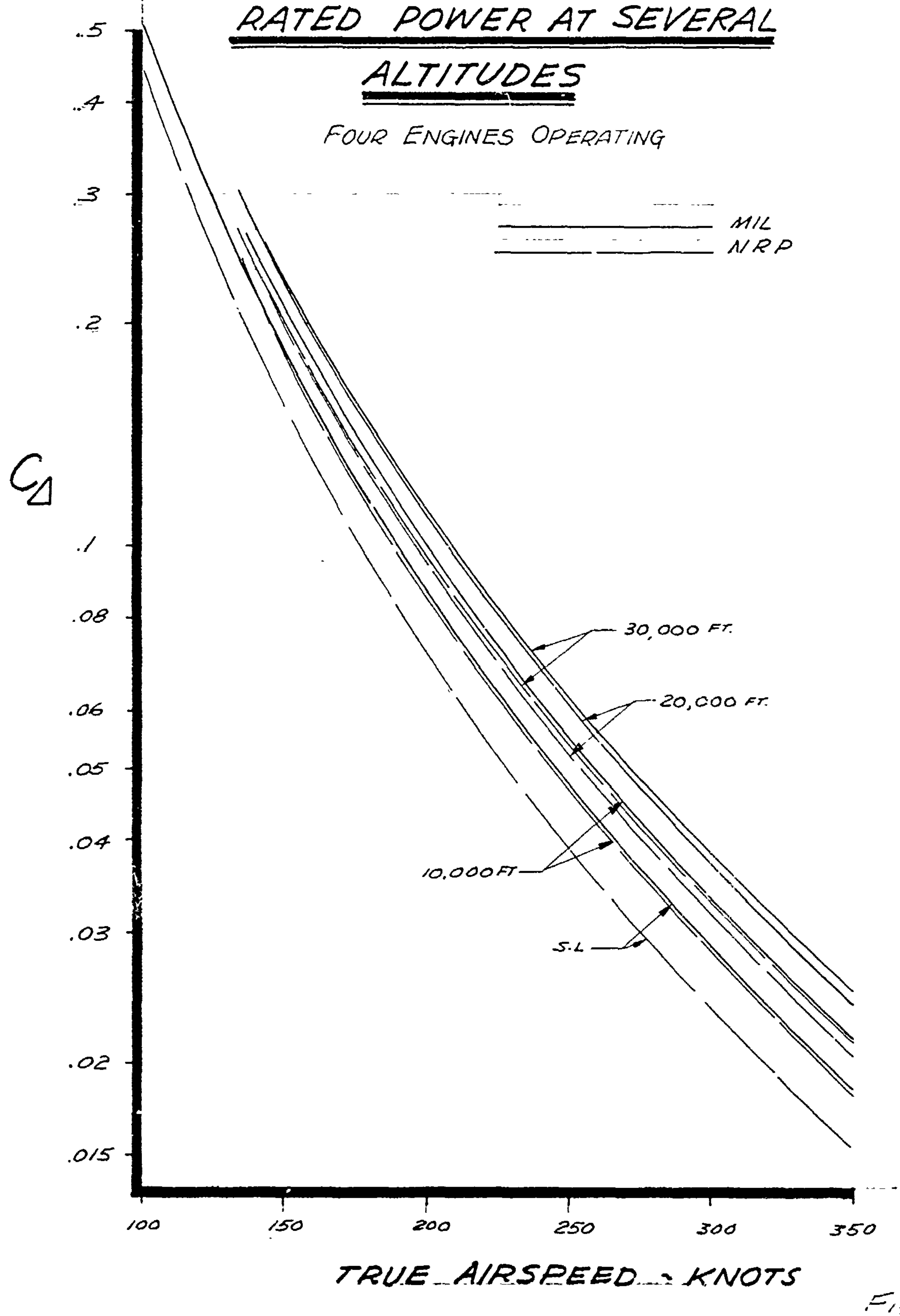

Fig 3

TABLE II

AERODYNAMIC SIGN CONVENTIONS

Item:	Positive When:
Lift, L (C_L)	Up
Drag, D (C_D)	Aft
Thrust, T ($C_\Delta = \frac{\Sigma T}{q S}$)	Forward
Pitching Moment, M (C_m)	Nose Up
Angle of Attack, α	Nose Up
Side Force, Y (C_y)	Right
Yawing Moment, N (C_n)	Nose Right
Angle of Yaw, ψ	Nose Right
Rolling Moment, L (C_l)	Right Wing Down
Elevator Angle, δ_e	Trailing Edge Down
Rudder Angle, δ_r	Trailing Edge Left
Aileron Angle, δ_a	Trailing Edge Down

LONGITUDINAL AERODYNAMIC CHARACTERISTICS

Aerodynamic data in pitch for the airplane and the airplane build-up are obtained principally from the low-and-high-speed wind tunnel tests of refs. 1, 2 and 3. Data on individual components not tested by Lockheed are obtained largely from publications of the NACA, specific references being noted as used. The airplane is conventional in all geometric and aerodynamic respects, presenting no unusual problems not capable of solution by standard methods.

AIRFOIL SECTION DATA

Airfoil section data for all lifting surfaces, together with effects of deflection of flaps or control surfaces are presented in figs. 4 through 11. These data are obtained from NACA publications, refs. 8, 9, 11-13, 15-21 and unpublished tests of the Lockheed XP2V-1.

AIRPLANE LIFT CHARACTERISTICS

Low Speed. -- Low speed lift characteristics for the airplane build-up are presented in figs. 12 and 13. These data are determined directly from the low speed wind tunnel tests, corrected for Reynold's No. effects.

Power Effects. -- Effects of power on the lift characteristics of the airplane with and without horizontal tail are given in figs. 15 through 19. These data are determined by interpolation and extrapolation from low speed wind tunnel tests. It will be noted that both lift curve slope and maximum attainable lift coefficient are increased with increasing power coefficient. The manner of obtaining power effects is discussed in the section on pitching moment characteristics below.

Mach Effects. -- Effects of compressibility on airplane build-up lift characteristics are shown in fig. 14. High speed wind tunnel tests show that all configurations which include the wing have a lift curve slope variation with Mach No. which is identical on a percentage basis, and that the incremental change in zero lift angle of attack is the same. Thus, these two simple curves are sufficient to describe the Mach effects on lift. These curves apply only to power-off cases; power effects should be ascertained from the low speed curves and added unchanged.

AIRPLANE DRAG CHARACTERISTICS

Low Speed. -- Drag characteristics for the airplane build-up are presented in figs. 20 and 21. These data are determined from the low speed wind tunnel tests, corrected for effects of Reynold's No. on lift.

Mach Effects. -- Effects of compressibility on the drag of the airplane in four stages of build-up are shown in figs. 22 and 23. Data are presented in the form of drag coefficient increments at several values of lift coefficient, to be added to low speed drag. These curves are obtained from an analysis of the low and high speed wind tunnel data.

AIRPLANE PITCHING MOMENT CHARACTERISTICS

Low Speed. -- Pitching moment characteristics for the airplane build-up are presented in figs. 24, 25 and 26. It is noted that the addition of the vertical tail to the wing - fuselage combination adds an appreciable and approximately constant, nose-down increment which will contribute to fuselage bending in the same manner as horizontal tail load. Additional configurations tested, for which no data are presented, include pylon tanks on and cargo doors in various positions. In testing with the complete airplane, addition of the pylon tanks caused a nose-down trim shift of $\Delta C_m = -.016$ while opening the upper cargo door caused a nose-up trim shift of $\Delta C_m = +.014$ and the lower, or ramp door caused a similar shift of approximately $\Delta C_m = +.0015$ per degree of door opening.

Mach Effects. -- Pitching moment coefficient curves are plotted for several Mach Numbers for each of several configurations in the airplane build-up, and presented in figs. 27 through 31.

Power Effects. -- Wind tunnel tests with power were made at very low tunnel speeds to enable attainment of large power coefficients with the model motors used. Due to the very low Reynold's Numbers of such tests, the absolute magnitude of the results are not deemed to be as trustworthy as those run at higher speeds. The incremental effects due to power are considered to be entirely reliable, and are used by adding them to proper basic power-off test results from normal tunnel speed runs. This procedure has been followed in the analysis of all power-on data presented herein.

Effects of power-on airplane pitching moment characteristics with and without horizontal tail and for various flap settings are presented in figs. 32 through 36. It will be noted that the effects of power are destabilizing for both configurations and all flap settings.

These power effects are absolute in value with respect to speed; to determine pitching moment at high speeds, the power-off value should first be ascertained for the proper Mach No. and an increment due to power obtained from these low speed curves to be added.

ELEVATOR CHARACTERISTICS

Elevator effectiveness is given in fig. 37, showing change in airplane pitching moment at constant lift coefficient. Values are presented for several lift coefficients and for flaps retracted and extended. Effects of Mach No. on elevator effectiveness are given in fig. 38.

Elevator hinge moment data are presented in figs. 39 and 40 for flaps extended and retracted. Values are given in each case for airplane angles of attack of zero and six degrees. From elevator floating characteristics, it has been ascertained that hinge moment for angles of attack greater than six degrees is the same as at six degrees; all variation of hinge moment with angle of attack is for angles less than six degrees, as noted on the figures, for all flap positions. Characteristics of the control and boost system are shown in figs. 77, 78 and 79, including a plot of the variation of pilot force with elevator hinge moment.

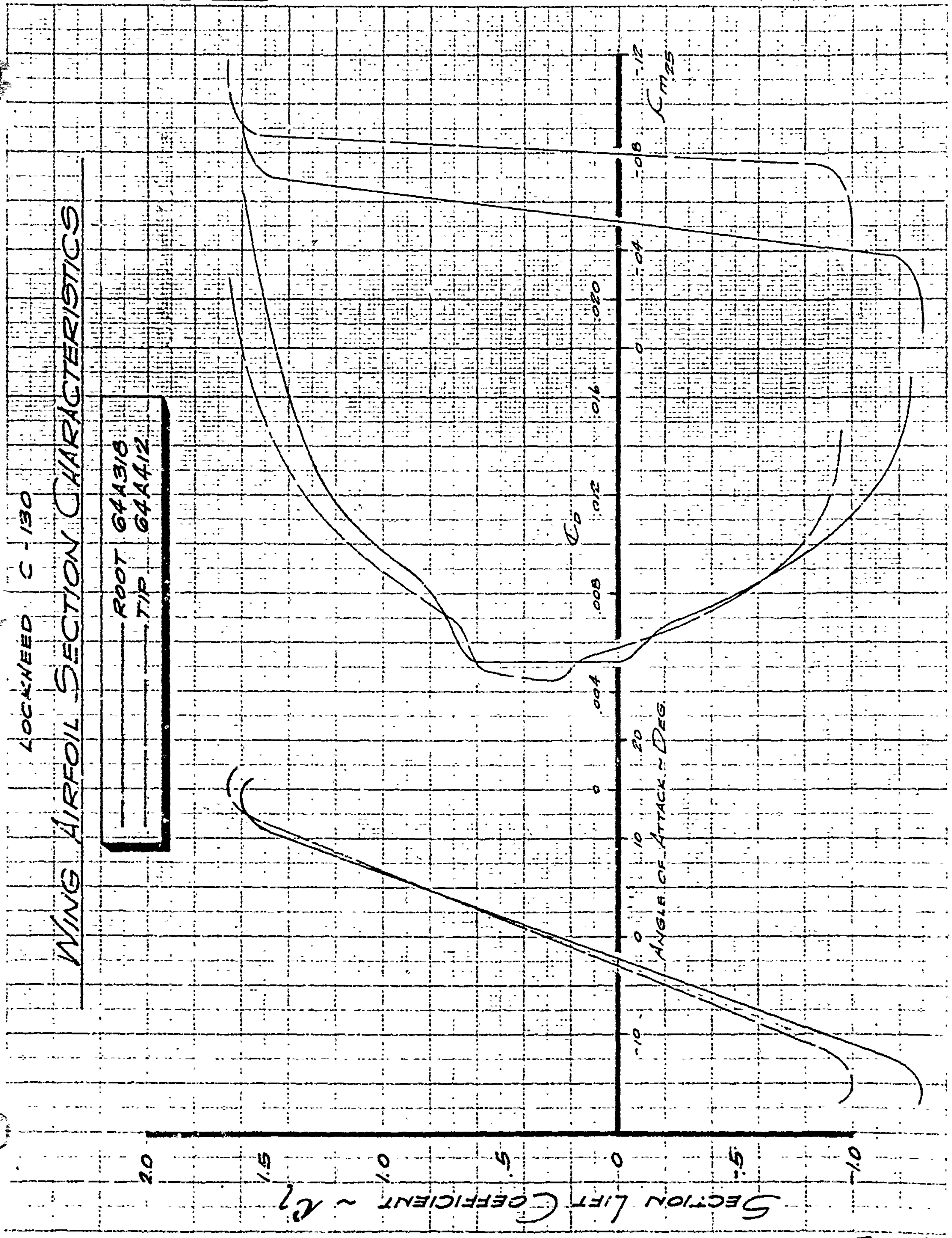
LOCKHEED C-130
WING AIRFOIL SECTION CHARACTERISTICS
ROOT 64A318
TIP 64A412
$C_{m_{.25}}$
-.12
-.08
-.04
0
C_D
.020
.016
.012
.008
.004
ANGLE OF ATTACK ~ DEG.
20
10
0
-10
SECTION LIFT COEFFICIENT ~ C_l
2.0
1.5
1.0
.5
0
-.5
-1.0

FIG. 4

LOCKHEED C-130

WING AIRFOIL SECTION LIFT CHARACTERISTICS WITH VARIOUS FLAP EXTENSIONS

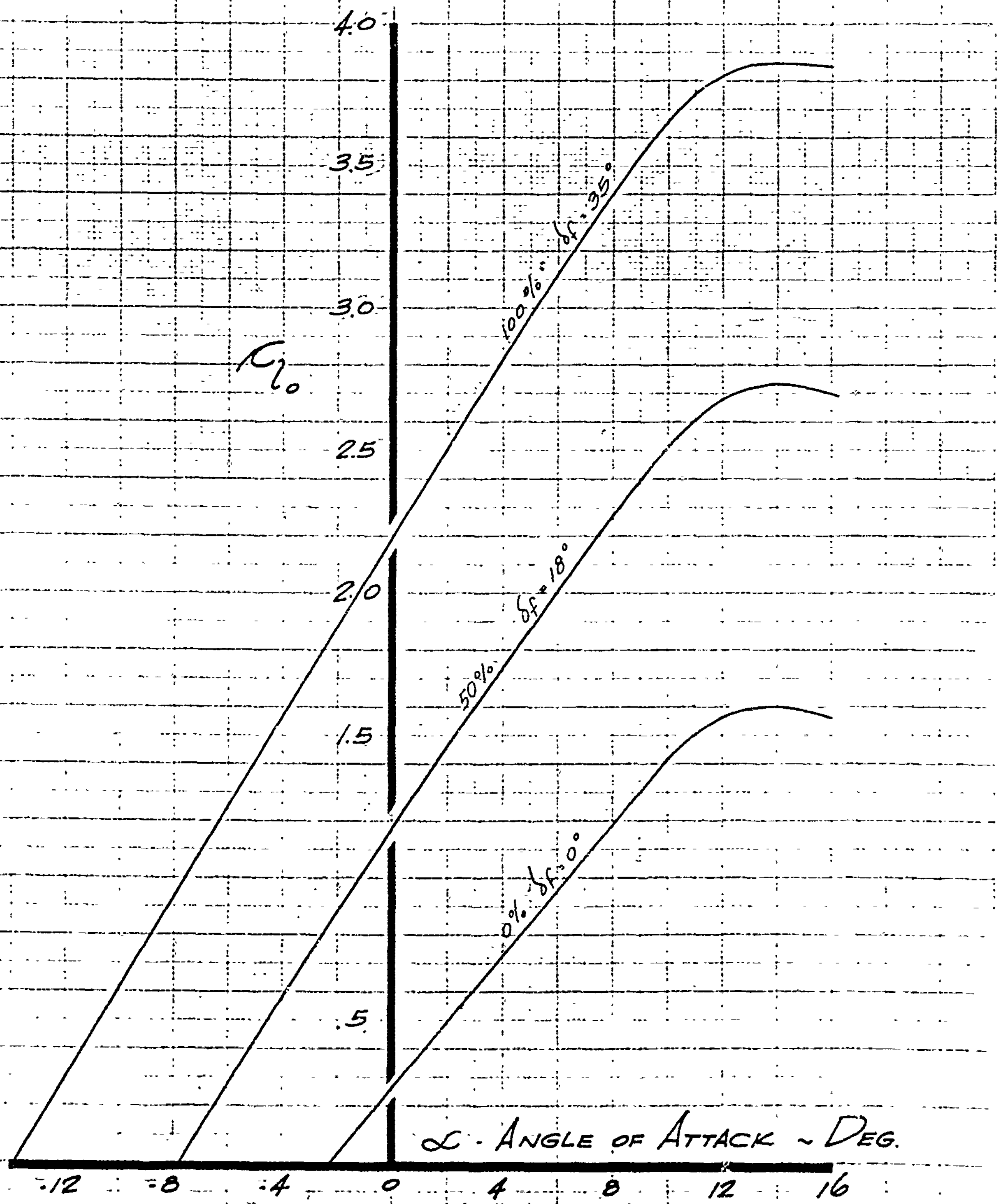

FIG. 5

PREPARED BY R.L.D
DATE 12-7-52
CHECKED BY

LOCKHEED AIRCRAFT CORPORATION

PAGE 18
MODEL C-130
REPORT NO. 9062

LOCKHEED C-130

WING AIRFOIL SECTION DRAG CHARACTERISTICS
WITH
VARIOUS FLAP EXTENSIONS

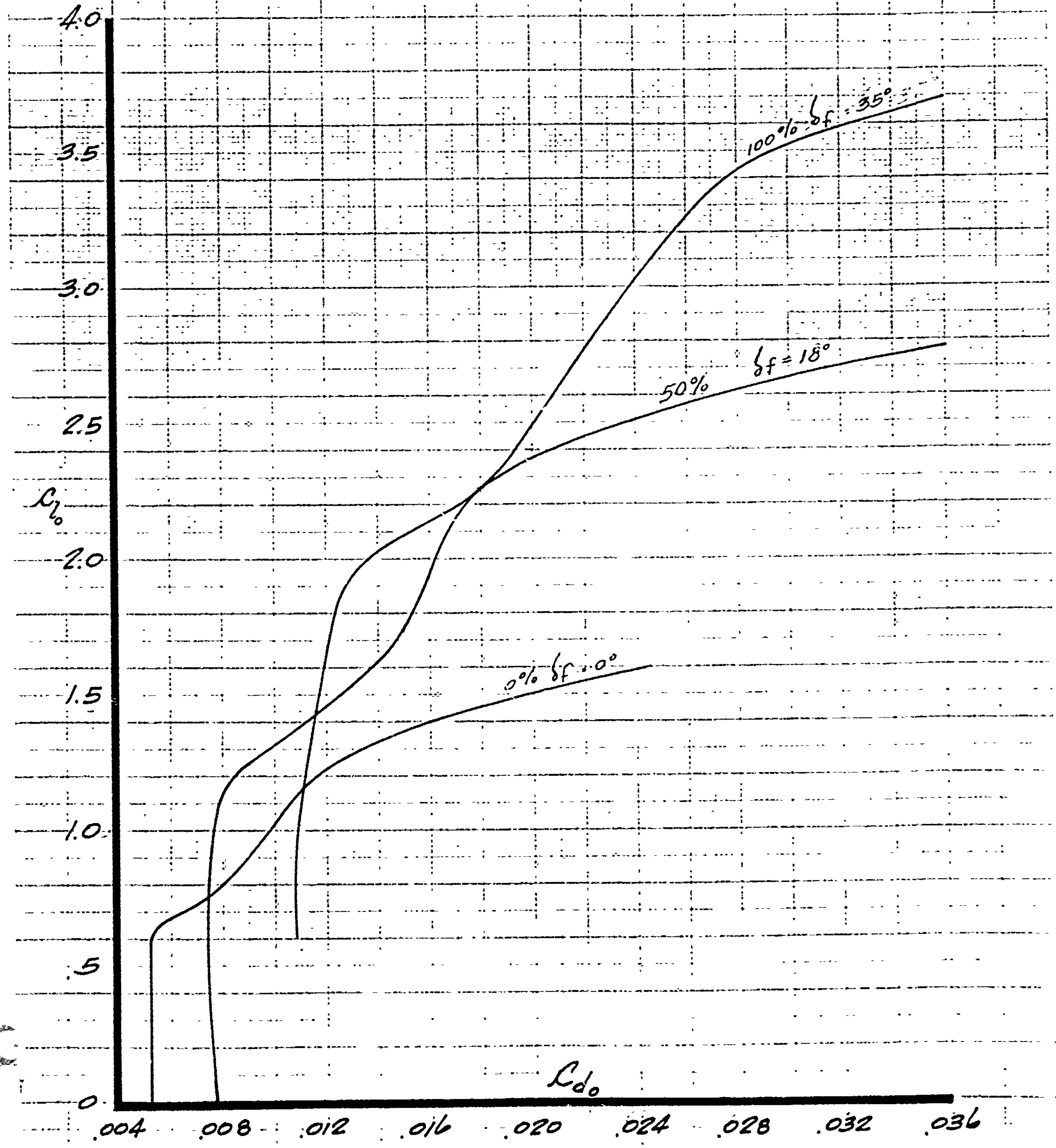

FIG. 6

PREPARED BY RLD
DATE 2-7-52
CHECKED BY

LOCKHEED AIRCRAFT CORPORATION

PAGE 19
MODEL C-130
REPORT NO 9062

LOCKHEED C-130

WING AIRFOIL SECTION PITCHING MOMENT CHARACTERISTICS WITH VARIOUS FLAP EXTENSIONS

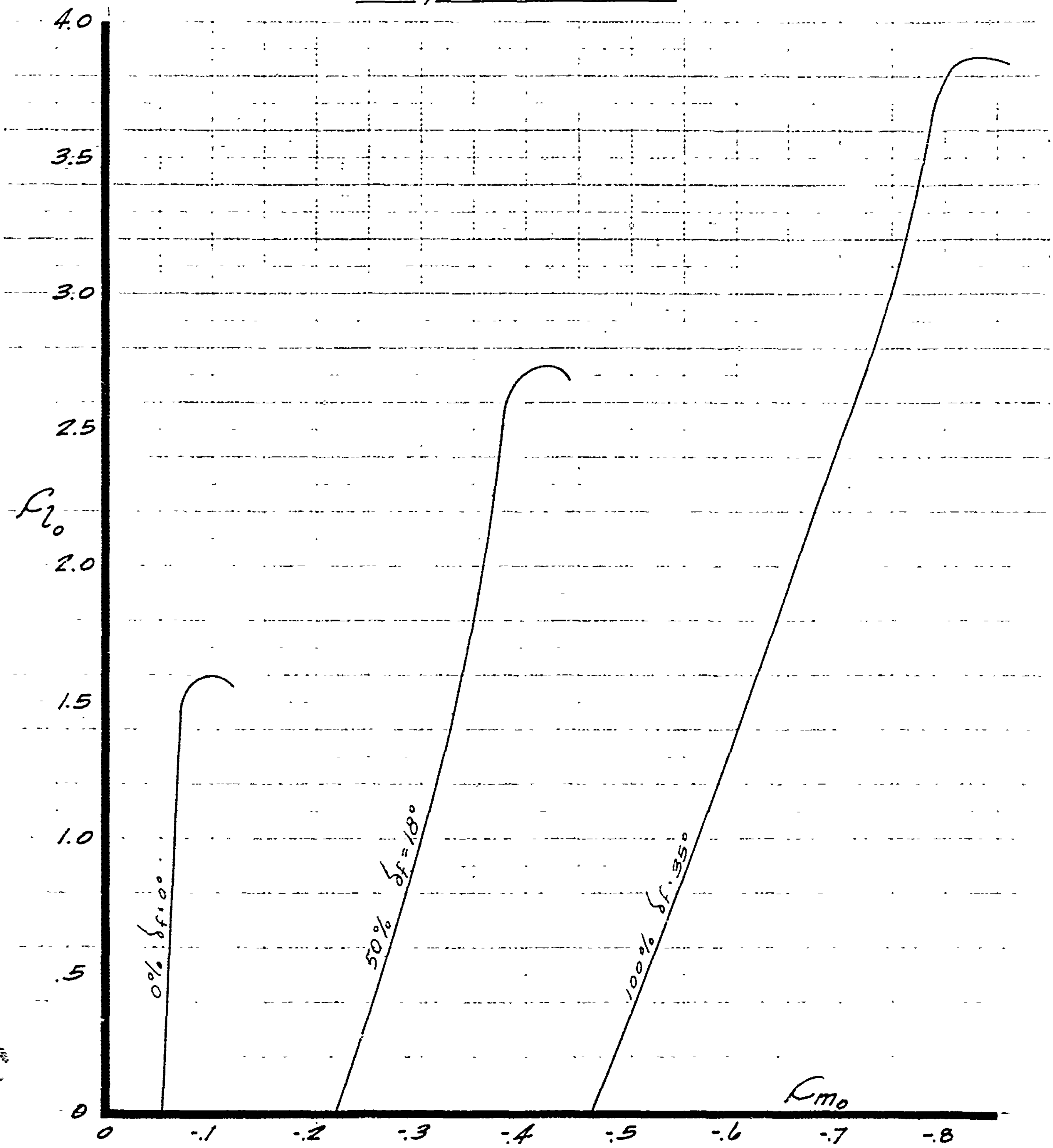

FIG. 7

FORM 527BA

LOCKHEED C-130

HORIZONTAL TAIL AIRFOIL SECTION CHARACTERISTICS

TR 824

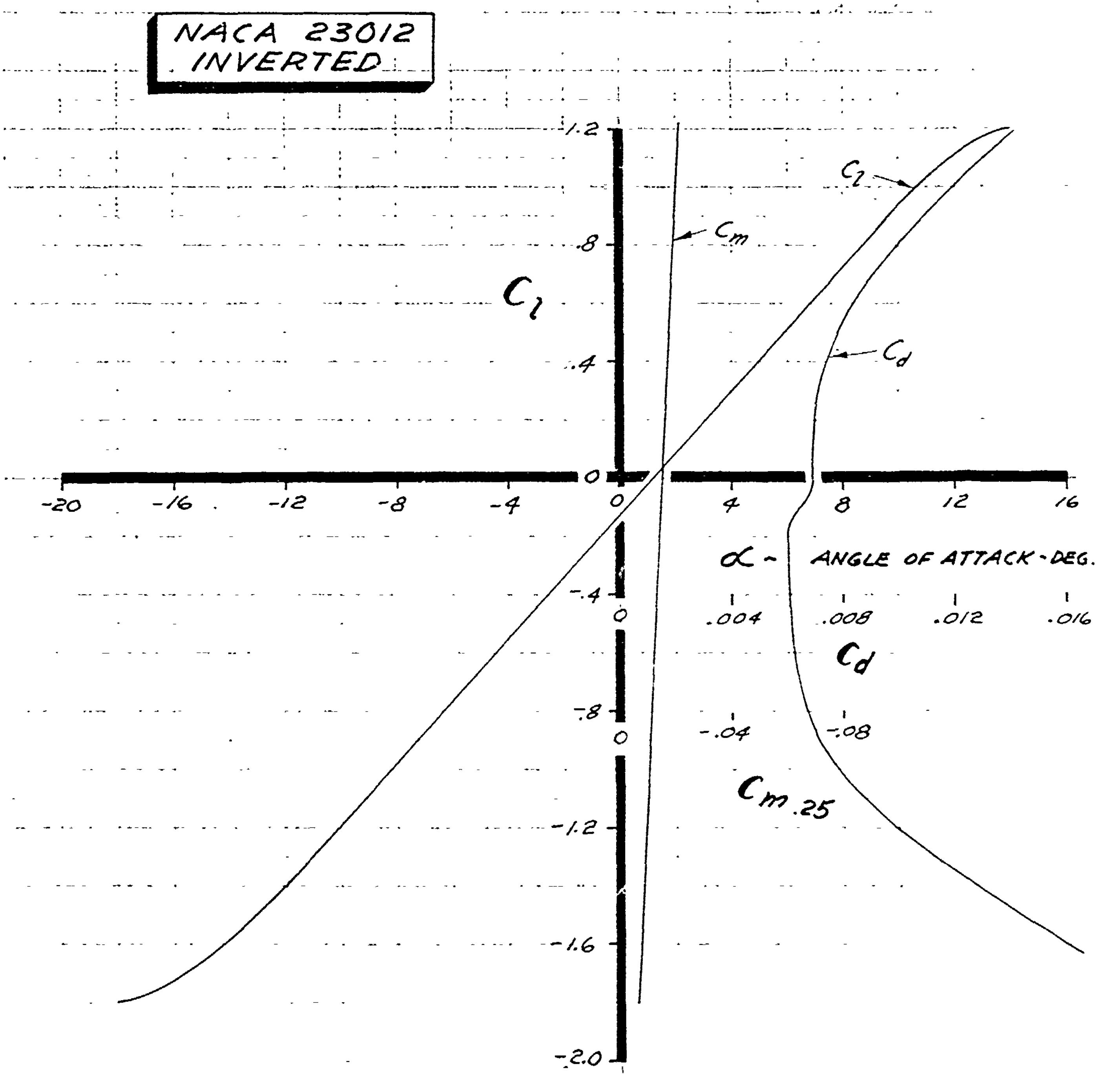

LOCKHEED C-130

HORIZONTAL TAIL AIRFOIL SECTION

PITCH CHARACTERISTICS DUE TO

ELEVATOR DEFLECTION

LOW SPEED

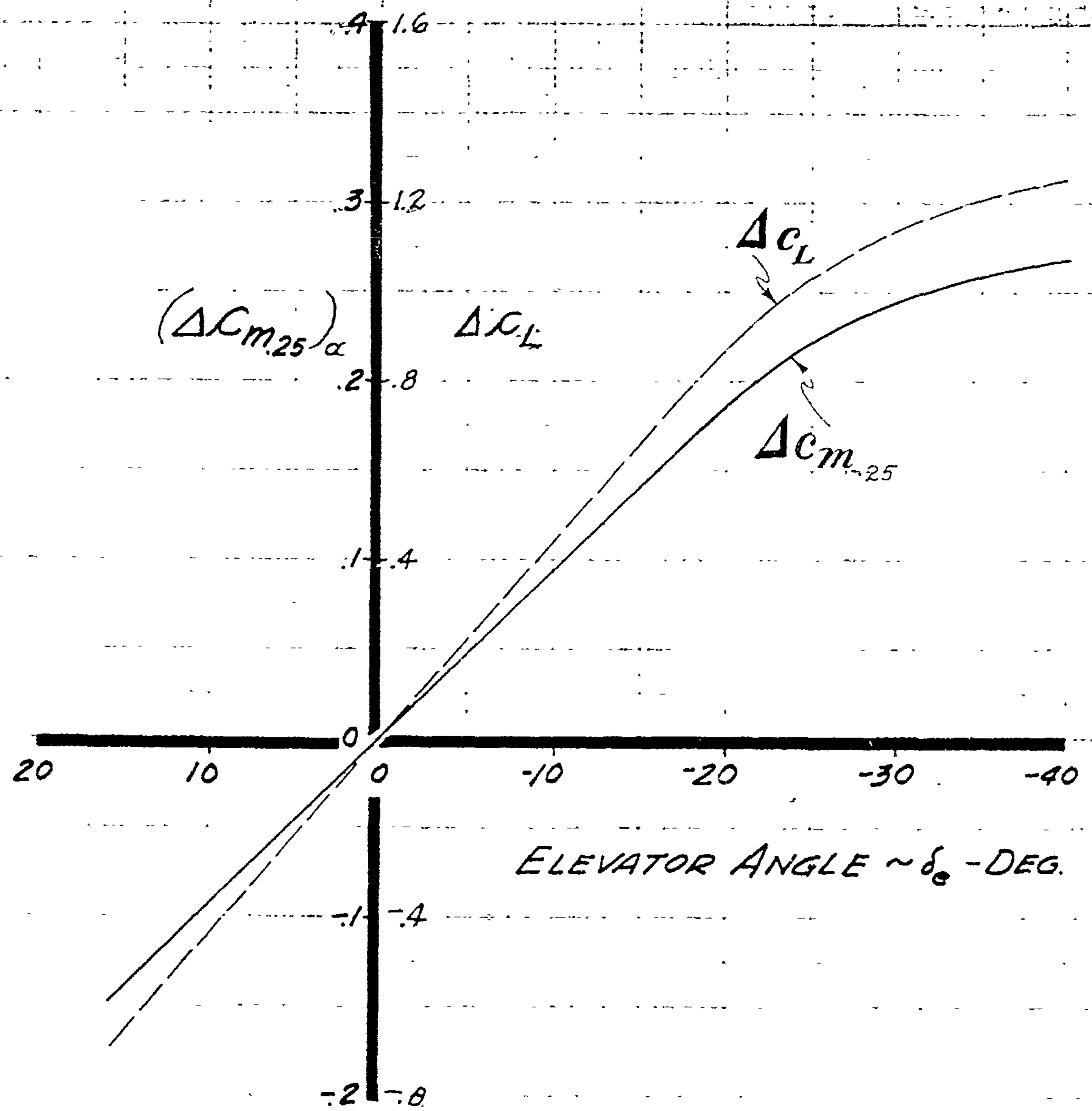

FIG. 9

TR 824 #903

LOCKHEED C-130

VERTICAL TAIL AIRFOIL

SECTION CHARACTERISTICS

NACA 64A015 AIRFOIL

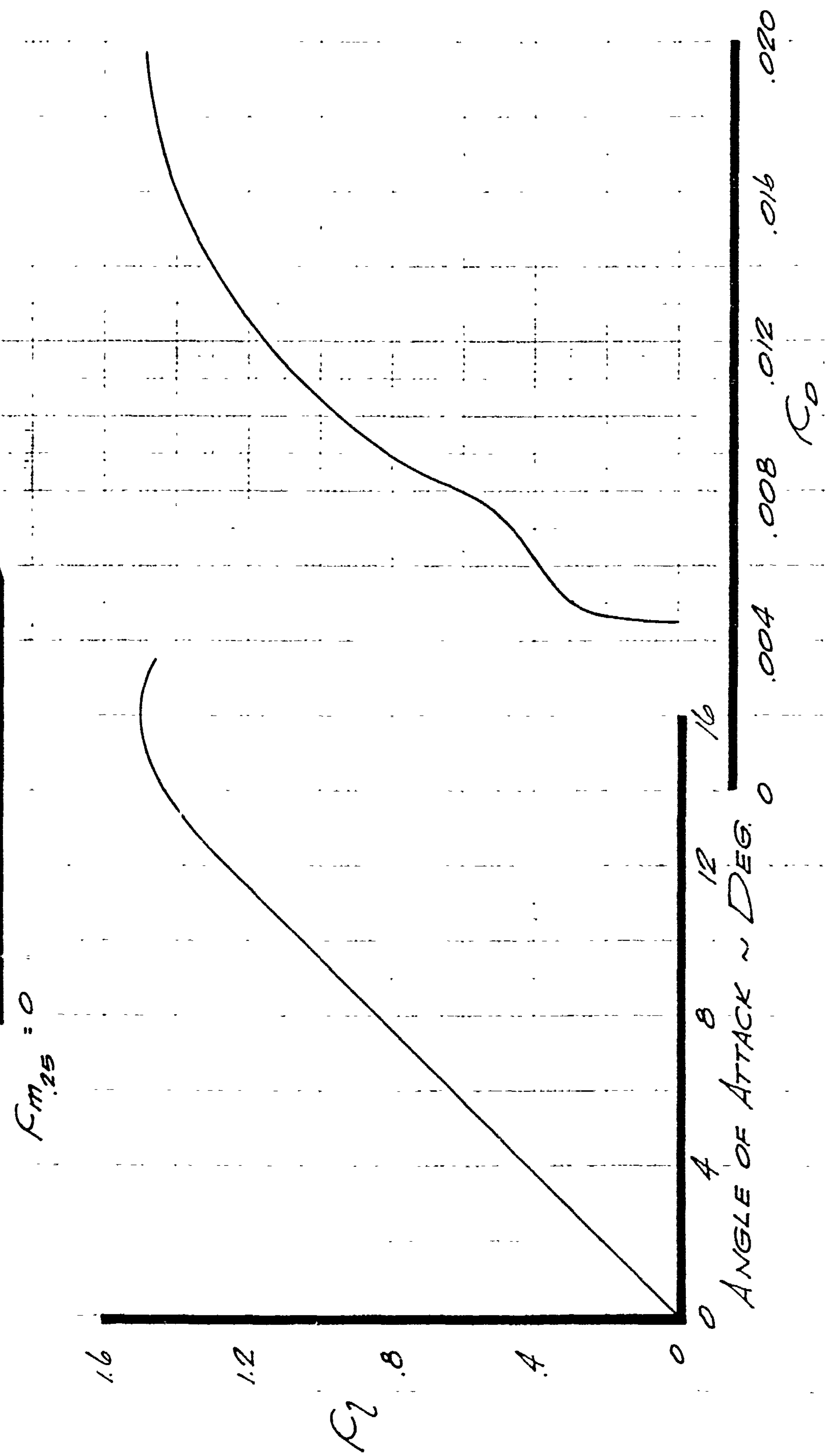

FIG. 10

PREPARED BY RLD
DATE 1-3-52
CHECKED BY

LOCKHEED AIRCRAFT CORPORATION

LOCKHEED C-130

EFFECT OF AILERON DEFLECTION ON WING AIRFOIL SECTION CHARACTERISTICS

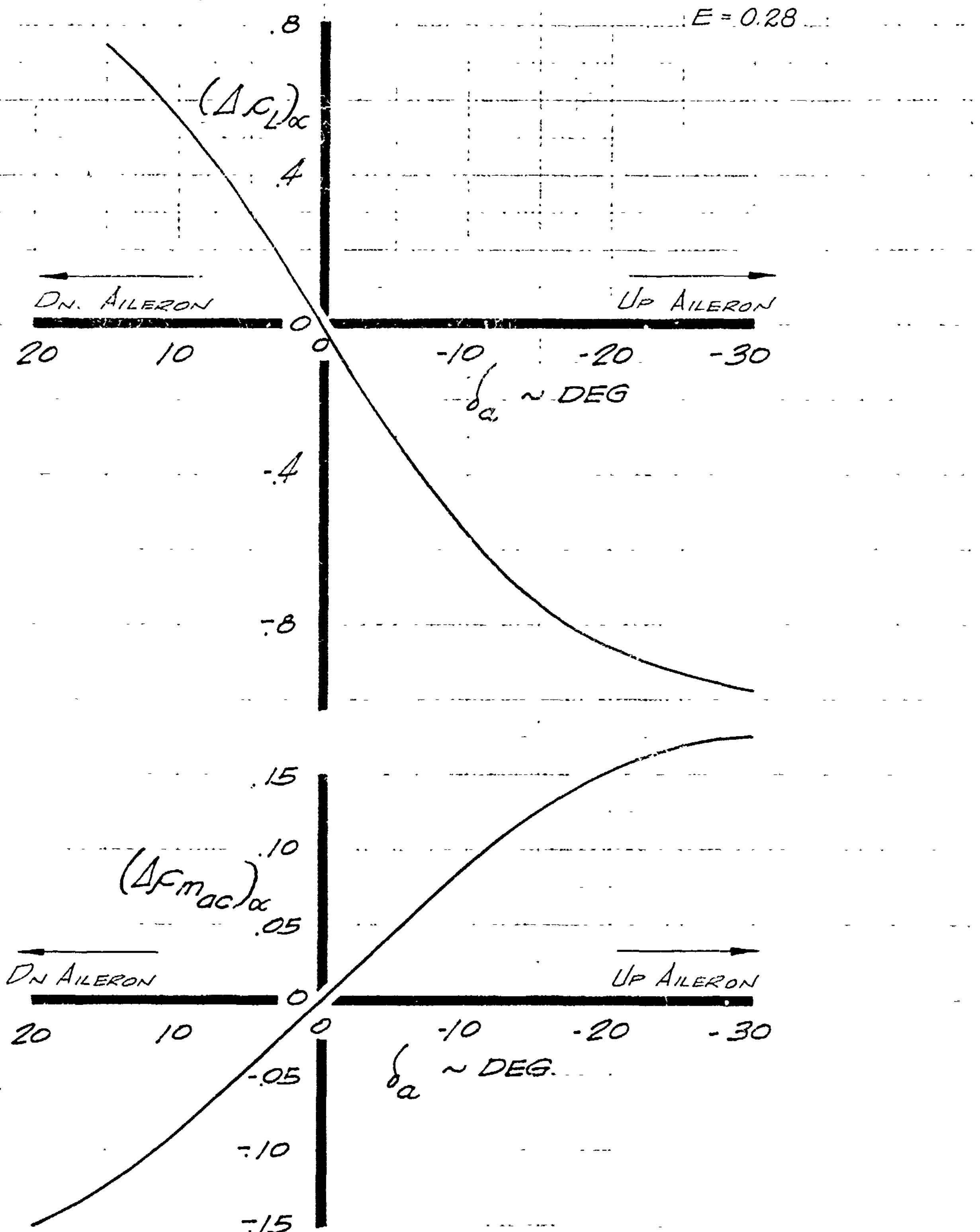

FIG. 11

RM 632, TN 763

RK 103, 111, 174

PREPARED BY R.L.D.
DATE 9-8-52
CHECKED BY

LOCKHEED AIRCRAFT CORPORATION

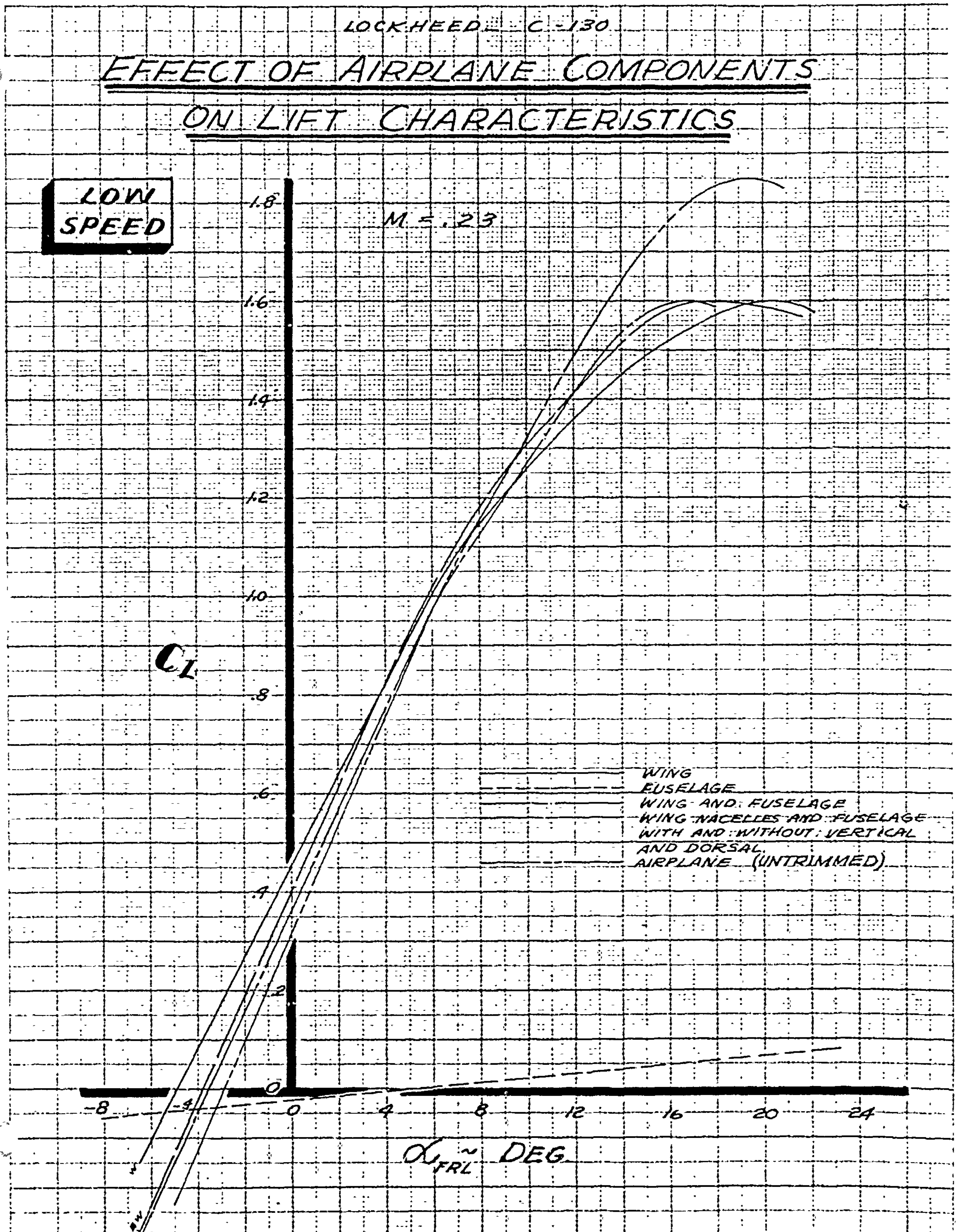

Fig. 12

LOCKHEED C-130

AIRPLANE LIFT CHARACTERISTICS WITH VARIOUS FLAP EXTENSIONS

POWER OFF

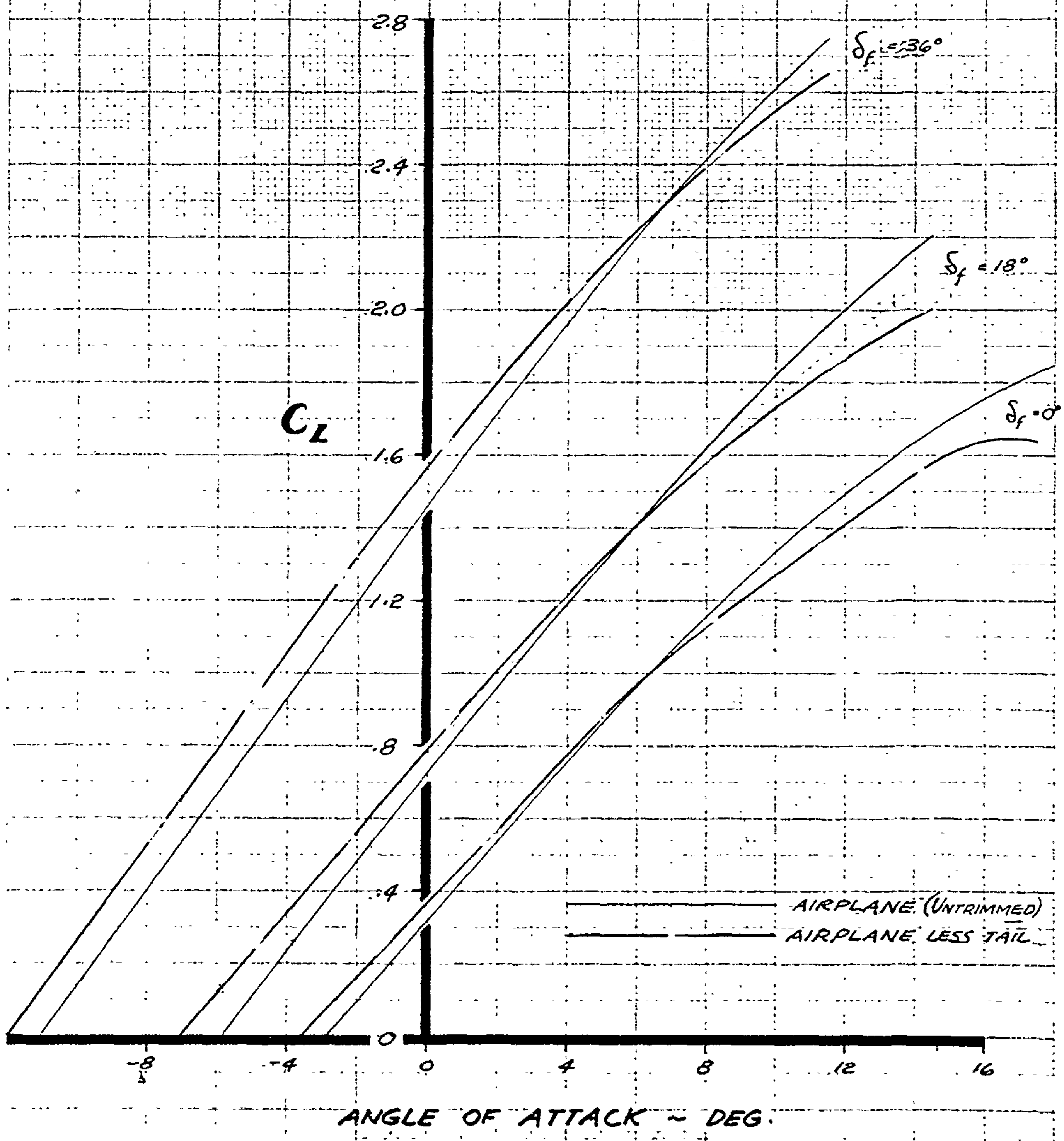

FIG. 13

PREPARED BY R.L.D.
DATE 9-8-52
CHECKED BY

LOCKHEED AIRCRAFT CORPORATION

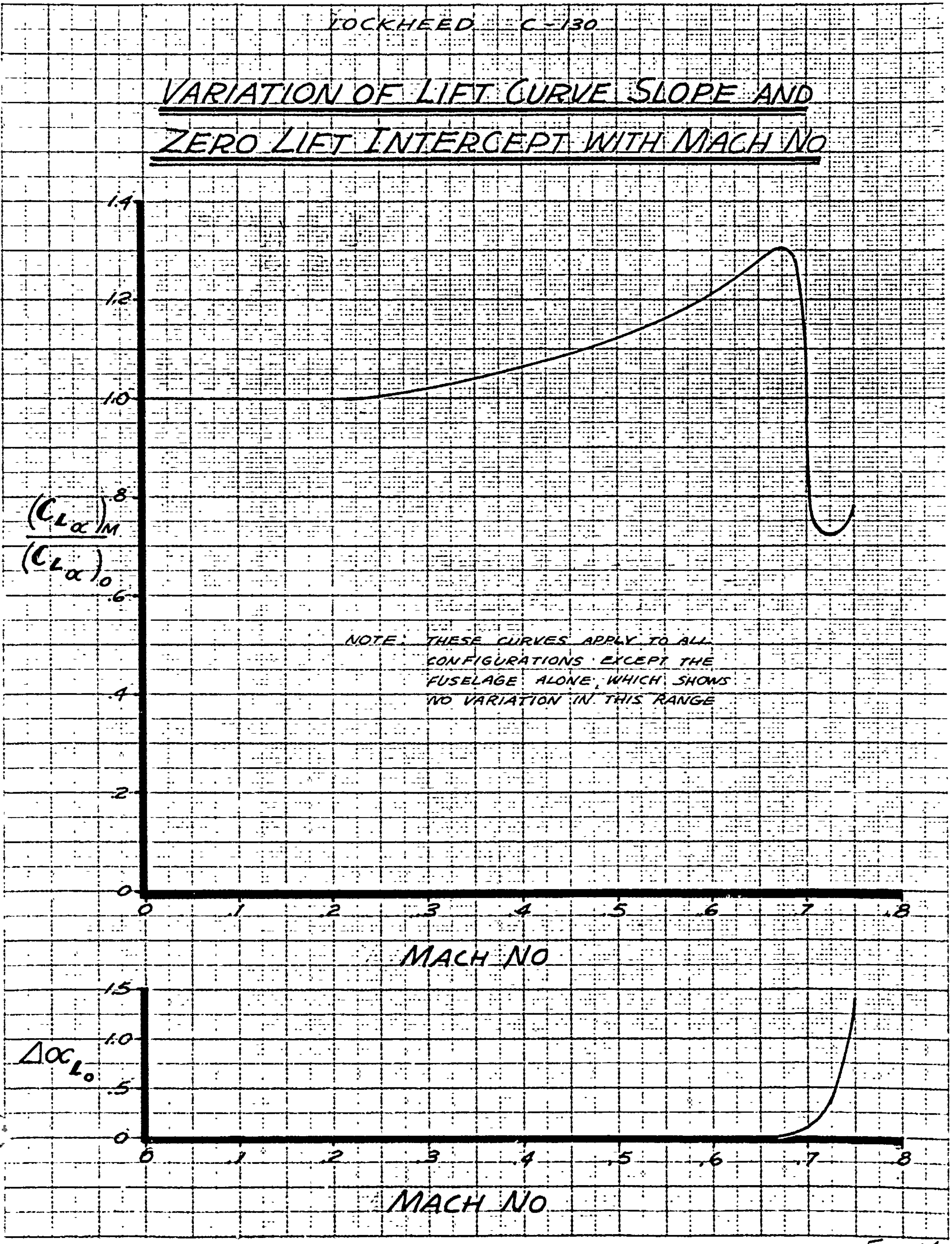

FIG. 14

FORM 327CA

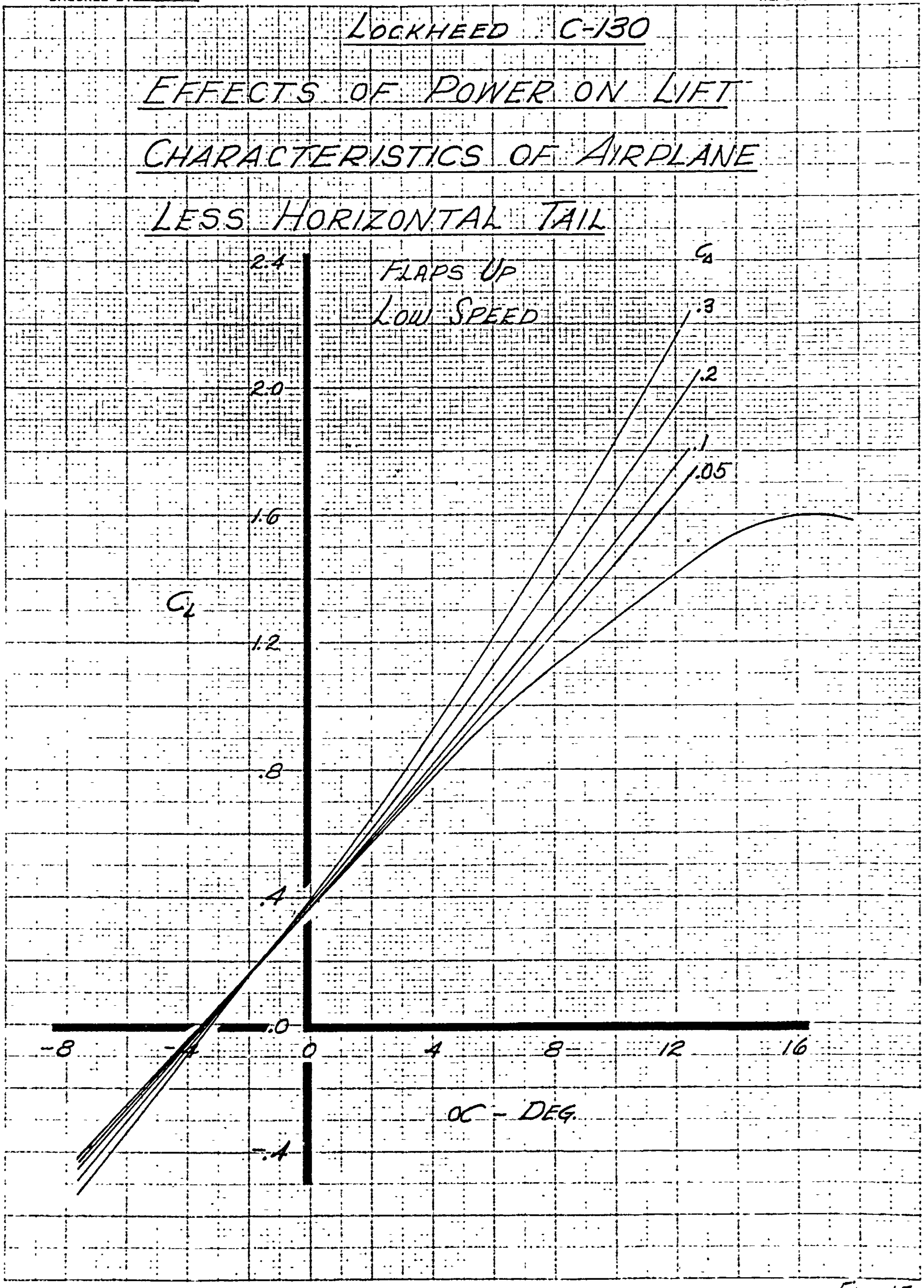
LOCKHEED C-130
EFFECTS OF POWER ON LIFT
CHARACTERISTICS OF AIRPLANE
LESS HORIZONTAL TAIL
FLAPS UP
LOW SPEED
C_s
.3
.2
.1
.05
C_L
2.4
2.0
1.6
1.2
.8
.4
0
-.4
-8
-4
0
4
8
12
16
α - DEG.

FIG. 15.

LOCKHEED C-130

EFFECTS OF POWER ON LIFT CHARACTERISTICS OF AIRPLANE LESS HORIZONTAL TAIL

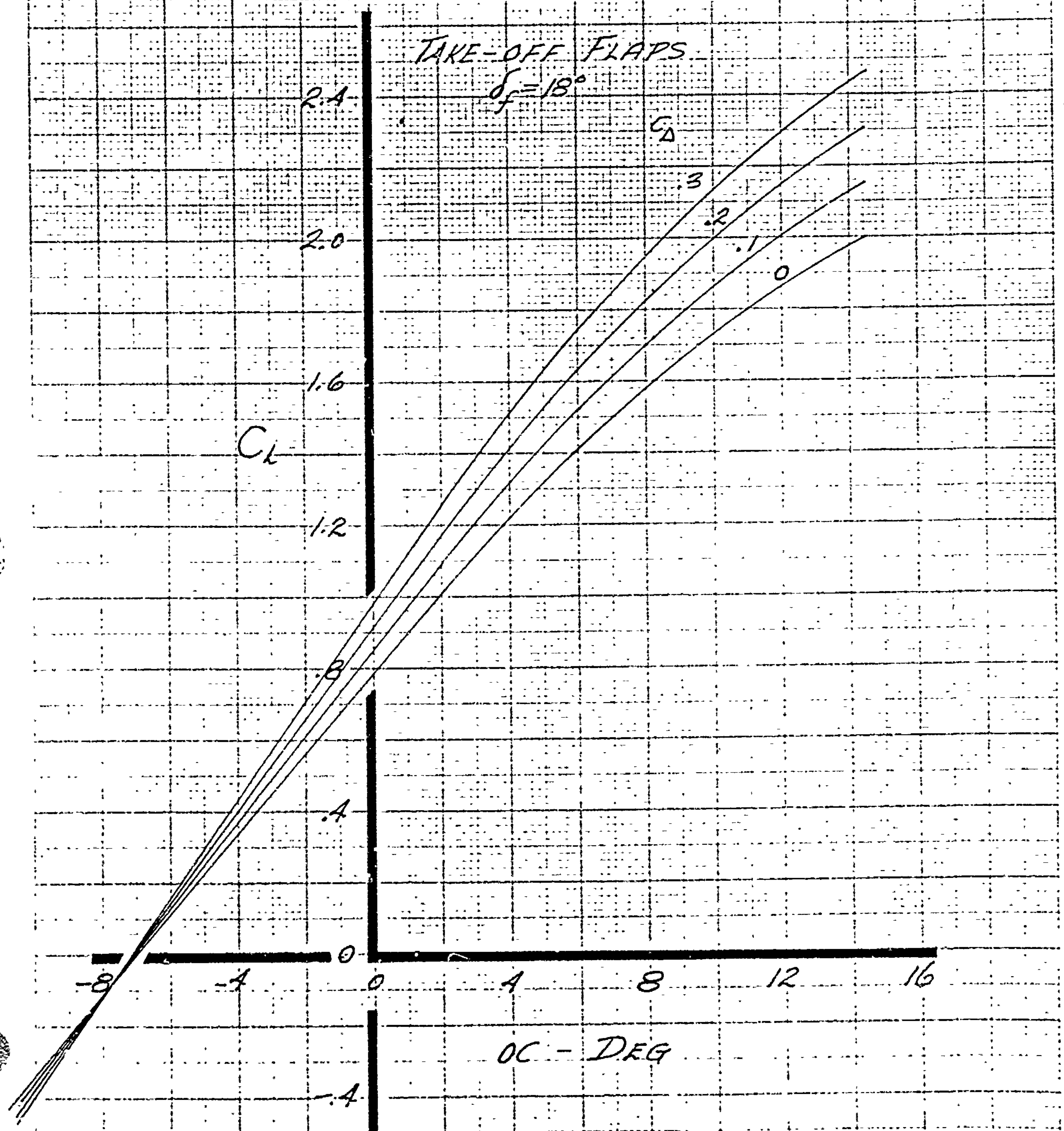

Fig. 16

LOCKHEED C-130

EFFECTS OF POWER ON LIFT CHARACTERISTICS OF AIRPLANE LESS HORIZONTAL TAIL

LANDING FLAPS - $\delta_f = 36°$

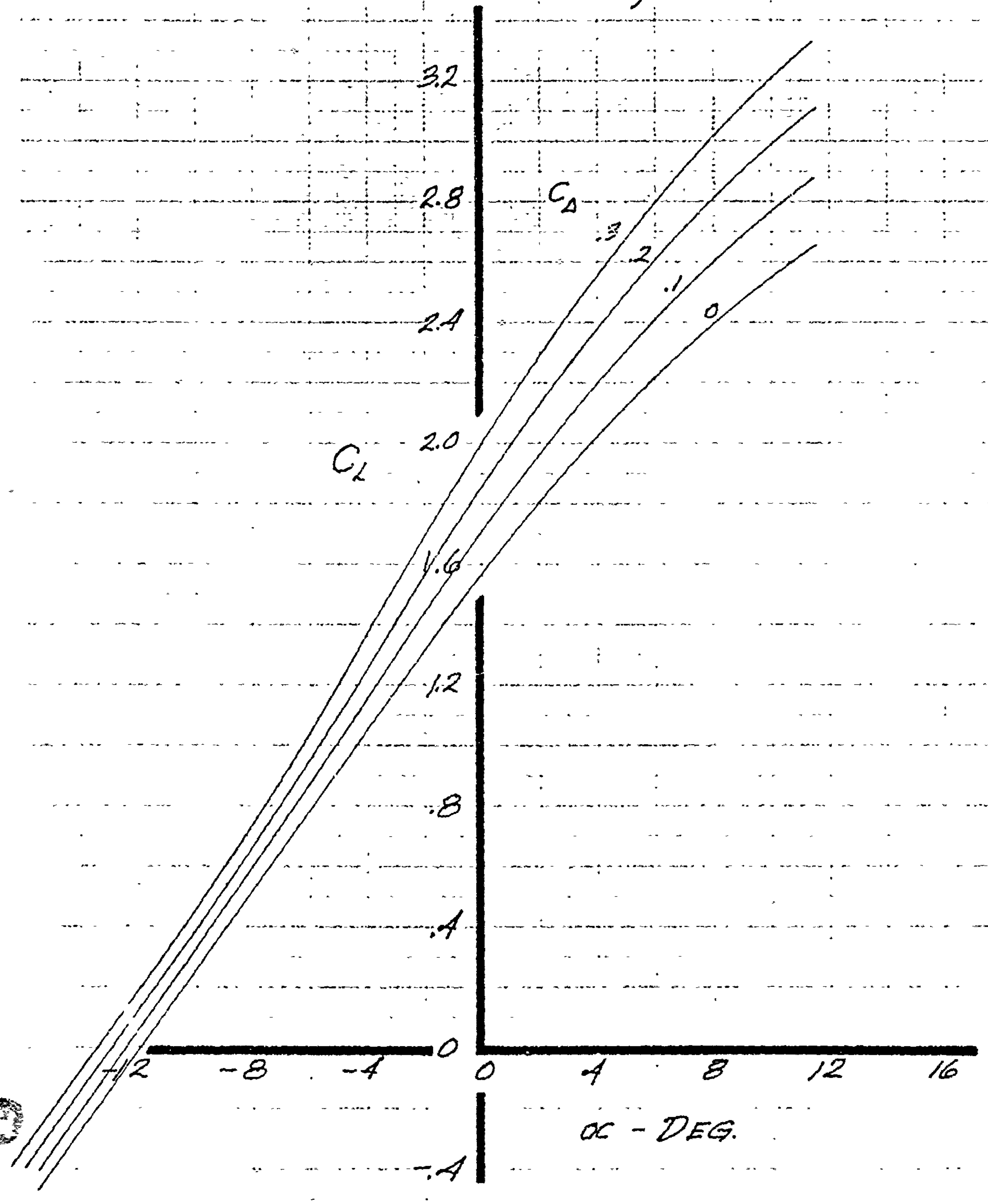

FIG. 17

LOCKHEED C-130

POWER EFFECTS ON AIRPLANE LIFT CHARACTERISTICS

LOW SPEED

$\delta_e = 0°$

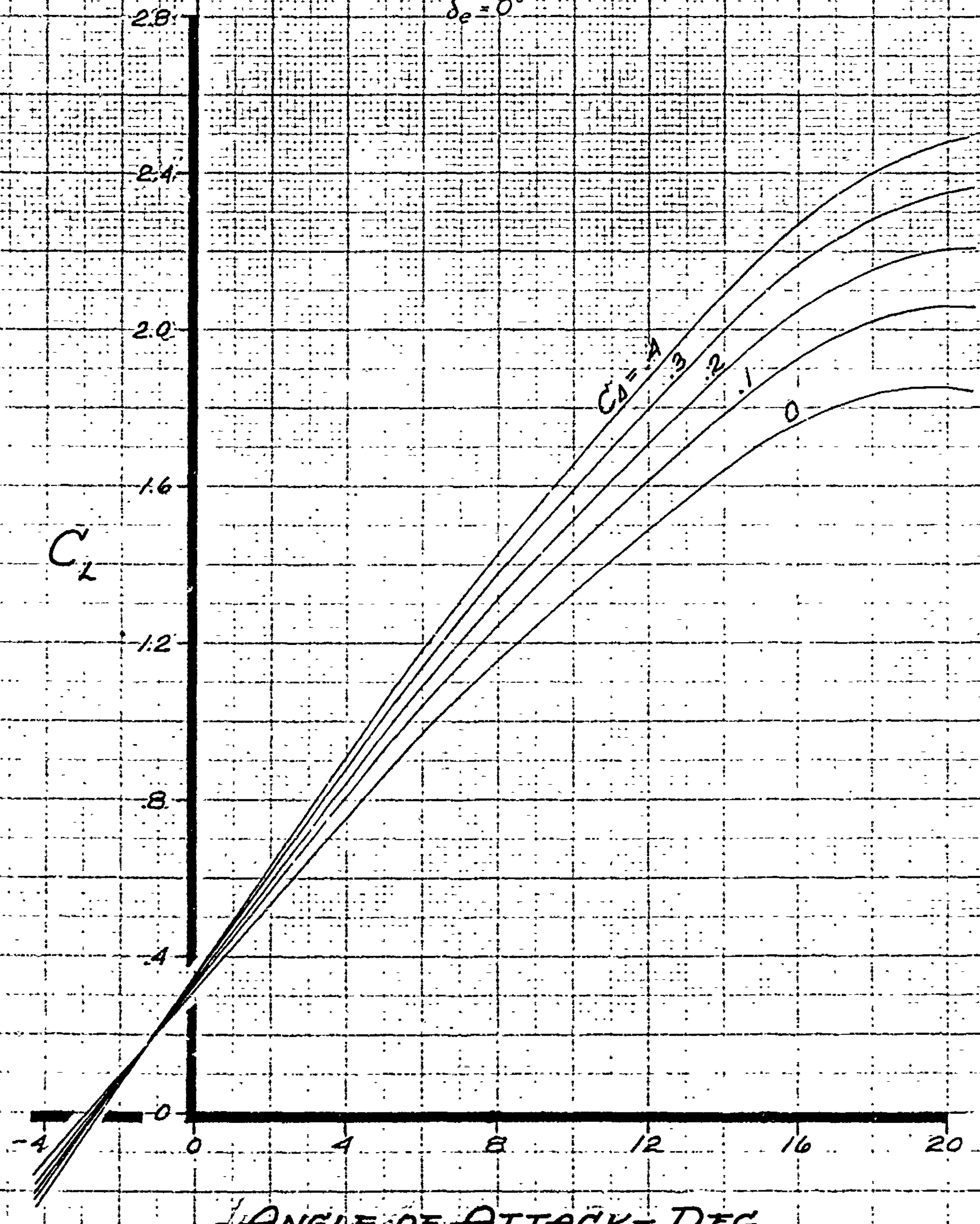

FIG. 18

LOCKHEED C-130

EFFECT OF POWER ON AIRPLANE LIFT CHARACTERISTICS

FLAPS DOWN 36°

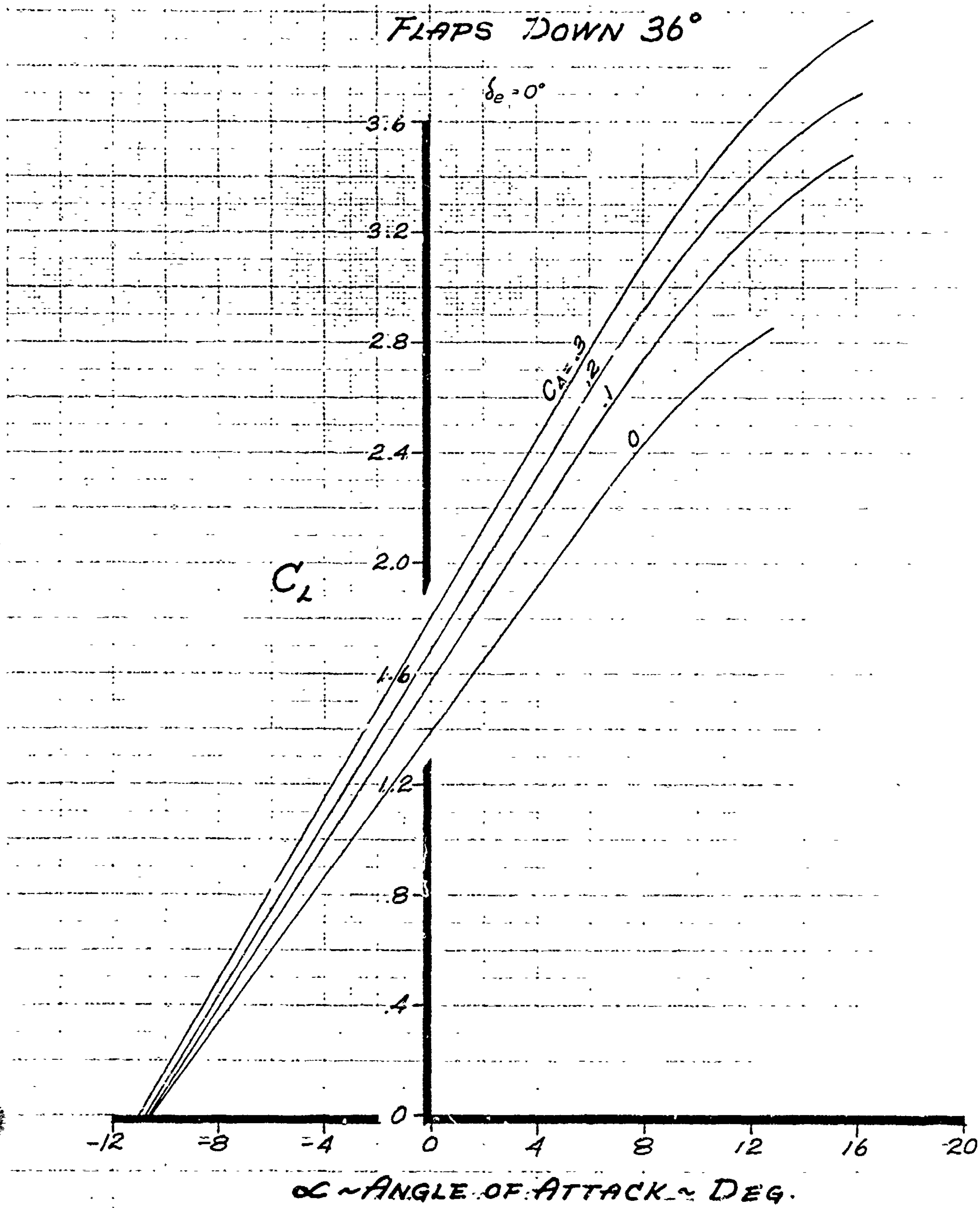

FORM 5278A

FIG. 19

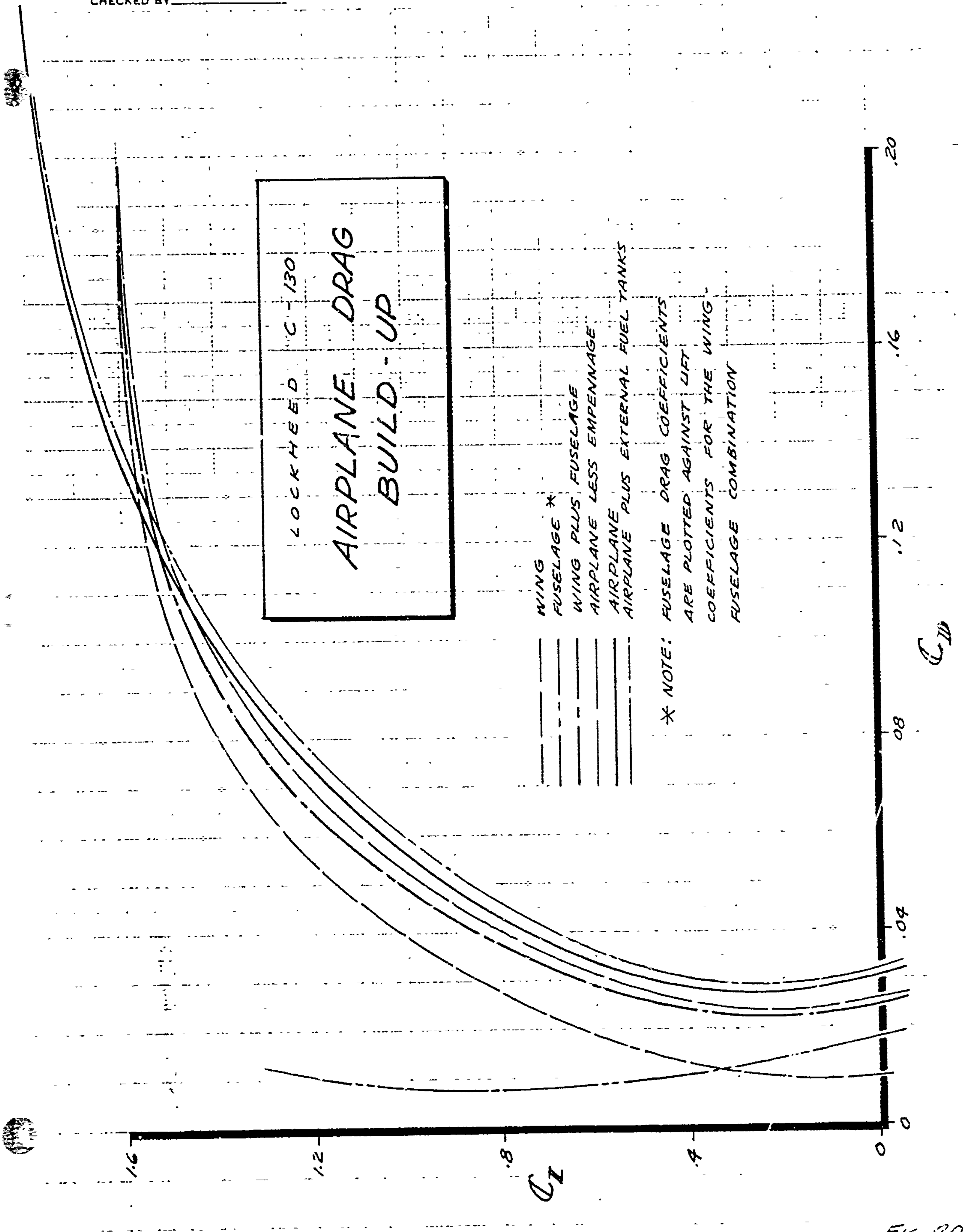
LOCKHEED C-130
AIRPLANE DRAG
BUILD-UP
WING
FUSELAGE *
WING PLUS FUSELAGE
AIRPLANE LESS EMPENNAGE
AIRPLANE
AIRPLANE PLUS EXTERNAL FUEL TANKS
* NOTE: FUSELAGE DRAG COEFFICIENTS
ARE PLOTTED AGAINST LIFT
COEFFICIENTS FOR THE WING-
FUSELAGE COMBINATION
C_L
1.6
1.2
.8
.4
0
C_D
0
.04
.08
.12
.16
.20

FIG. 20

PREPARED BY
DATE
CHECKED BY

LOCKHEED AIRCRAFT CORPORATION

PAGE 33
MODEL C-130
REPORT NO. 9062

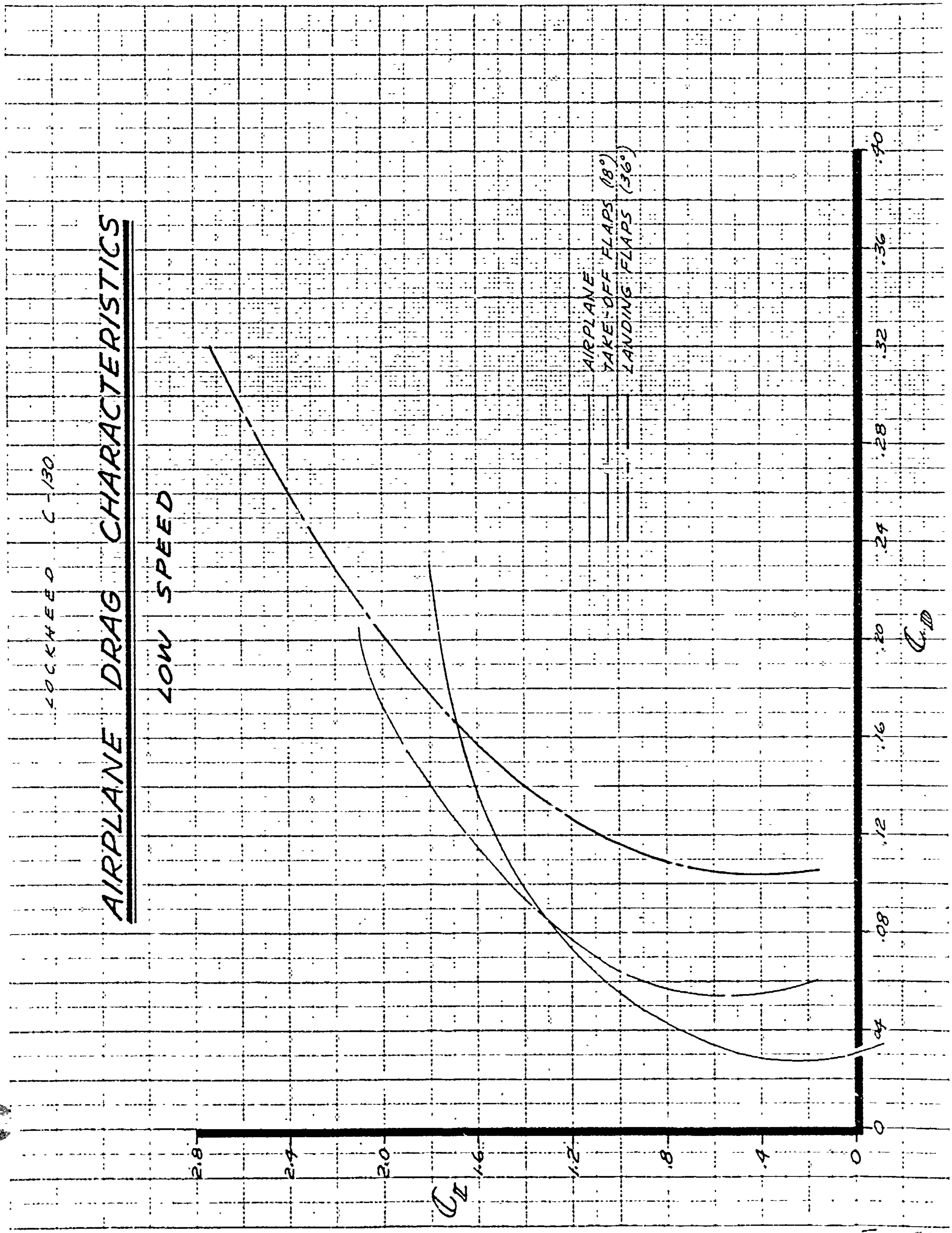

FIG. 21

FORM 3278A

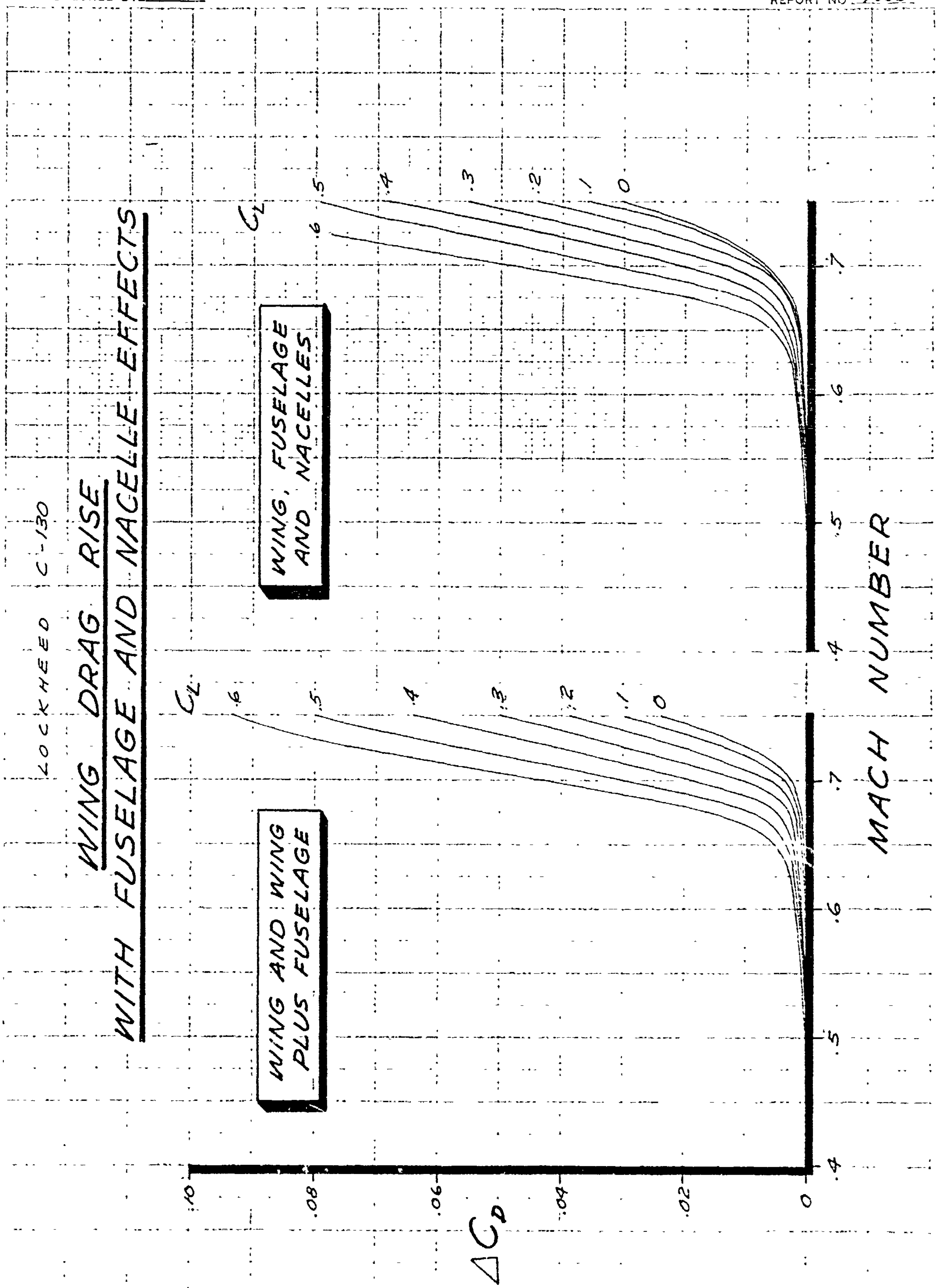
LOCKHEED C-130
WING DRAG RISE
WITH FUSELAGE AND NACELLE EFFECTS
WING, FUSELAGE AND NACELLES
WING AND WING PLUS FUSELAGE
C_L
0 .1 .2 .3 .4 .5 .6
ΔC_D
.10 .08 .06 .04 .02 0
.4 .5 .6 .7
MACH NUMBER

Fig. 22

LOCKHEED C-130

AIRPLANE DRAG RISE

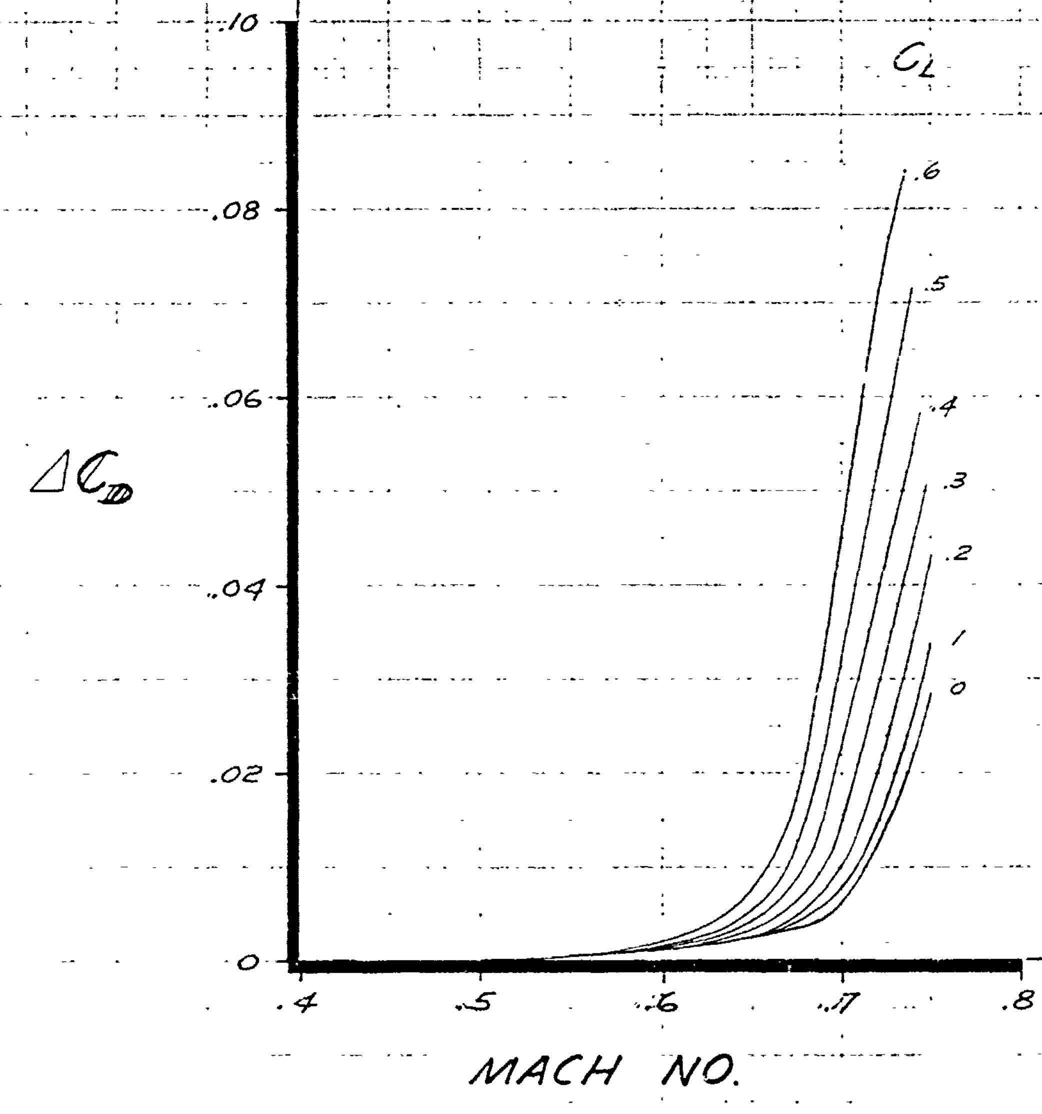

LOCKHEED. C-130

EFFECT OF AIRPLANE COMPONENTS ON PITCHING MOMENTS

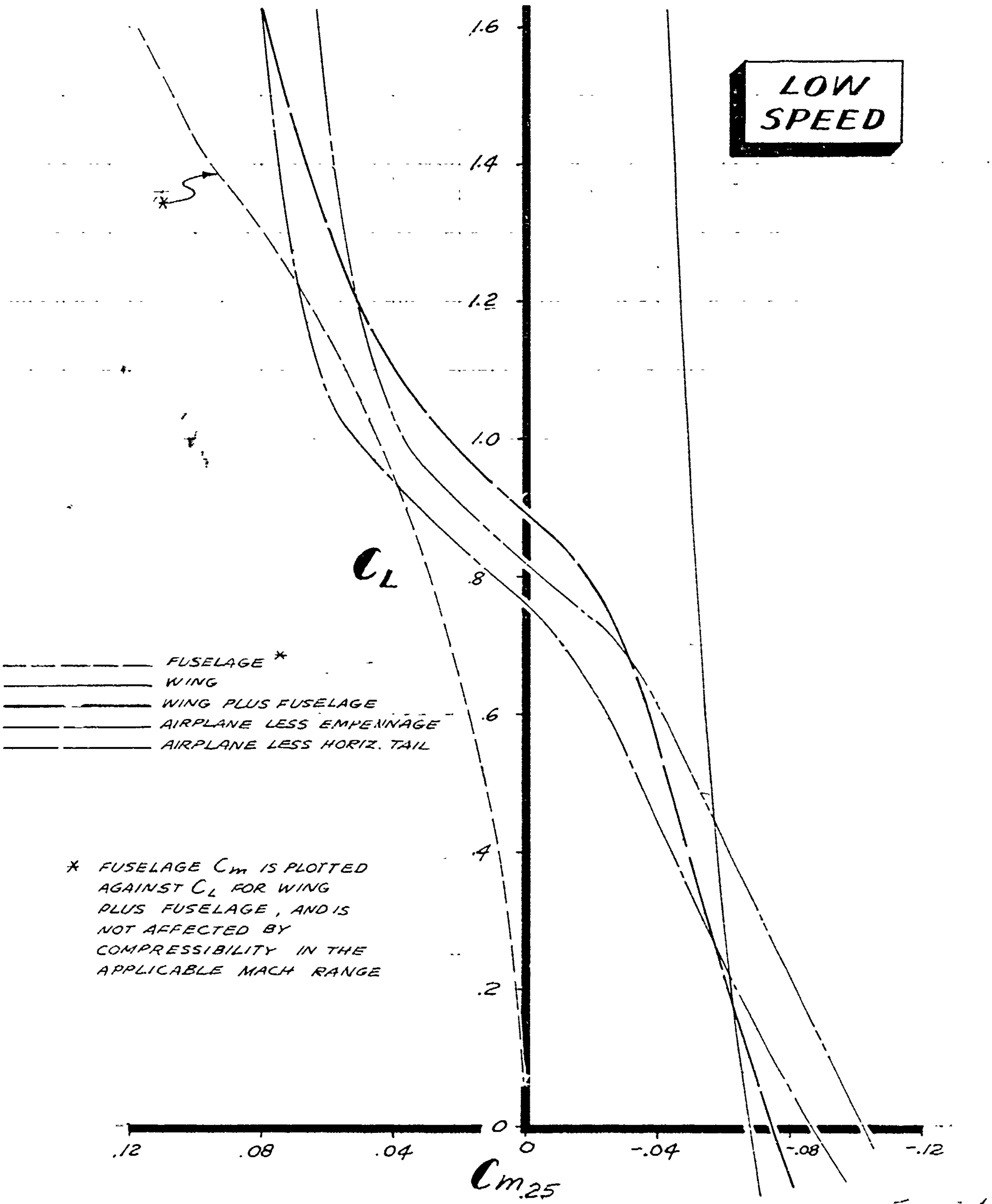

F-24

LOCKHEED C-130

AIRPLANE - LESS - TAIL PITCHING MOMENT FOR VARIOUS FLAP DEFLECTIONS

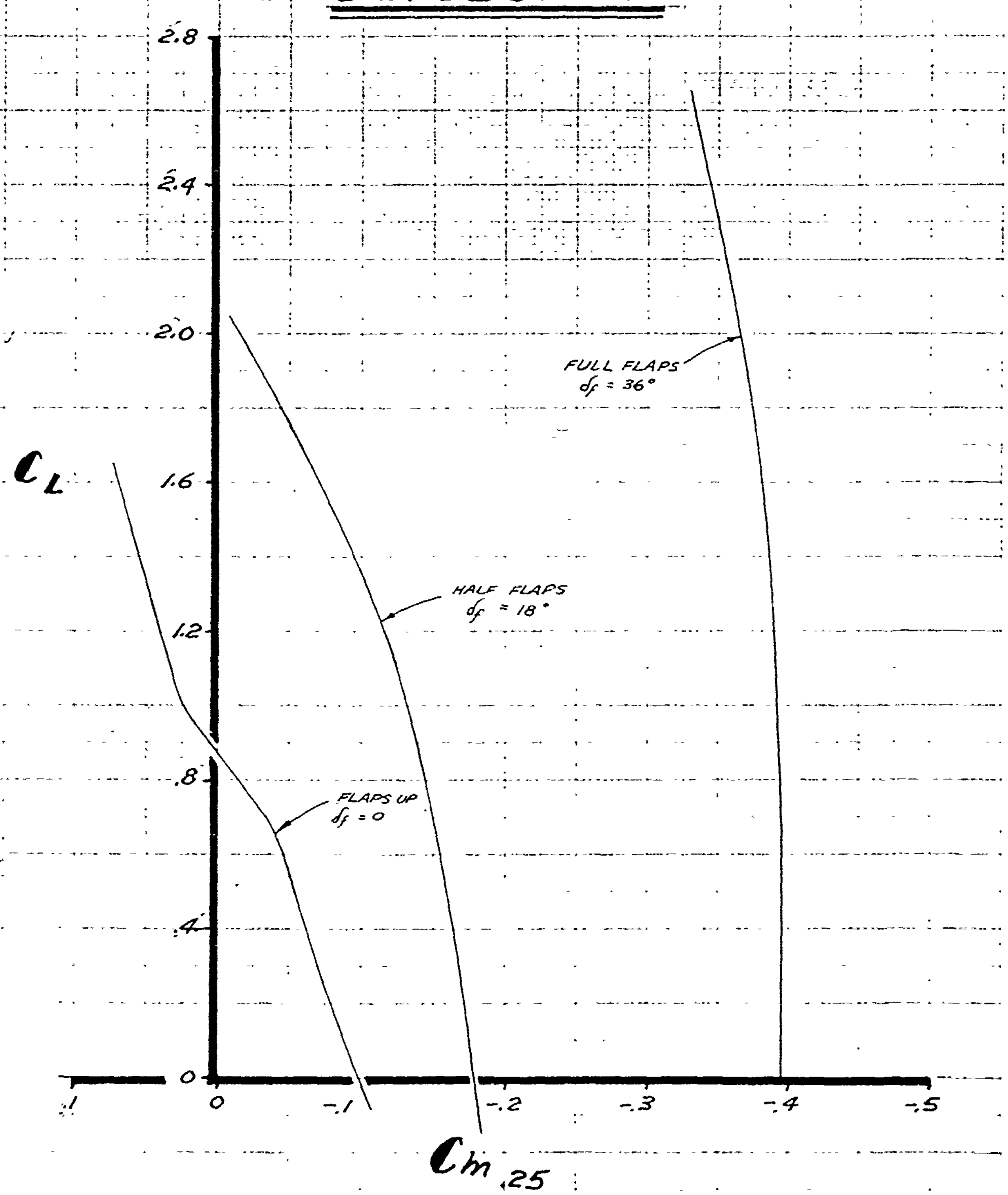

FIG. 25

LOCKHEED C-130

AIRPLANE PITCHING MOMENT CHARACTERISTICS FOR VARIOUS FLAP POSITIONS

LOW SPEED

$i_s = -1.75$ $\delta_e = 0°$
POWER OFF

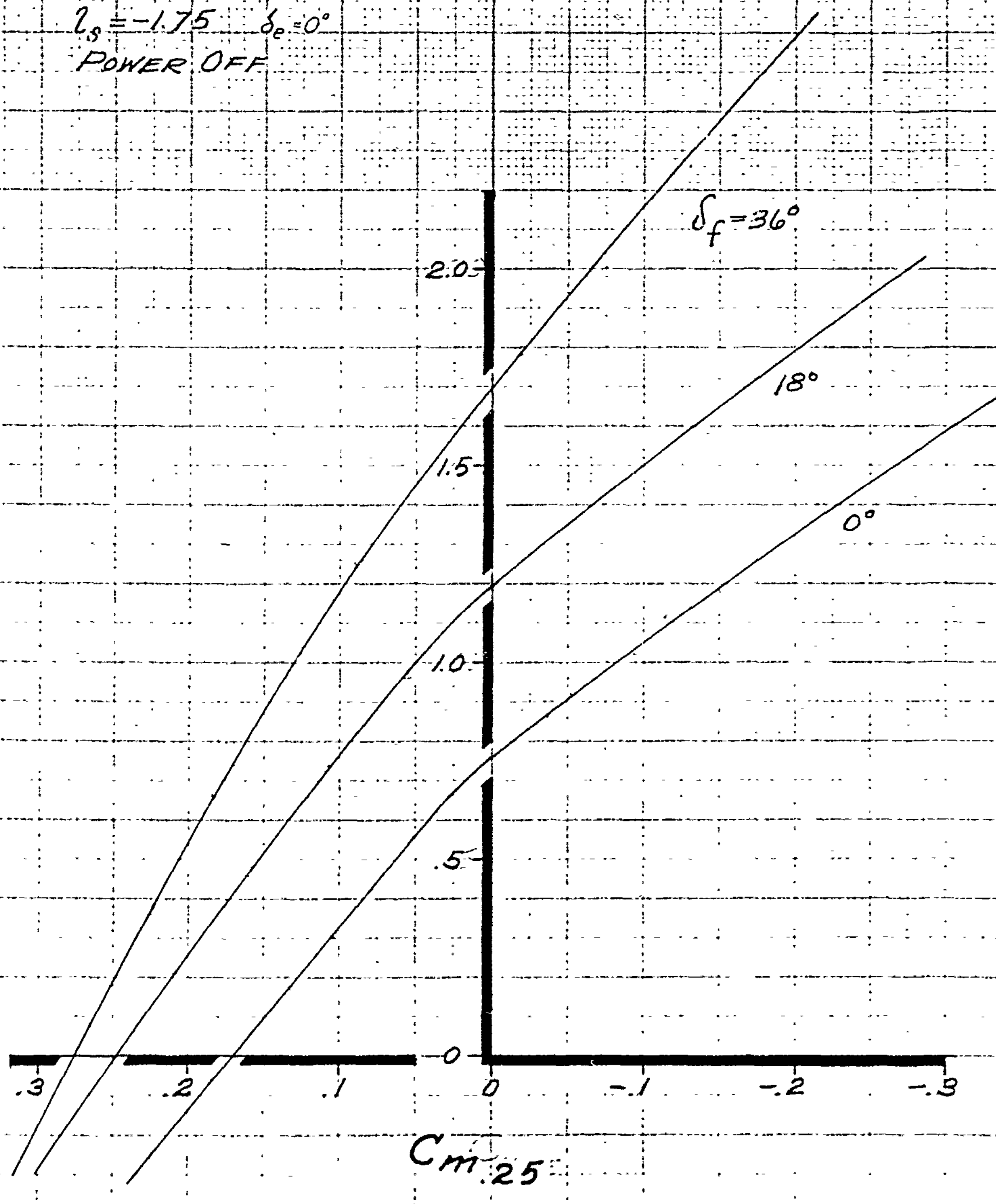

Fig. 26

LOCKHEED C-130

PITCHING MOMENTS AT SEVERAL MACH NOS. FOR WING

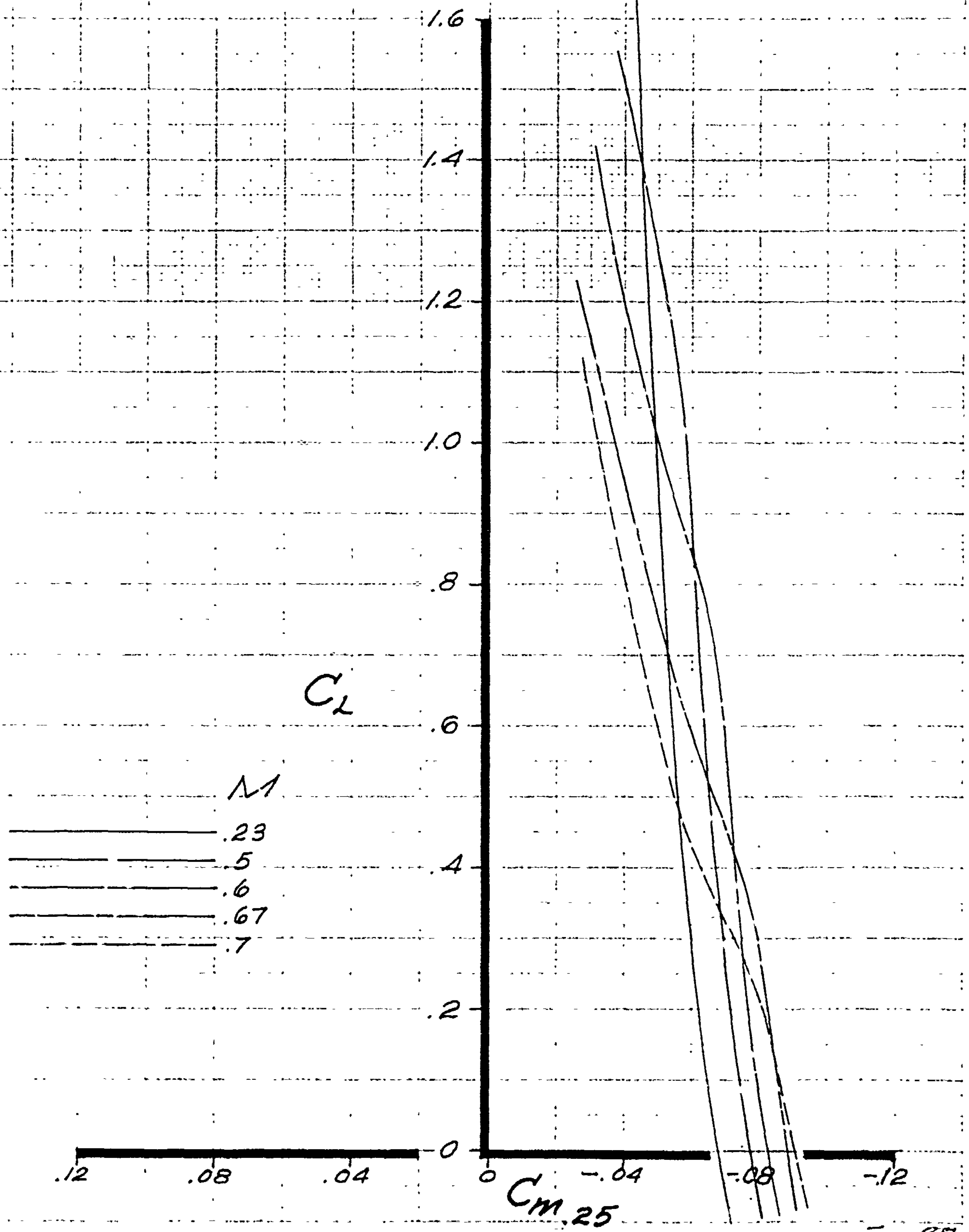

FIG. 27

LOCKHEED C-130

PITCHING MOMENT AT SEVERAL MACH NOS. FOR WING PLUS FUSELAGE

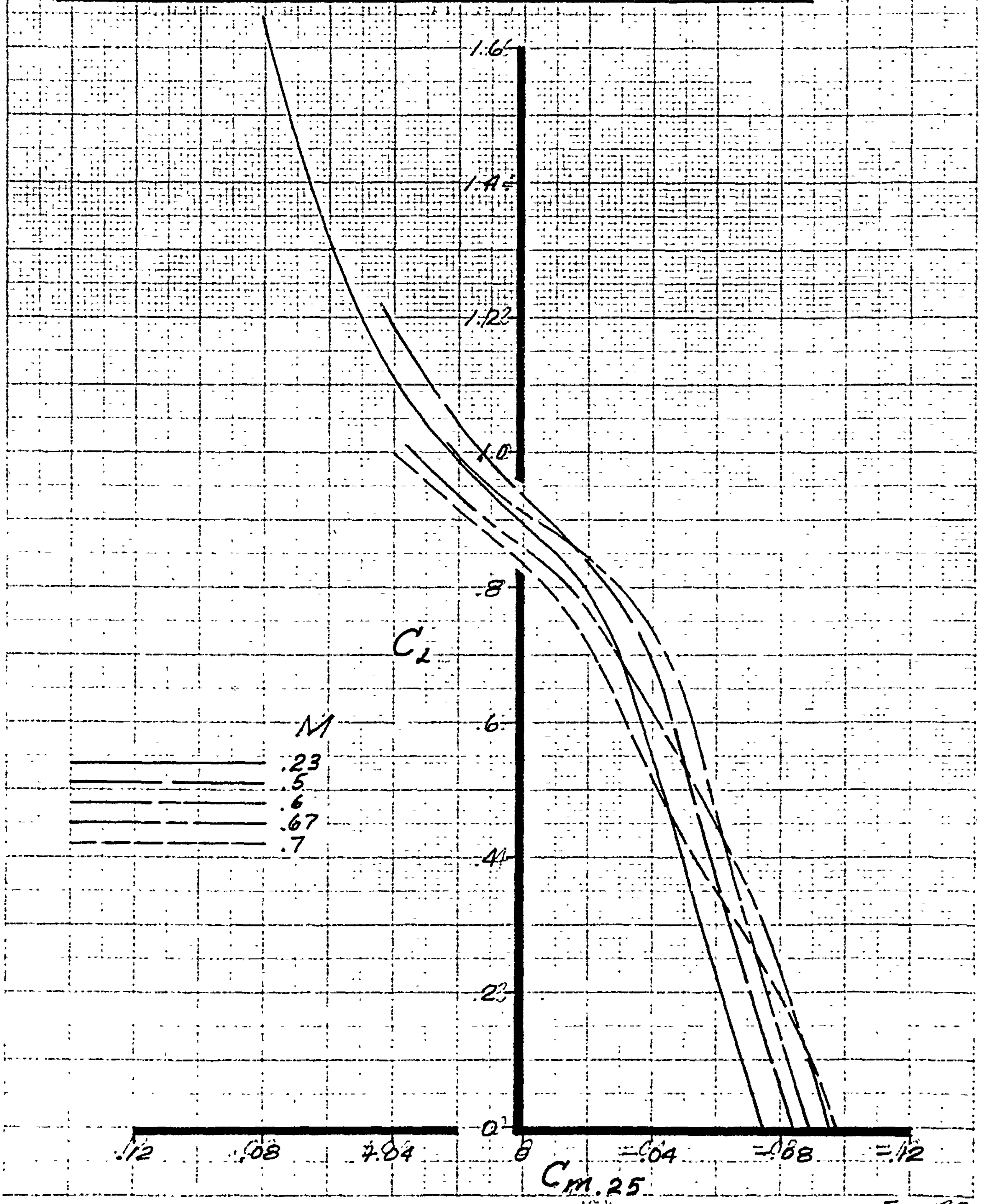

FIG. 28

LOCKHEED C-130

PITCHING MOMENT AT SEVERAL MACH NOS FOR AIRPLANE LESS EMPENNAGE

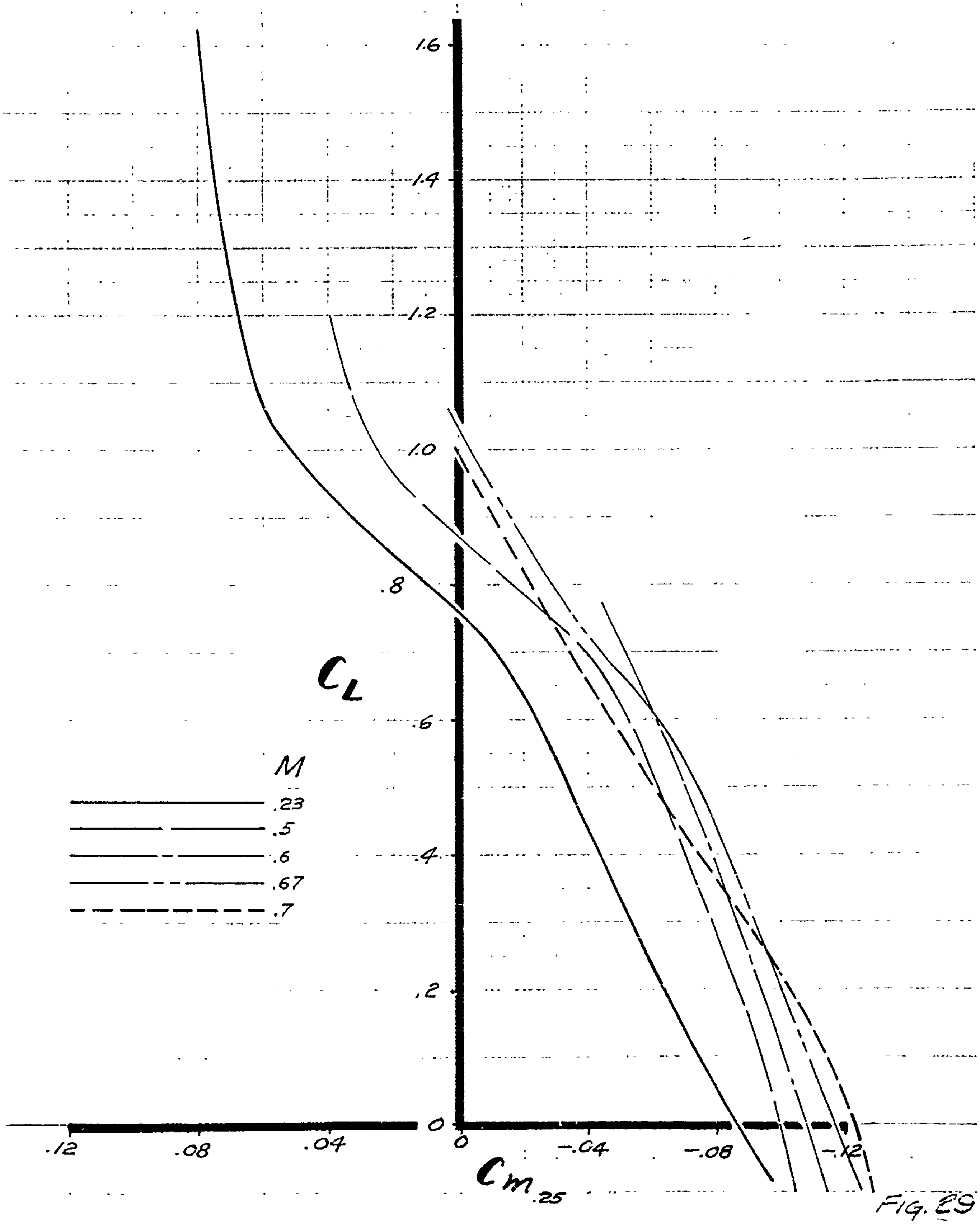

FIG. 29

LOCKHEED C-130

PITCHING MOMENT AT SEVERAL MACH NOS. FOR AIRPLANE LESS HORIZONTAL TAIL

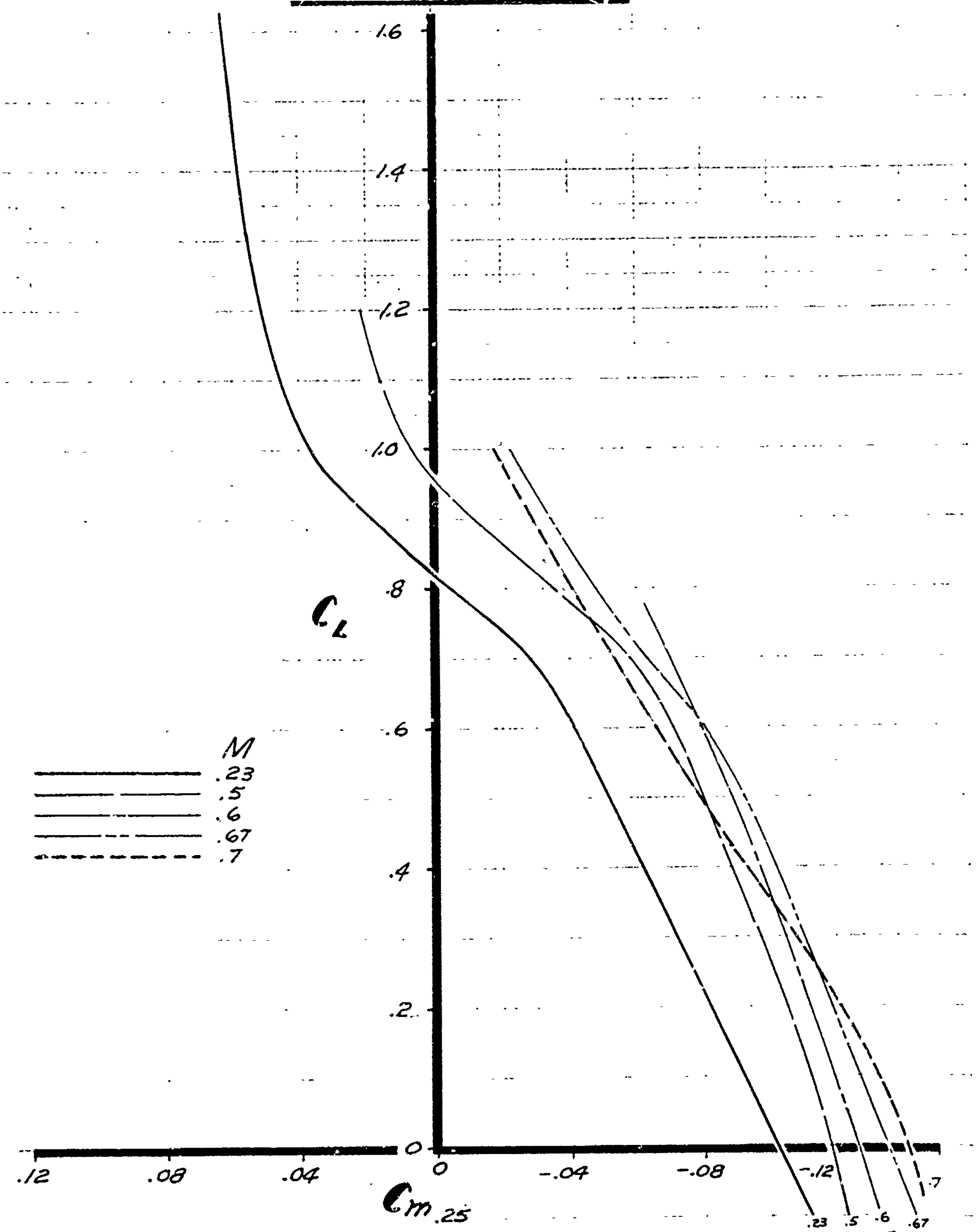

FIG. 30

LOCKHEED C-130

PITCHING MOMENTS AT SEVERAL MACH NOS FOR COMPLETE AIRPLANE

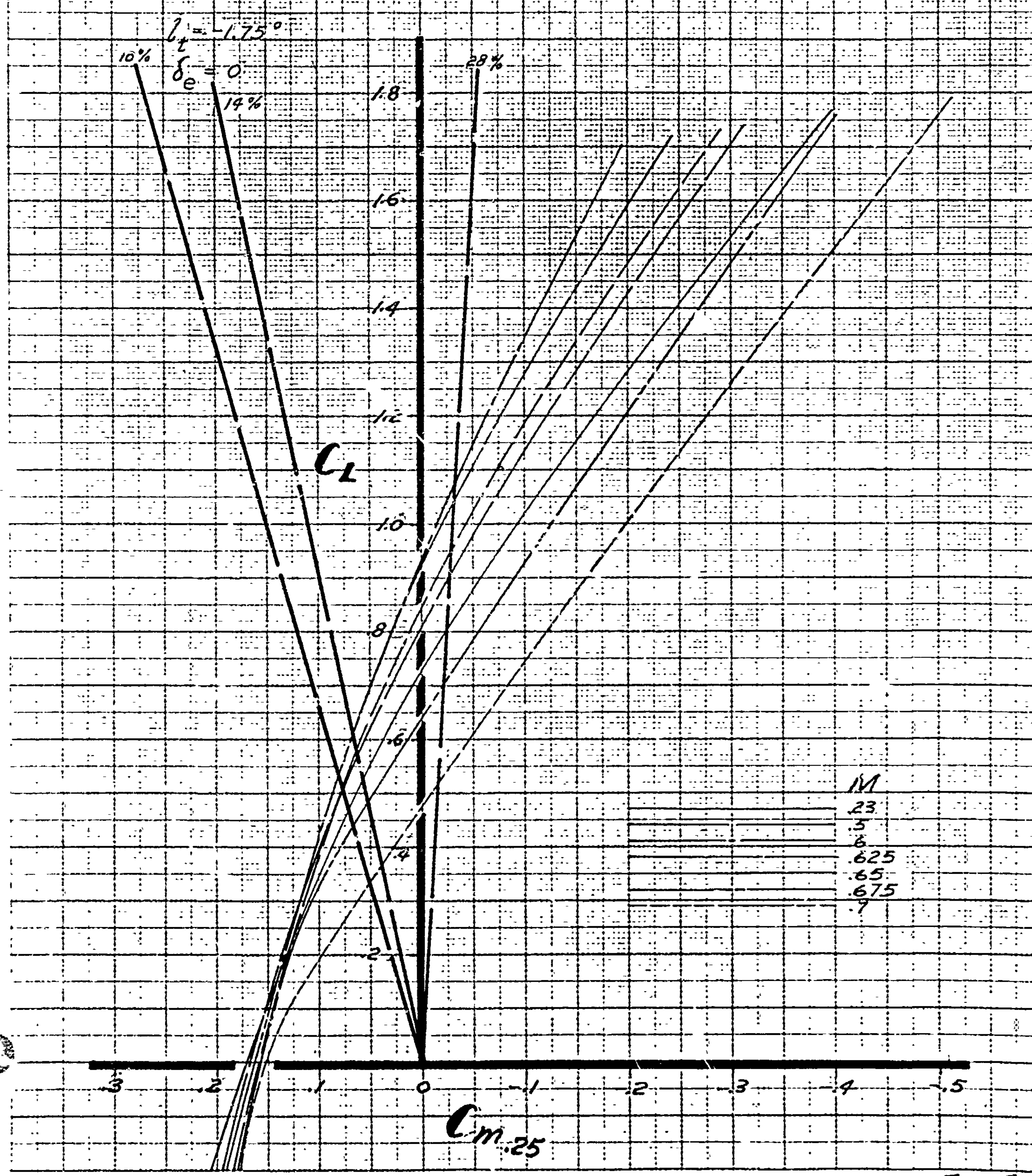

FIG. 31

PREPARED BY K.L.P.
DATE 11-21-52
CHECKED BY

LOCKHEED AIRCRAFT CORPORATION

PAGE 44
MODEL C-130
REPORT NO 9062

LOCKHEED C-130

EFFECTS OF POWER ON PITCHING CHARACTERISTICS OF AIRPLANE LESS HORIZONTAL TAIL

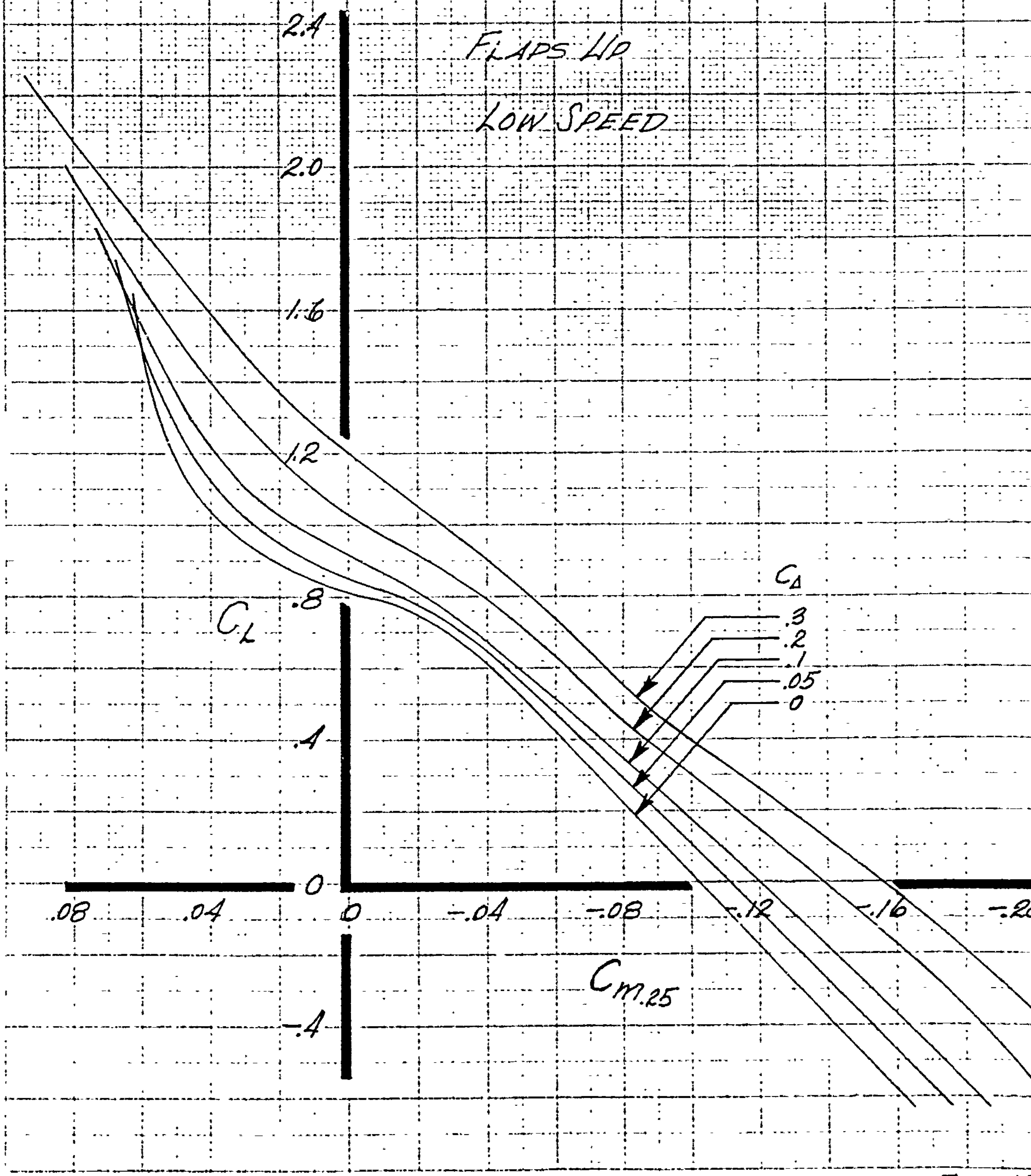

FORM 5270

FIG. 32

LOCKHEED C-130

EFFECTS OF POWER ON PITCHING CHARACTERISTICS OF AIRPLANE LESS HORIZONTAL TAIL

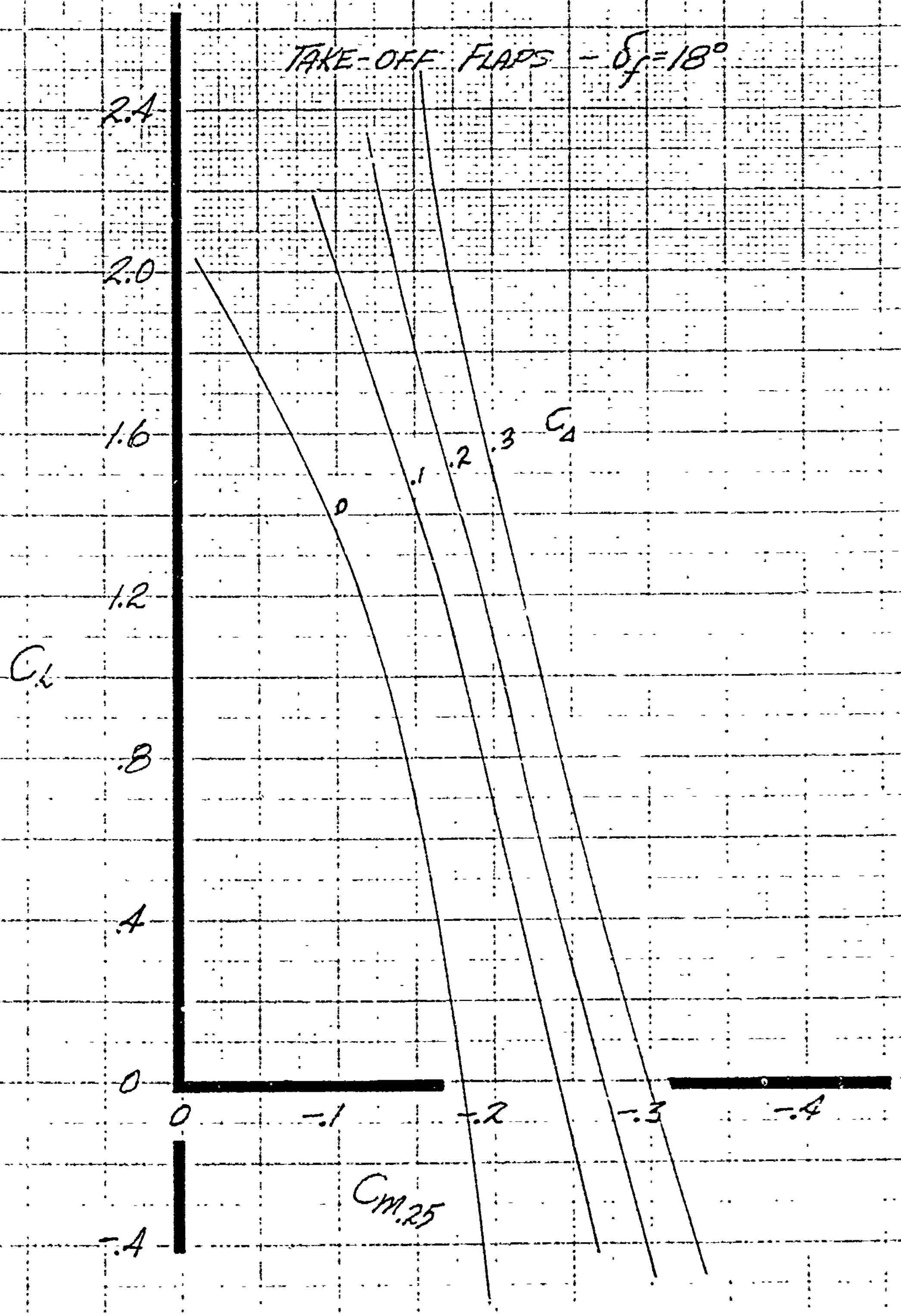

PREPARED BY	R.L.D.
DATE	11-25-52
CHECKED BY	

LOCKHEED AIRCRAFT CORPORATION

PAGE	46
MODEL	C-130
REPORT NO	9062

LOCKHEED C-130
EFFECTS OF POWER ON PITCHING CHARACTERISTICS OF AIRPLANE LESS HORIZONTAL TAIL

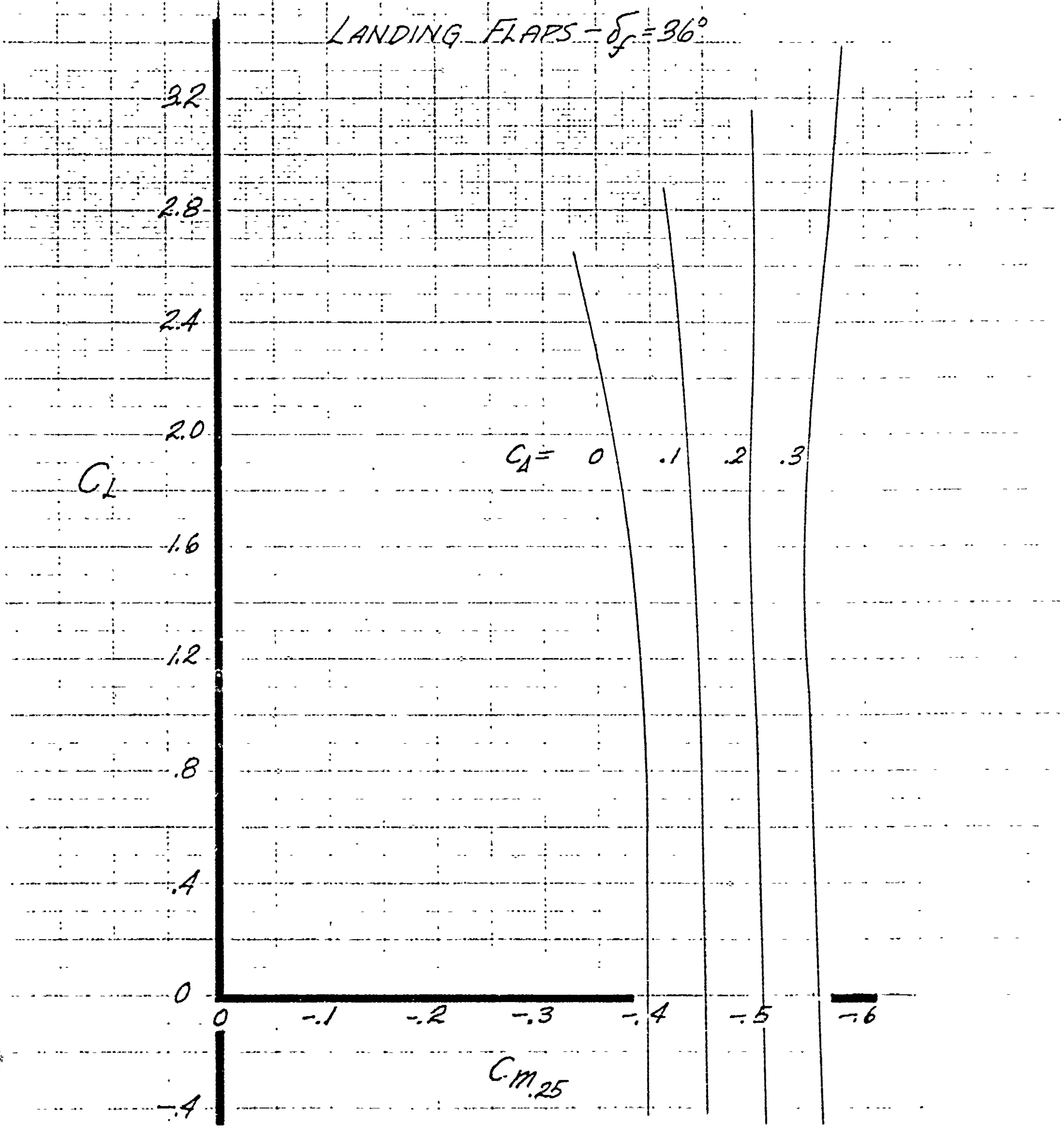

FORM 3278A

FIG. 34

LOCKHEED C-130

POWER EFFECTS ON AIRPLANE PITCHING MOMENT COEFFICIENTS

LOW SPEED

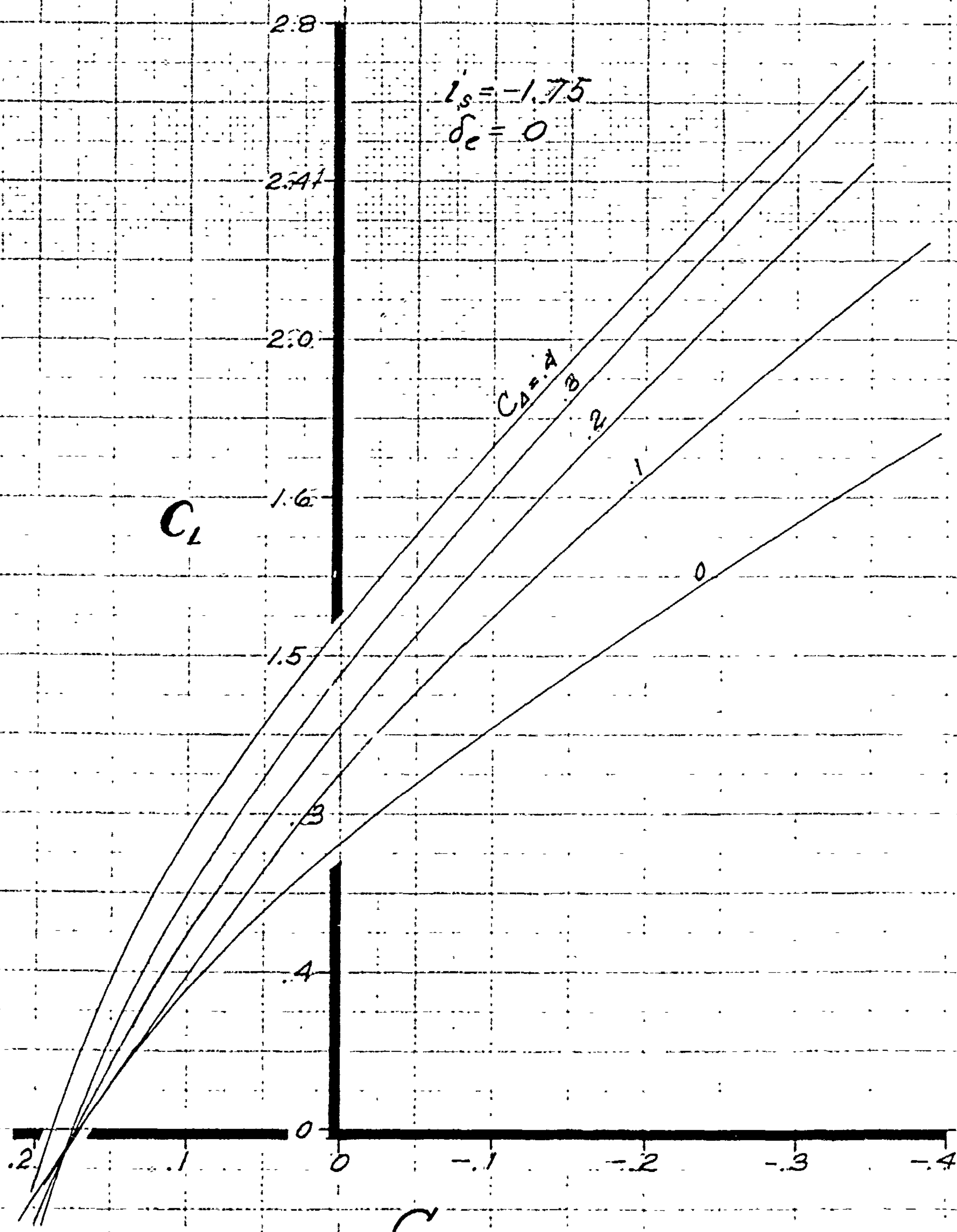

FIG 35

LOCKHEED C-130

EFFECTS OF POWER ON PITCH CHARACTERISTICS OF AIRPLANE

FLAPS DOWN 36°

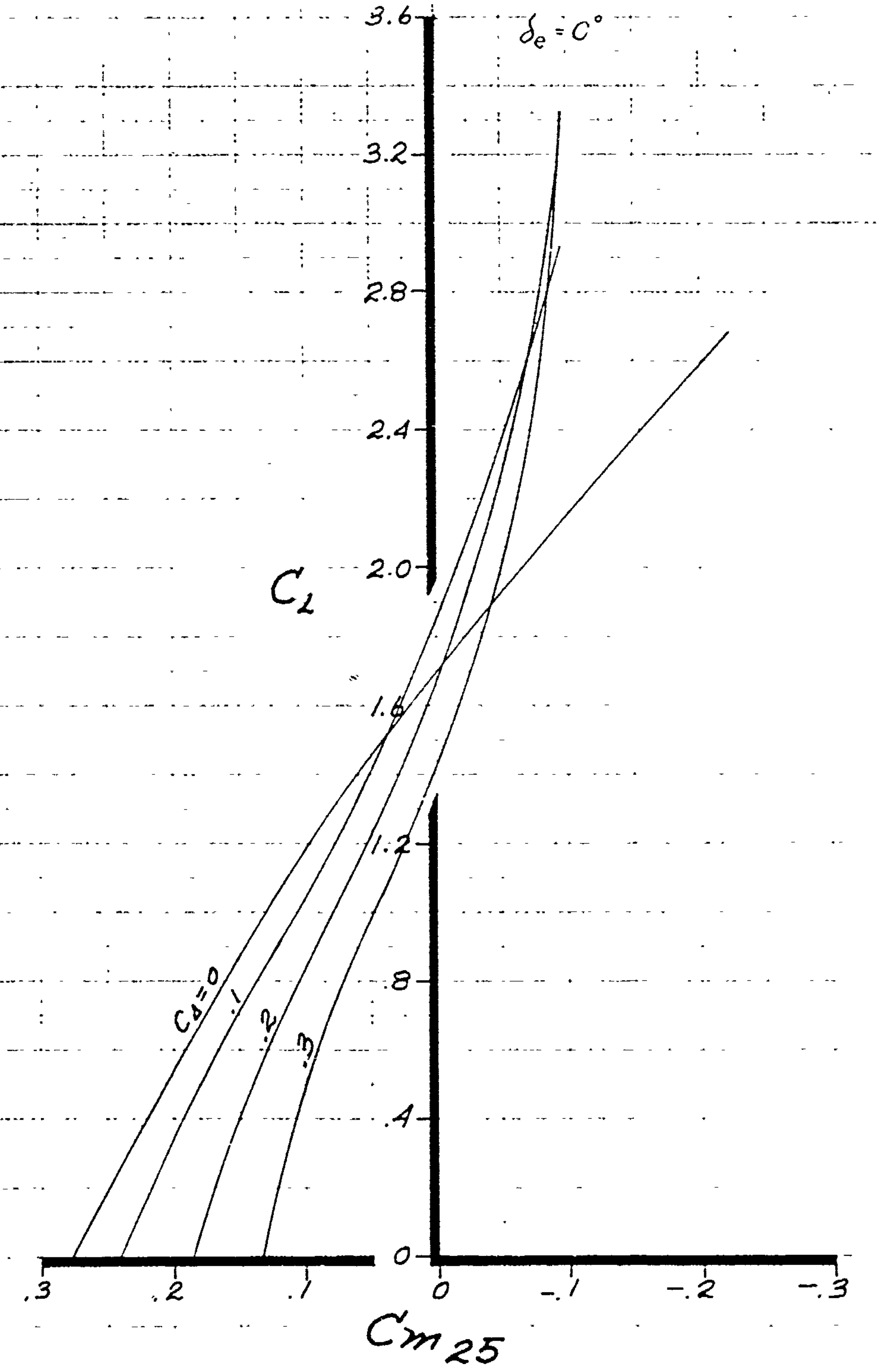

Fig. 36

LOCKHEED C-130

ELEVATOR EFFECTIVENESS

LOW SPEED

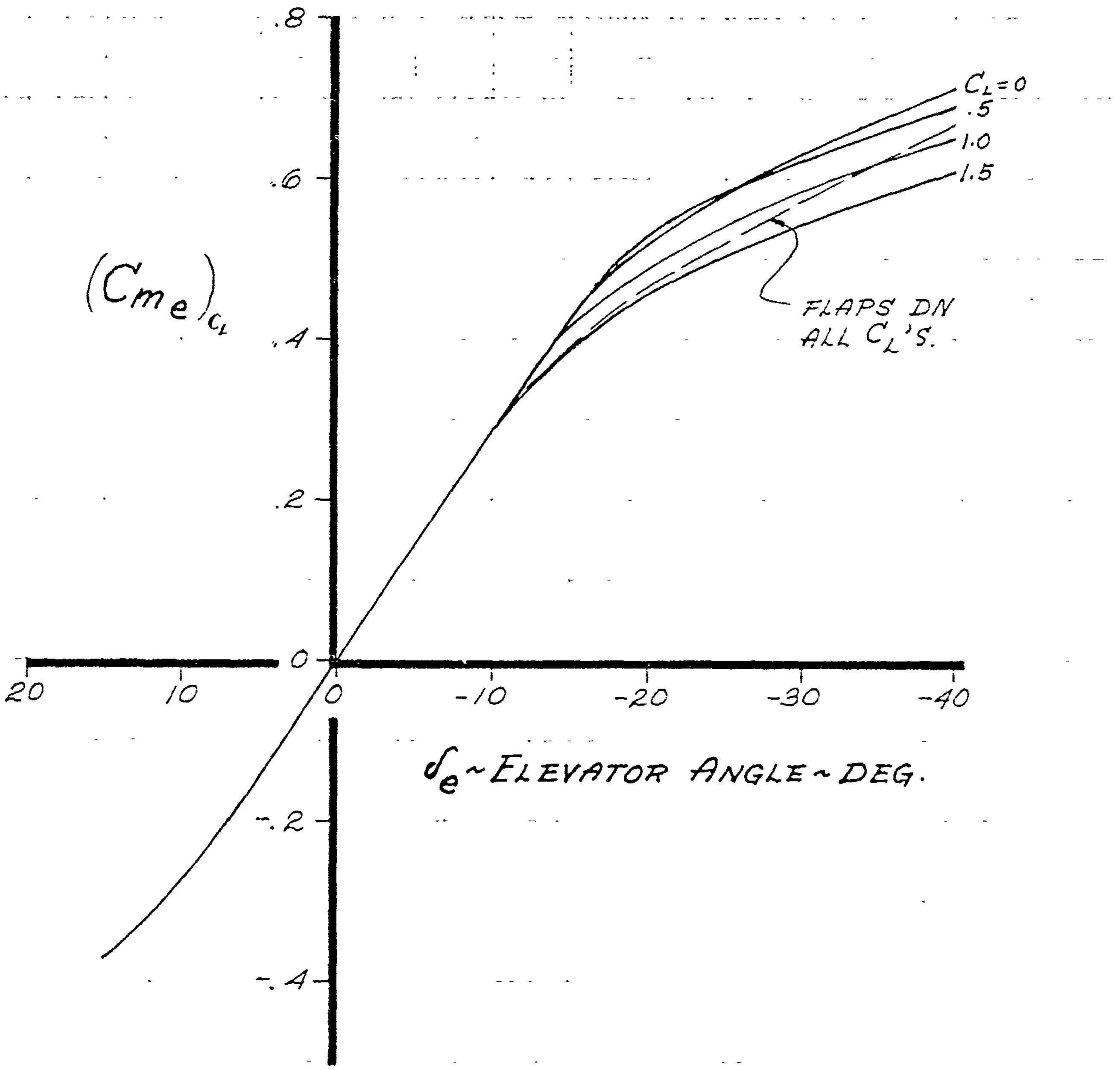

LOCKHEED C-130

VARIATION OF ELEVATOR EFFECTIVENESS WITH MACH NO

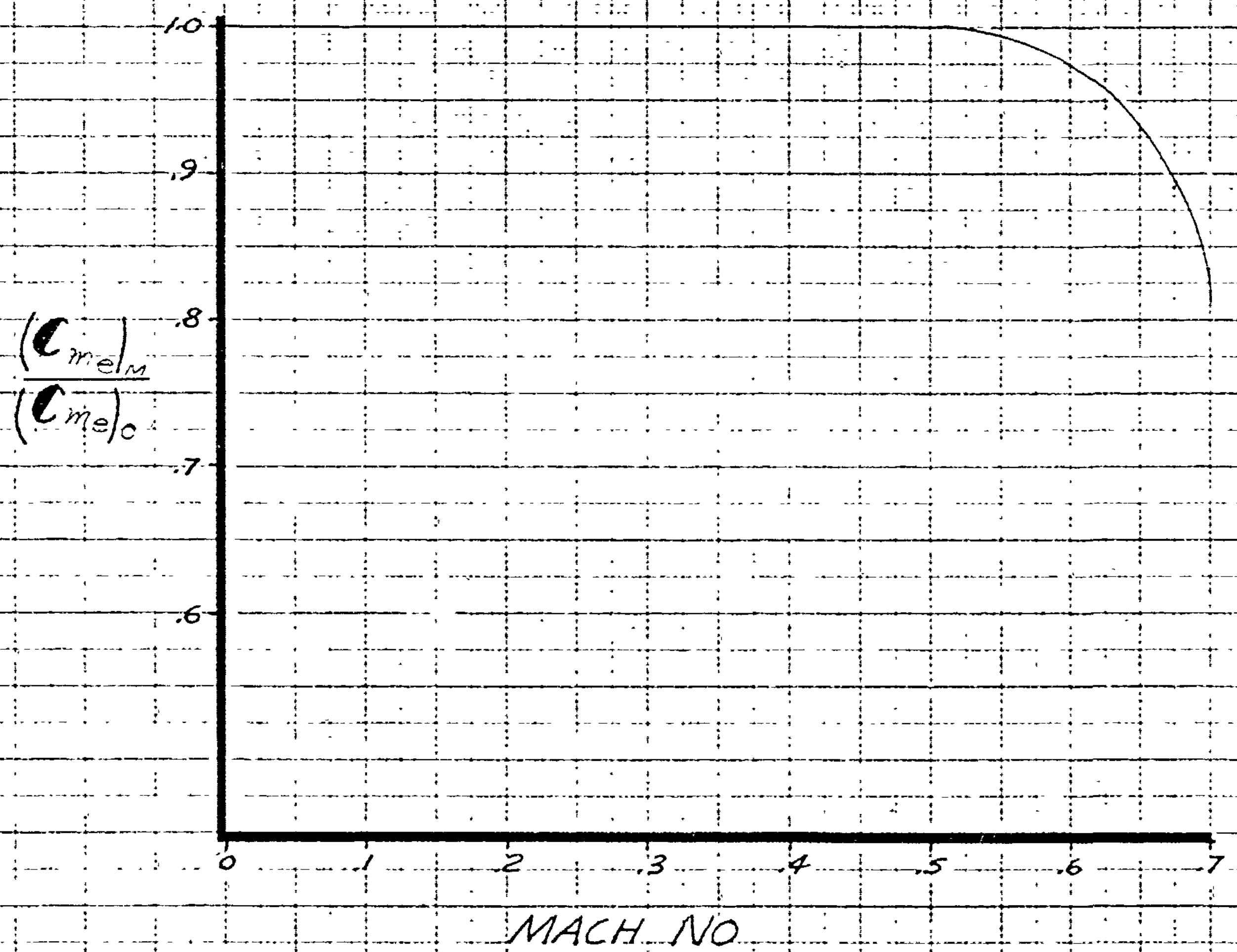

FIG 38

LOCKHEED C-130

ELEVATOR HINGE MOMENT CHARACTERISTICS

LOW SPEED - FLAPS UP

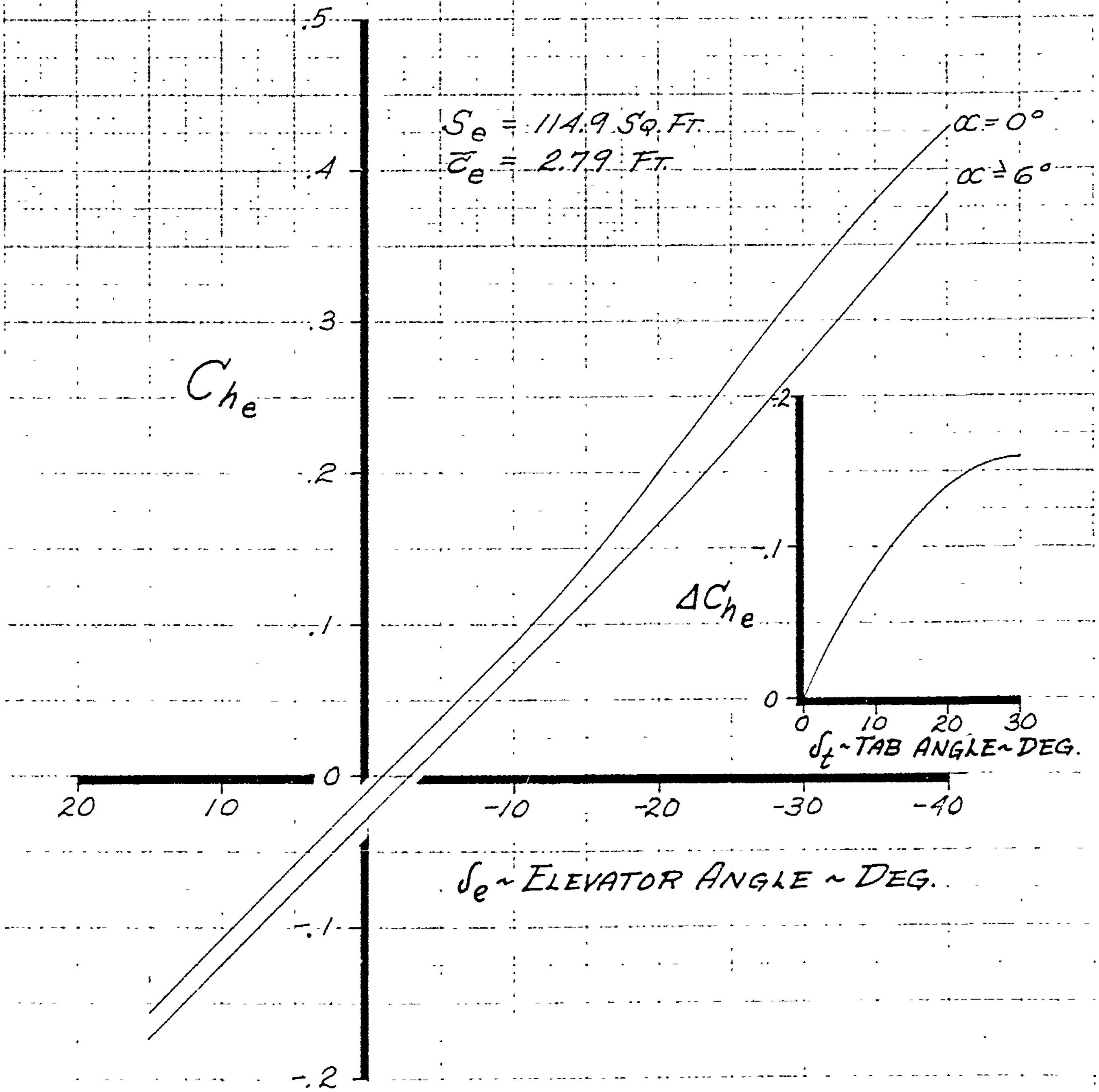

LOCKHEED C-130

ELEVATOR HINGE MOMENT CHARACTERISTICS

LOW SPEED FLAPS DOWN

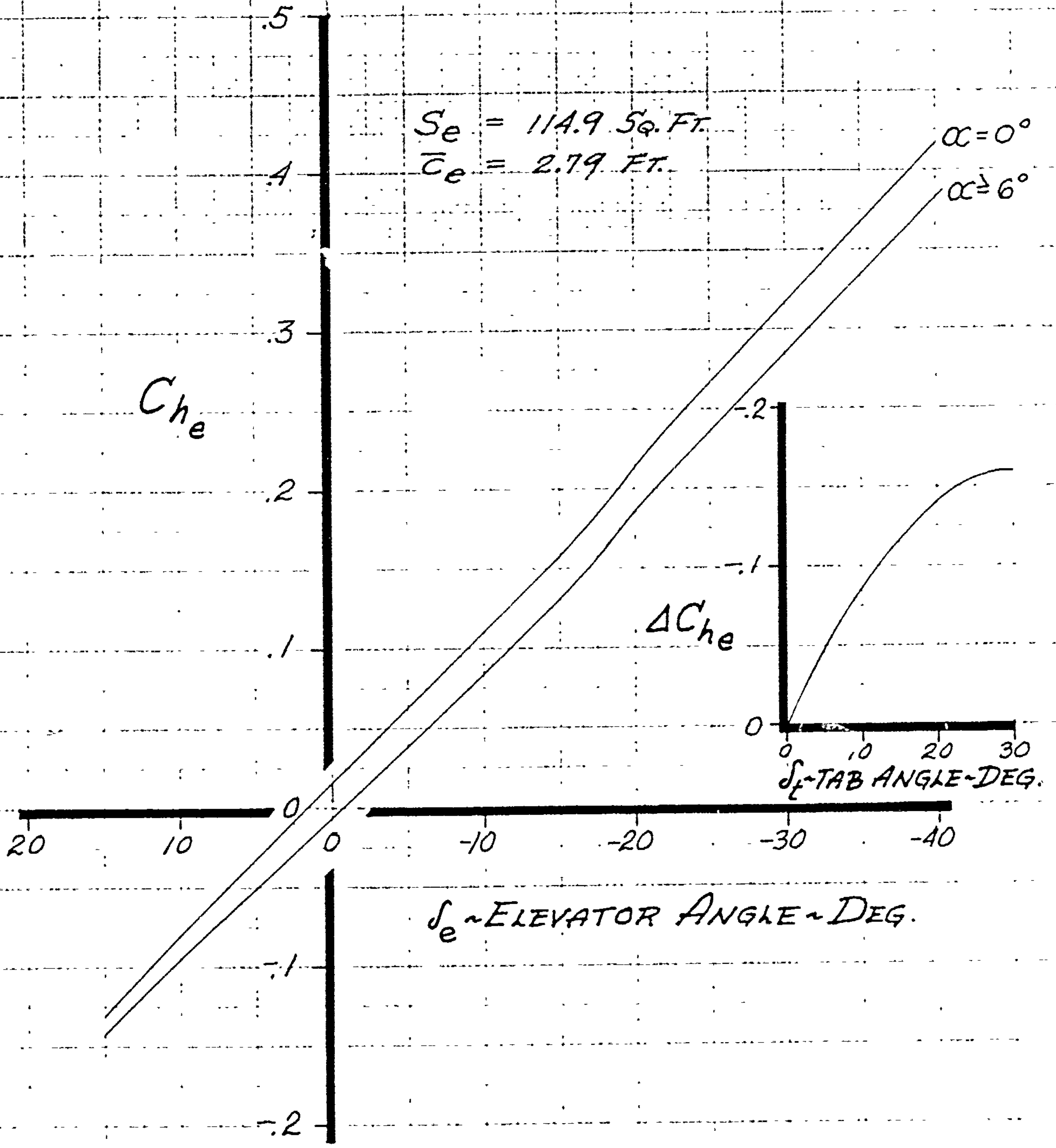

FORM 5270

FIG. 40

DIRECTIONAL AERODYNAMIC CHARACTERISTICS

Directional aerodynamic characteristics for the airplane and airplane build-up are obtained principally from the test results of refs. 1, 2 and 3. Where data from any other source is used, proper reference is made in the test.

SIDE FORCE CHARACTERISTICS

Variations of side force coefficient with yaw angle for the airplane build-up for low speeds is given in fig. 41. From many test results it has been ascertained that airplane less tail side force characteristics do not change appreciably with increasing Mach No., but that the force on the vertical tail varies according to the Prandtl-Glauert relation. Effect of compressibility on airplane side force and vertical tail normal force has been determined on this basis, and is presented in fig. 47. Effects of power on airplane side force with and without the vertical tail are given in fig. 42 as obtained from wind tunnel test results. As with other power effects, these are not subject to compressibility correction but should be added as increments to corrected power-off values. The manner of determining power effects from tunnel test is discussed in the section on pitching moment characteristics on pg. 14.

YAWING MOMENT CHARACTERISTICS

The variation of yawing moment coefficient with yaw angle for the airplane build-up is given in fig. 44 for low speeds. These curves are applicable to all flap settings. As is the case with side force, effects of compressibility are confined to the contribution of the vertical tail, and the effects of Mach Number on airplane directional stability, power-off, presented in fig. 47 are determined on that basis. Power effects for flaps retracted and extended are presented in figs. 45 and 46 to be used as increments applied to data corrected for compressibility. See the discussion of power effects on pitching moment characteristics, pg. 14, for the manner of obtaining all power effects.

RUDDER CHARACTERISTICS

Rudder effectiveness, including tabs, is presented in fig. 48 for all flap settings. Rudder hinge moment coefficient characteristics are shown in fig. 49, including trim tab effects. The values for zero yaw angle are obtained directly from wind tunnel tests, while effects of yaw angle are inferred from rudder floating characteristics observed in the tunnel and comparison with other similar surfaces. For the range of Mach Numbers in which critical design air loads will be produced, there are no changes in any of the aerodynamic characteristics of the rudder. The characteristics of the rudder control and boost system are shown in figs. 80 through 83, including a plot of the variation of rudder pedal force with rudder hinge moment.

PREPARED BY R.L.D.
DATE 6-17-52
CHECKED BY

LOCKHEED AIRCRAFT CORPORATION

PAGE 55
MODEL C-130
REPORT NO. 9062

LOCKHEED C-130

SIDE FORCE CHARACTERISTICS

LOW SPEED

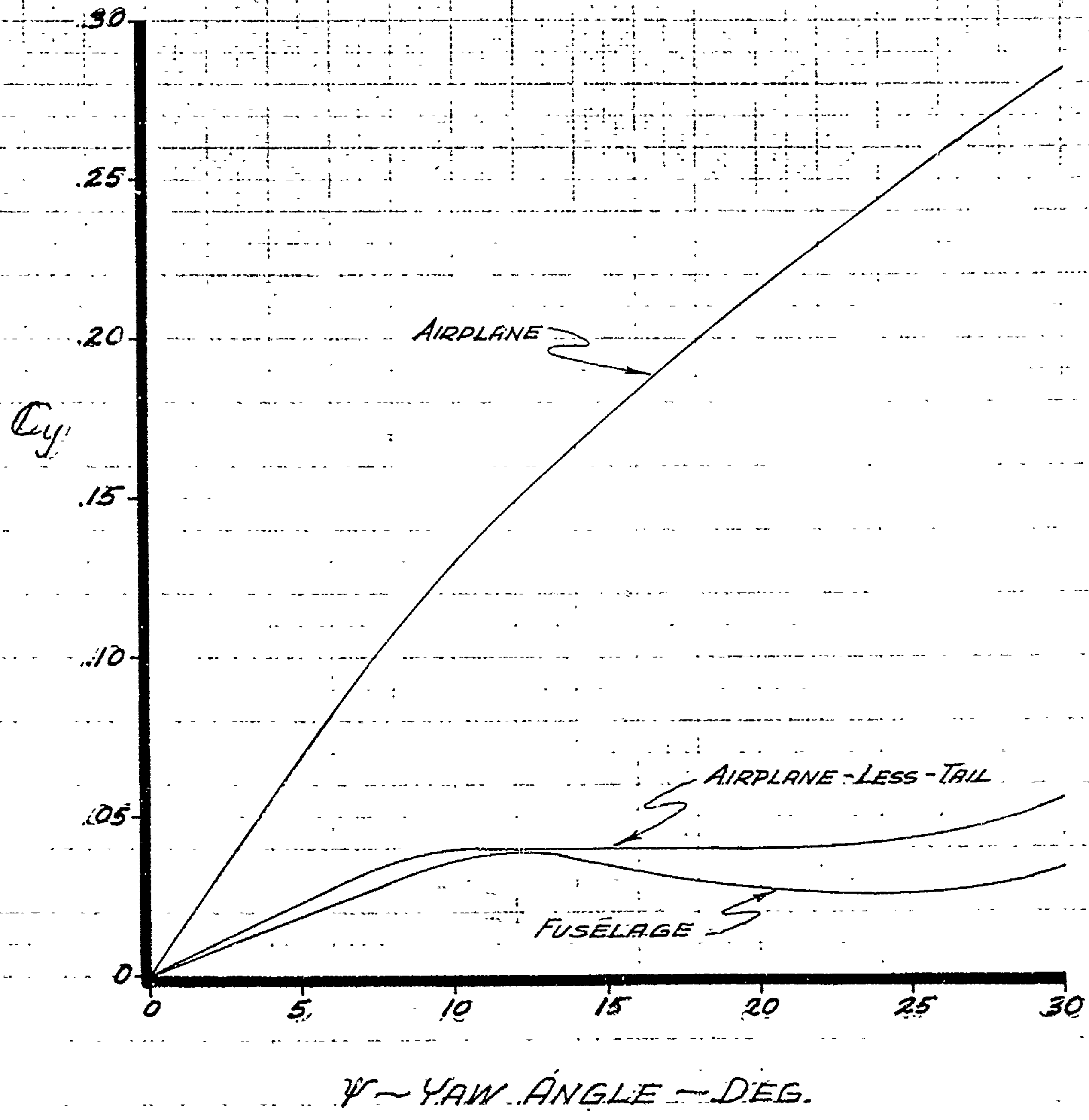

FORM 5278A

FIG. 41

PREPARED BY R.L.D.
DATE 12-11-52
CHECKED BY

LOCKHEED AIRCRAFT CORPORATION

LOCKHEED C-130

EFFECTS OF POWER ON AIRPLANE SIDE FORCE CHARACTERISTICS

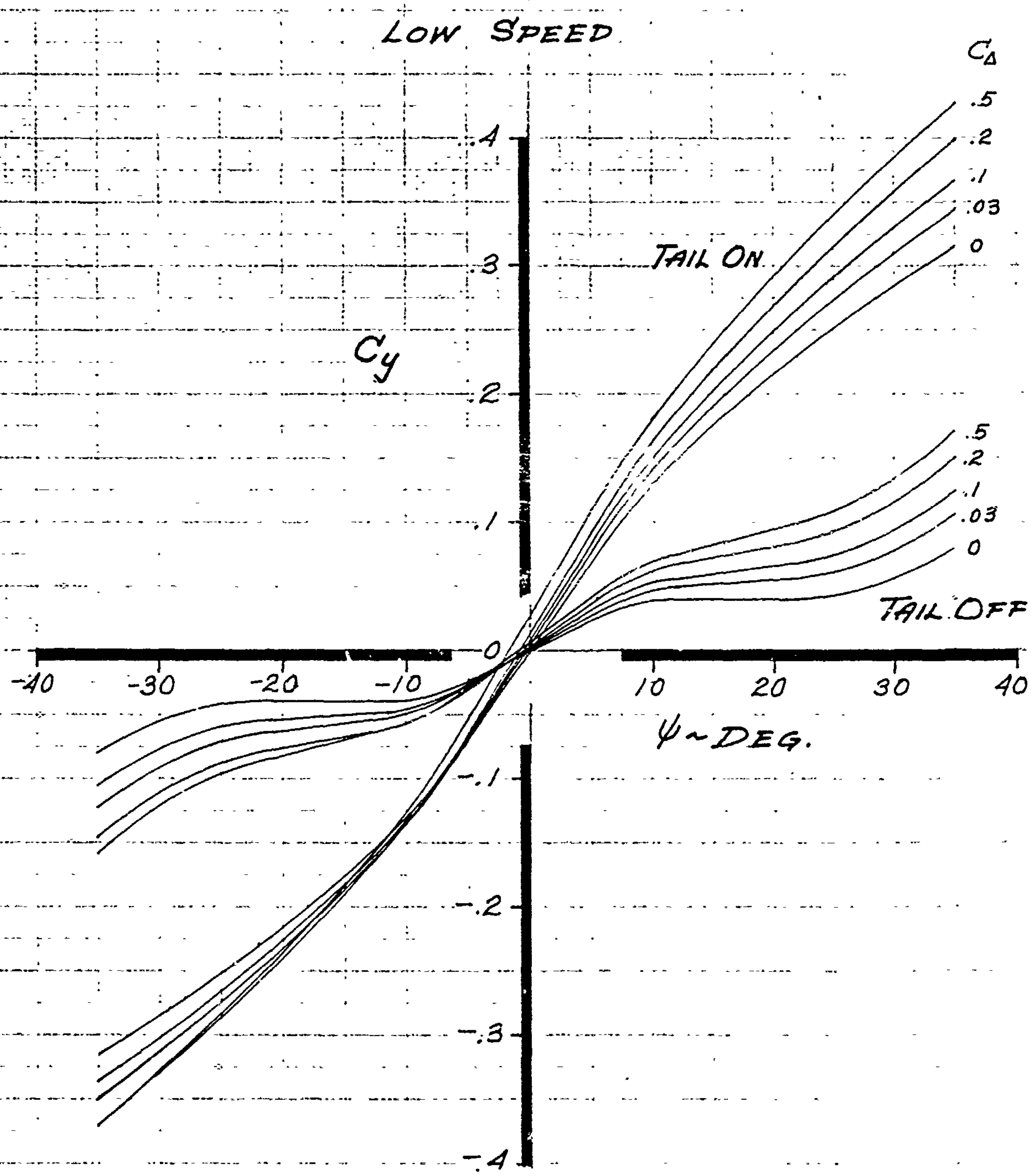

FIG. 42

LOCKHEED C-130

EFFECTS OF POWER ON AIRPLANE SIDE FORCE CHARACTERISTICS

LANDING FLAPS

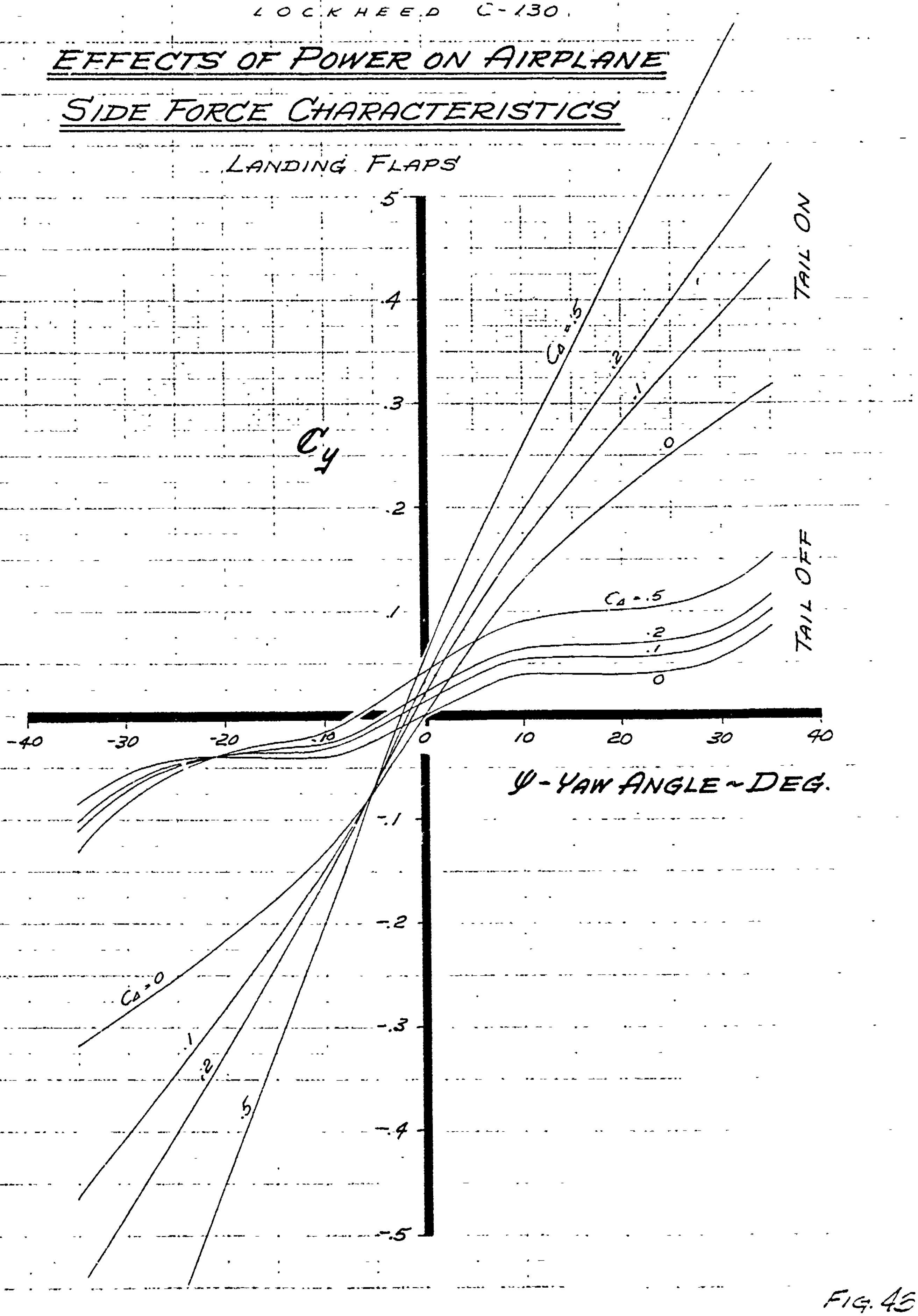

FIG. 45

PREPARED BY R.L.D.
DATE 6-13-52
CHECKED BY

LOCKHEED AIRCRAFT CORPORATION

PAGE 58
MODEL C-130
REPORT NO. 9062

LOCKHEED C-130

YAWING MOMENT CHARACTERISTICS

LOW SPEED

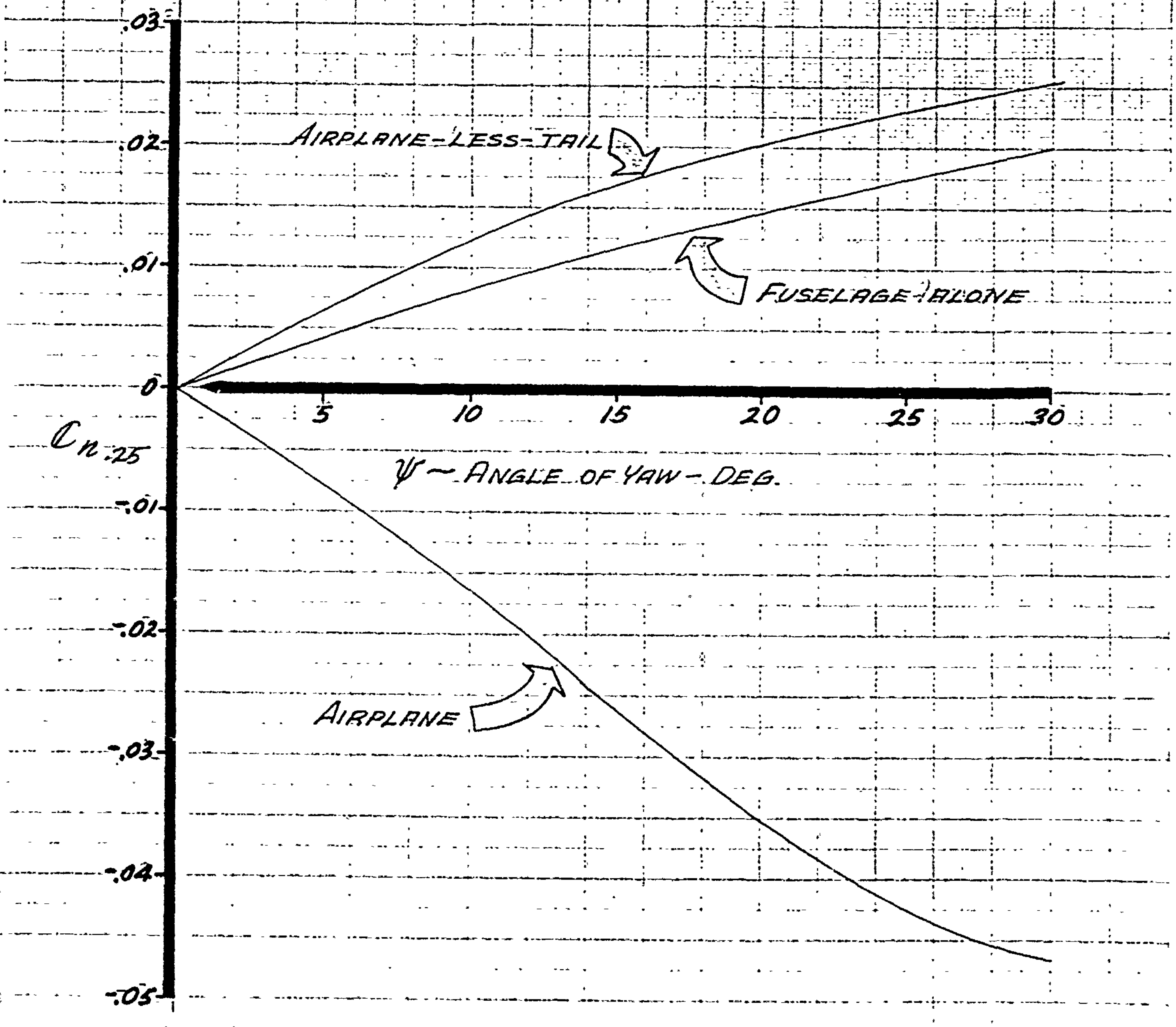

FORM 3278A

FIG. 44

PREPARED BY R.L.D.
DATE 12-8-52
CHECKED BY

LOCKHEED AIRCRAFT CORPORATION

LOCKHEED C-130

EFFECTS OF POWER ON CHARACTERISTICS IN YAW OF AIRPLANE WITH/WITHOUT TAIL

LOW SPEED

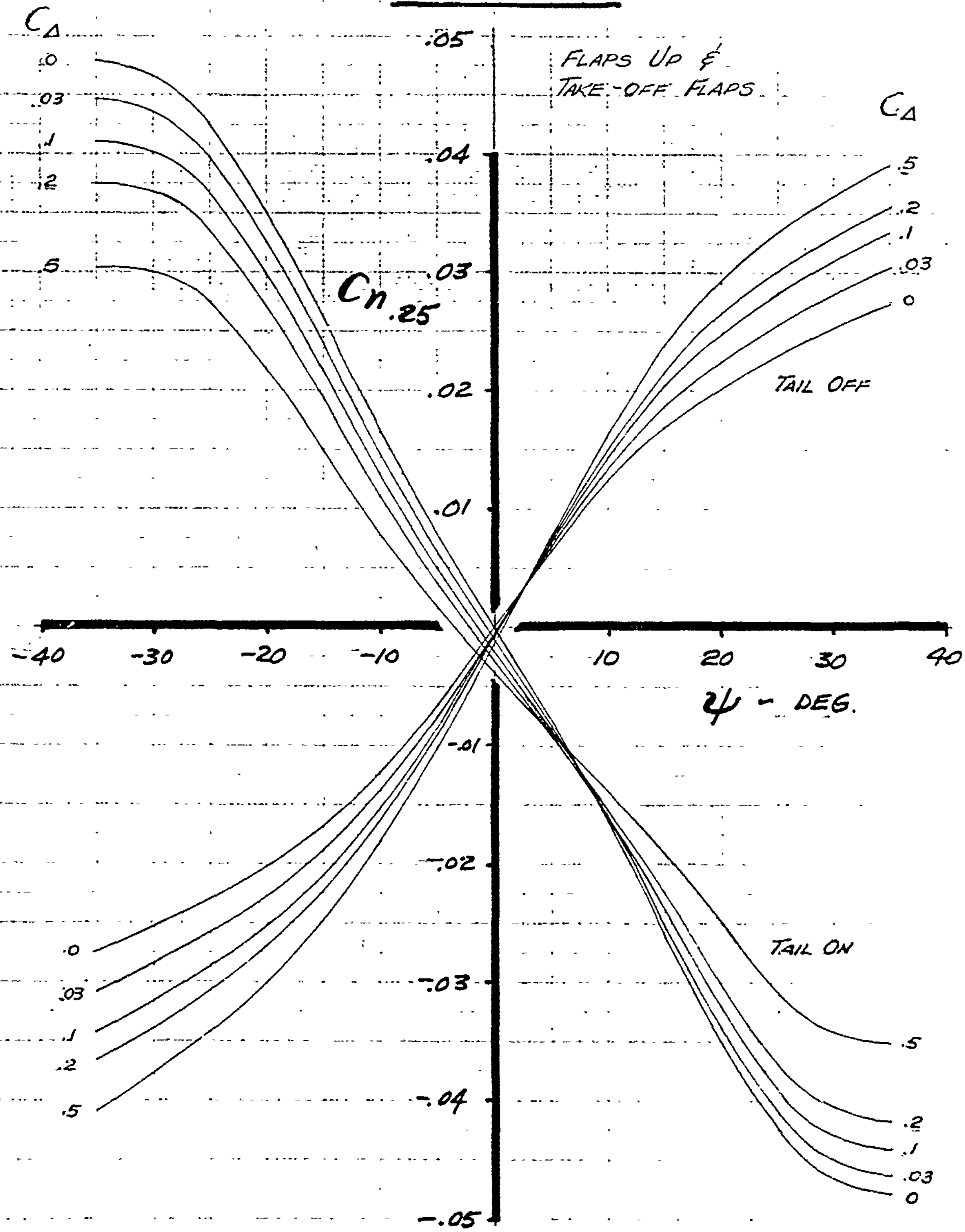

FORM 5278A

FIG. 45

LOCKHEED C-130

EFFECTS OF POWER ON AIRPLANE YAWING MOMENT CHARACTERISTICS

LANDING FLAPS

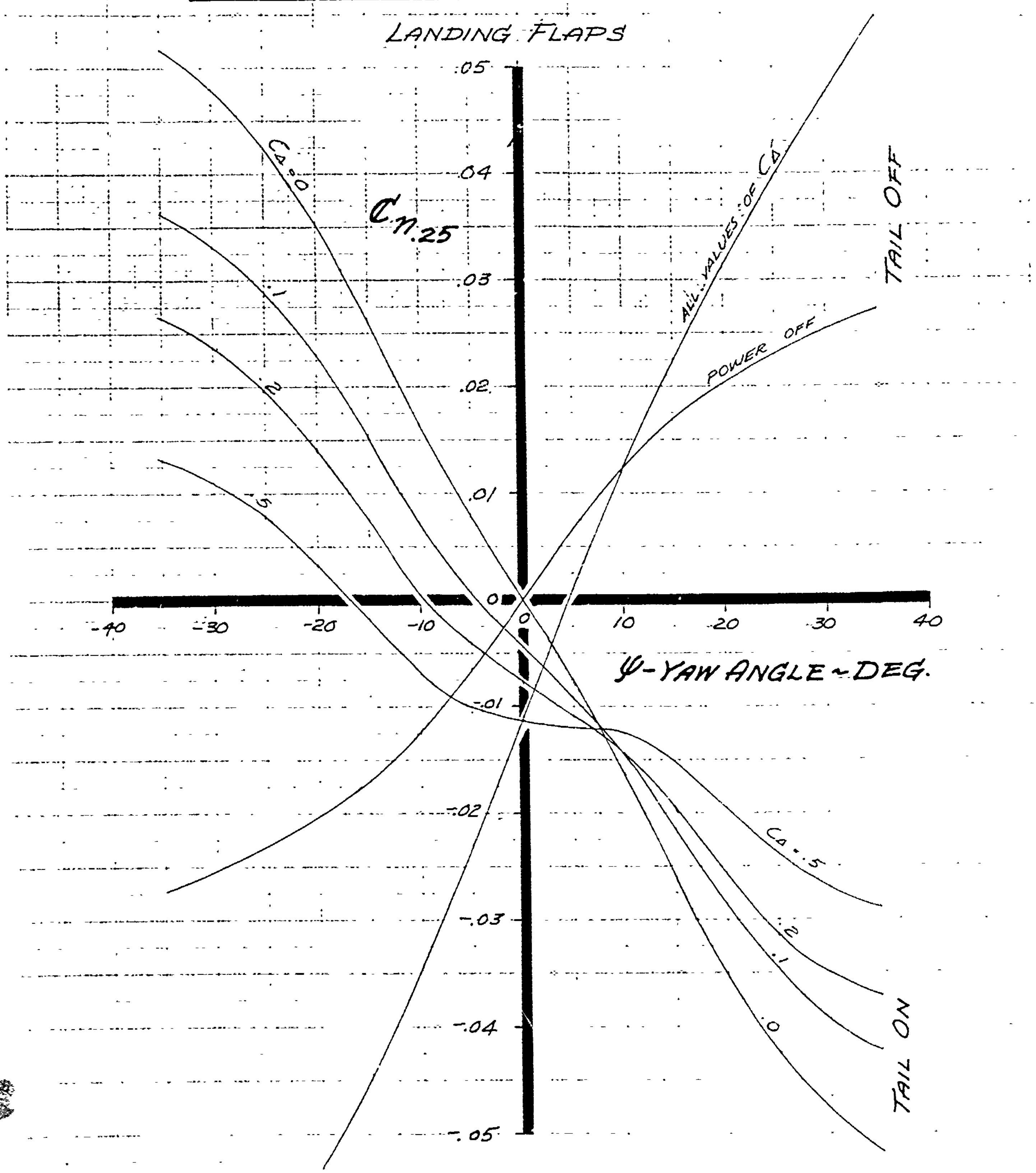

FIG. 46

LOCKHEED C-130

VARIATION OF AIRPLANE YAWING CHARACTERISTICS WITH MACH NO.

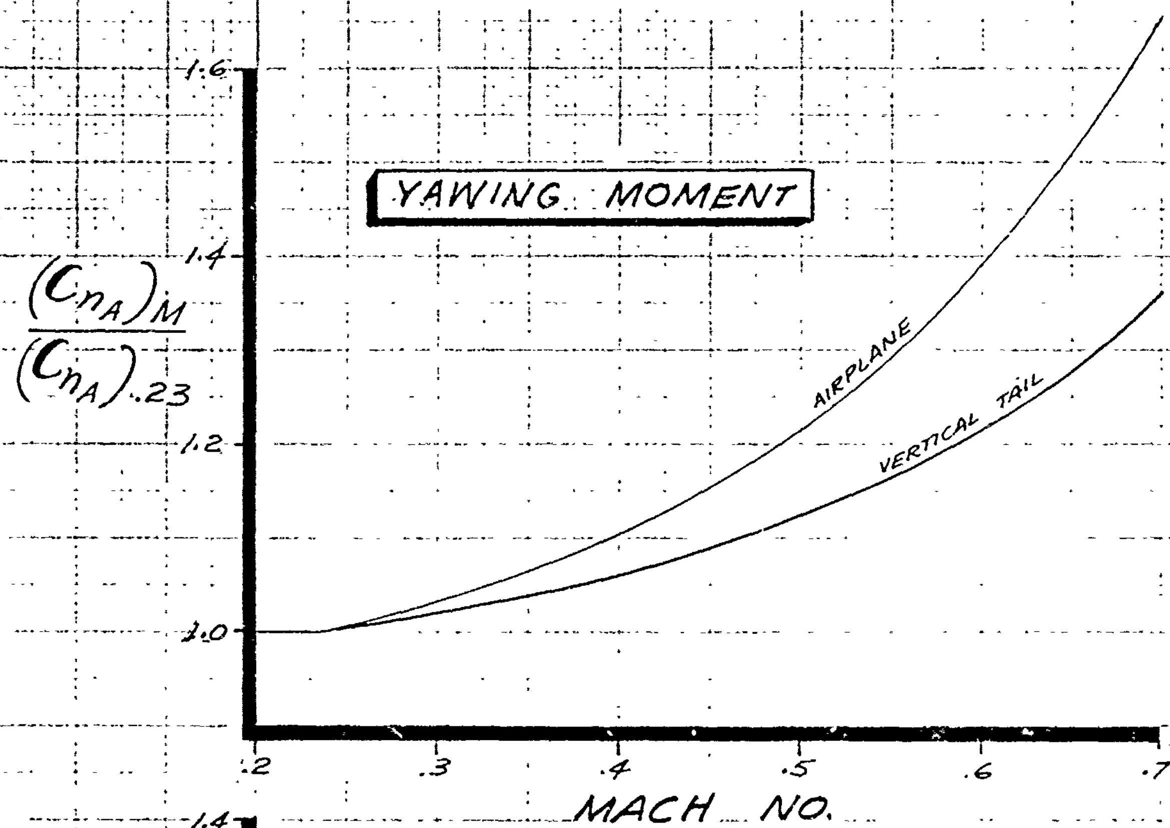

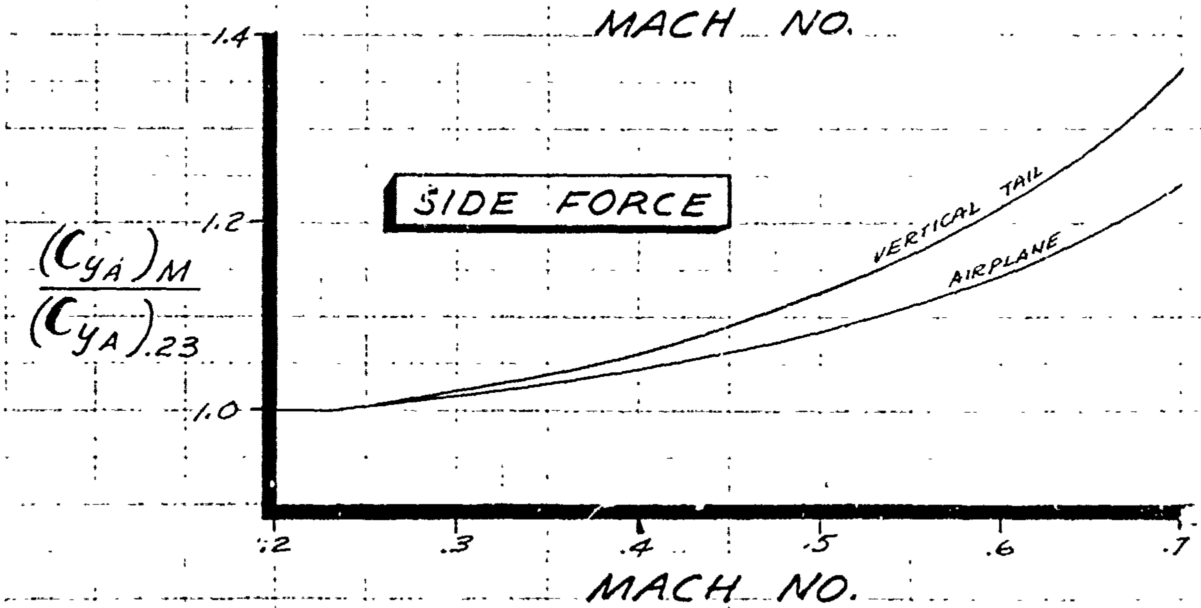

FIG. 47

LOCKHEED C-130

RUDDER EFFECTIVENESS CHARACTERISTICS

LOW SPEED

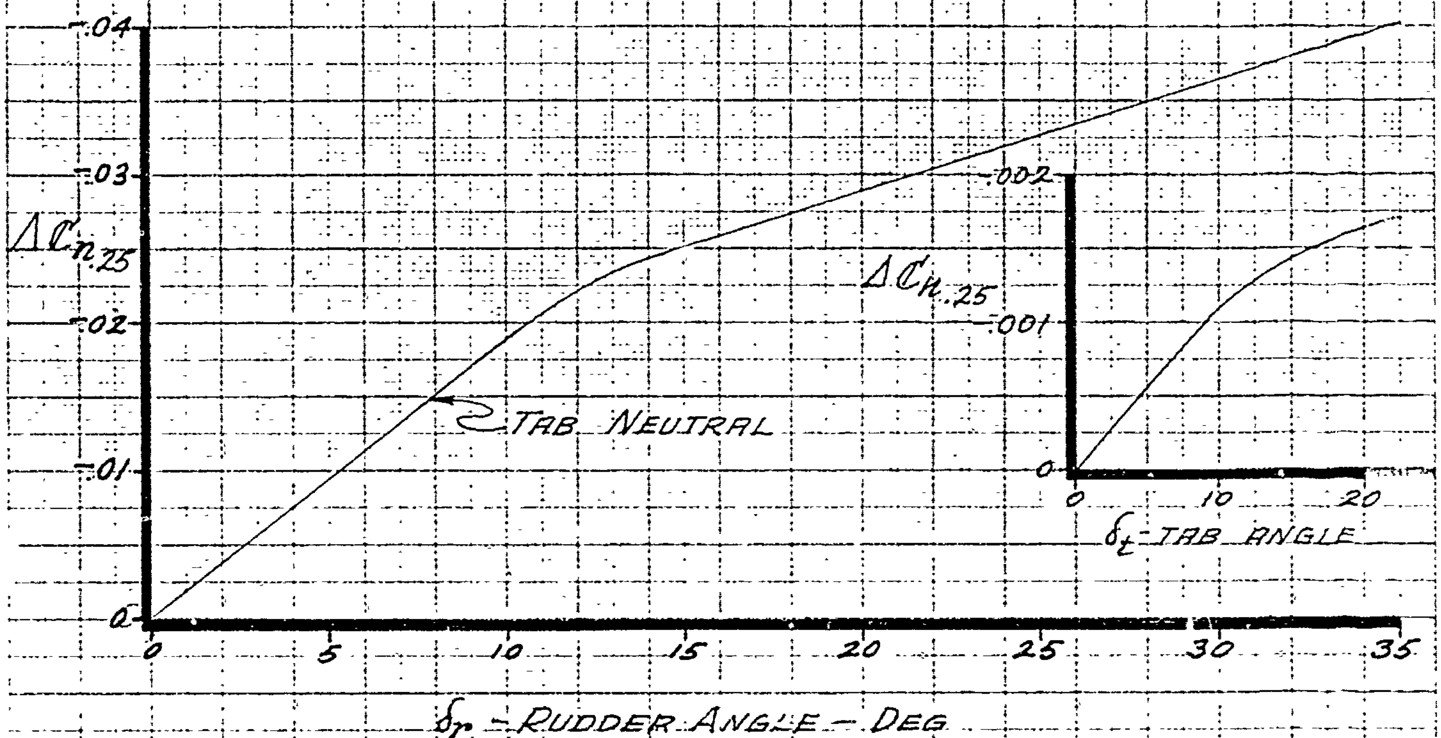

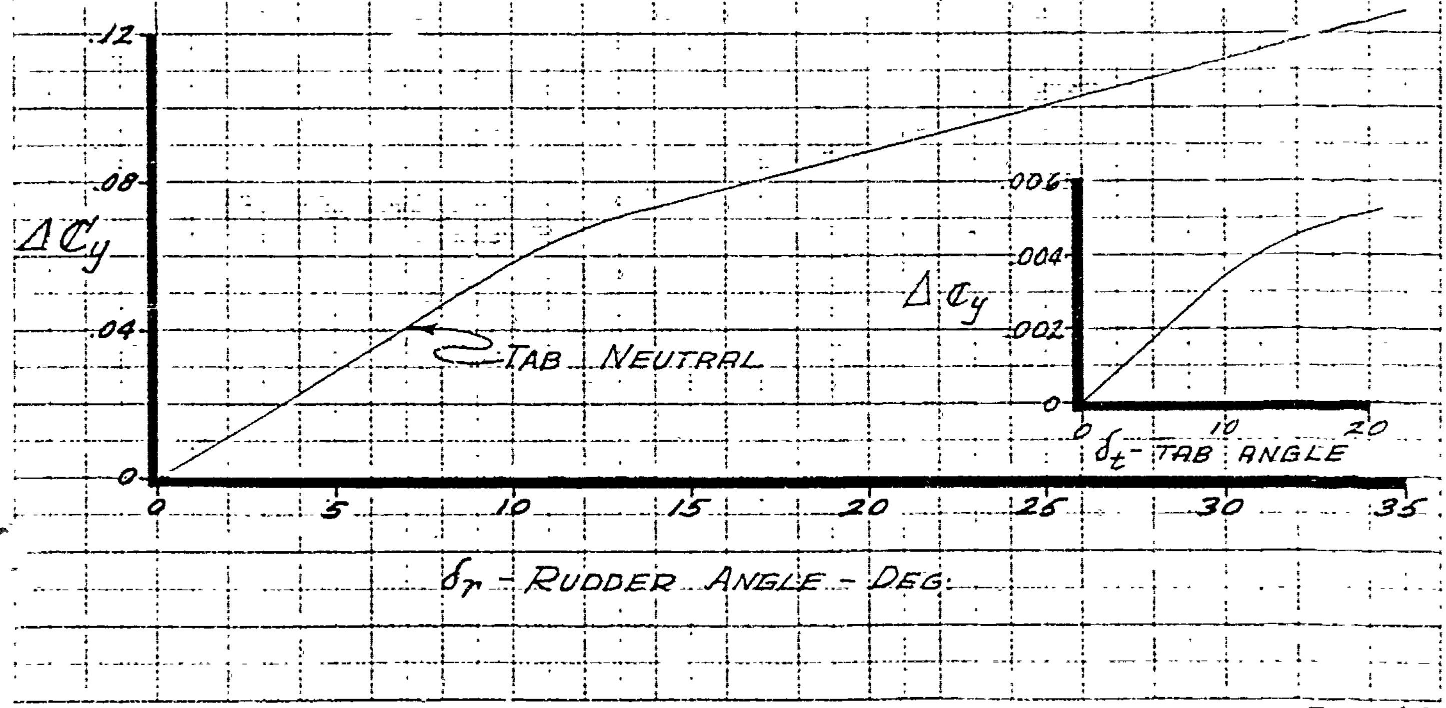

PREPARED BY

DATE

CHECKED BY

LOCKHEED AIRCRAFT CORPORATION

LOCKHEED C-130

RUDDER HINGE MOMENT COEFFICIENTS

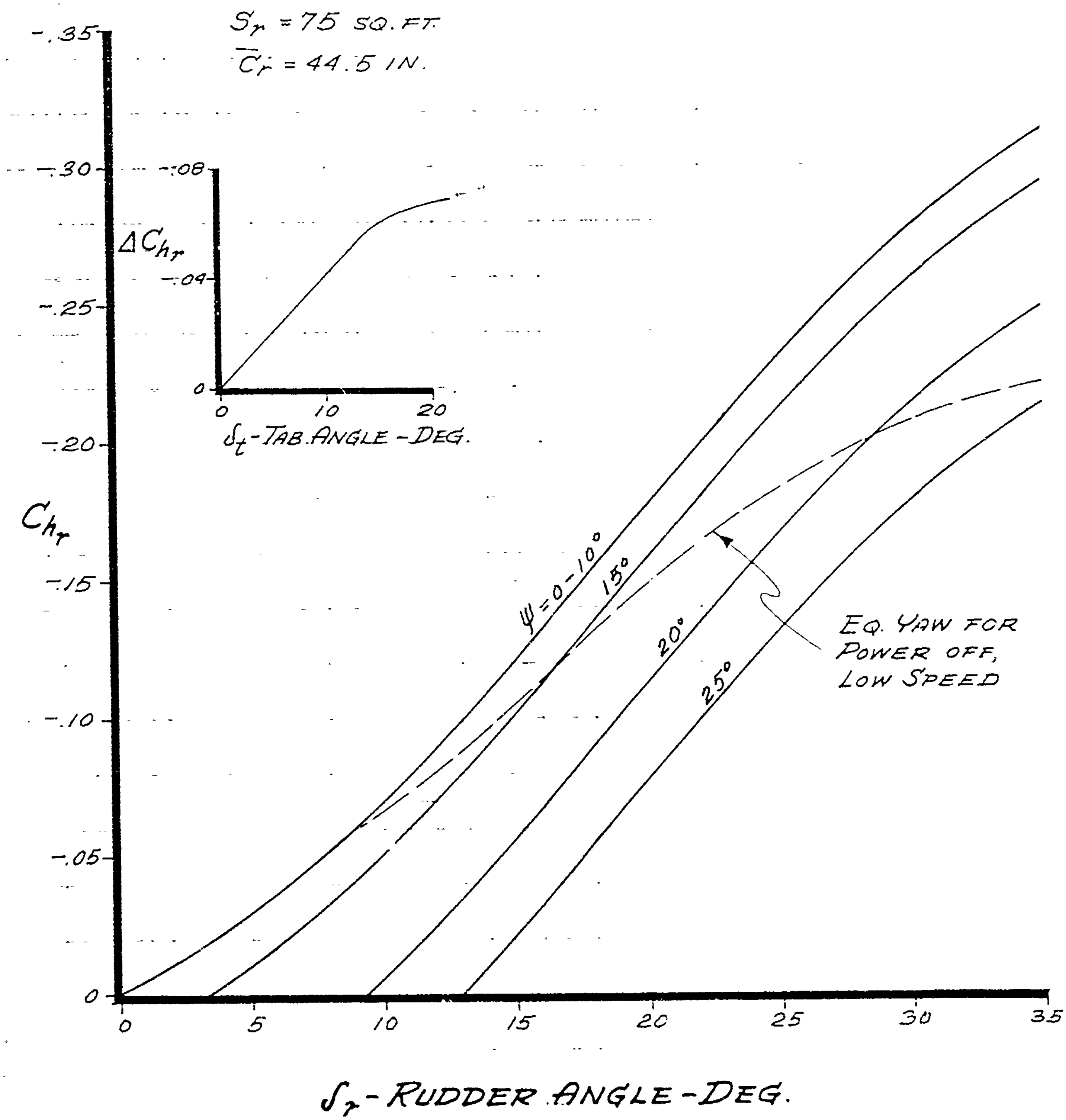

FORM 5278A

Fig. 48

LATERAL AERODYNAMIC CHARACTERISTICS

DIHEDRAL EFFECT

Airplane roll due to yaw for all angles of attack and flap settings is given in fig. 50 for power off. Application of power tends to reduce the dihedral effect by approximately C_Δ X 60% for flaps up. At high speeds, the power off curve may be corrected by the Prandtl-Glauert factor to account for compressibility in the Mach No. range wherein critical loads will occur.

DAMPING IN ROLL

The low speed value of the roll damping coefficient is determined on the basis of geometric parameters from ref. 10. The variation of the coefficient with Mach Number above 0.2 is according to the Prandtl-Glauert relation, which is valid in the Mach Number range in which critical air loads will be acting. Fig. 51 presents this data.

AILERON CHARACTERISTICS

Aileron effectiveness for flaps retracted and extended for all speeds is given in figs. 52 and 53. Values are given for various lift coefficients; intermediate values of effectiveness may be obtained by interpolation and extrapolation. Aileron hinge moment coefficients are presented in fig. 54 for all flap settings and all speeds. Values of hinge moment coefficient are given for two airplane angles of attack, from which values for other angles may be determined by interpolation and extrapolation. These hinge moment coefficients have been estimated from the data of refs. 4, 7 and 10.

Characteristics of the aileron control and boost system are given in figs. 84, 85 and 86. In figs 87 and 88 are shown plots of pilot force and aileron hinge moment versus wheel angle for several speeds, showing the effects of the boost ratio and boost cut-off and the relationship between pilot force and aileron hinge moment.

LOCKHEED C-130

DIHEDRAL EFFECT

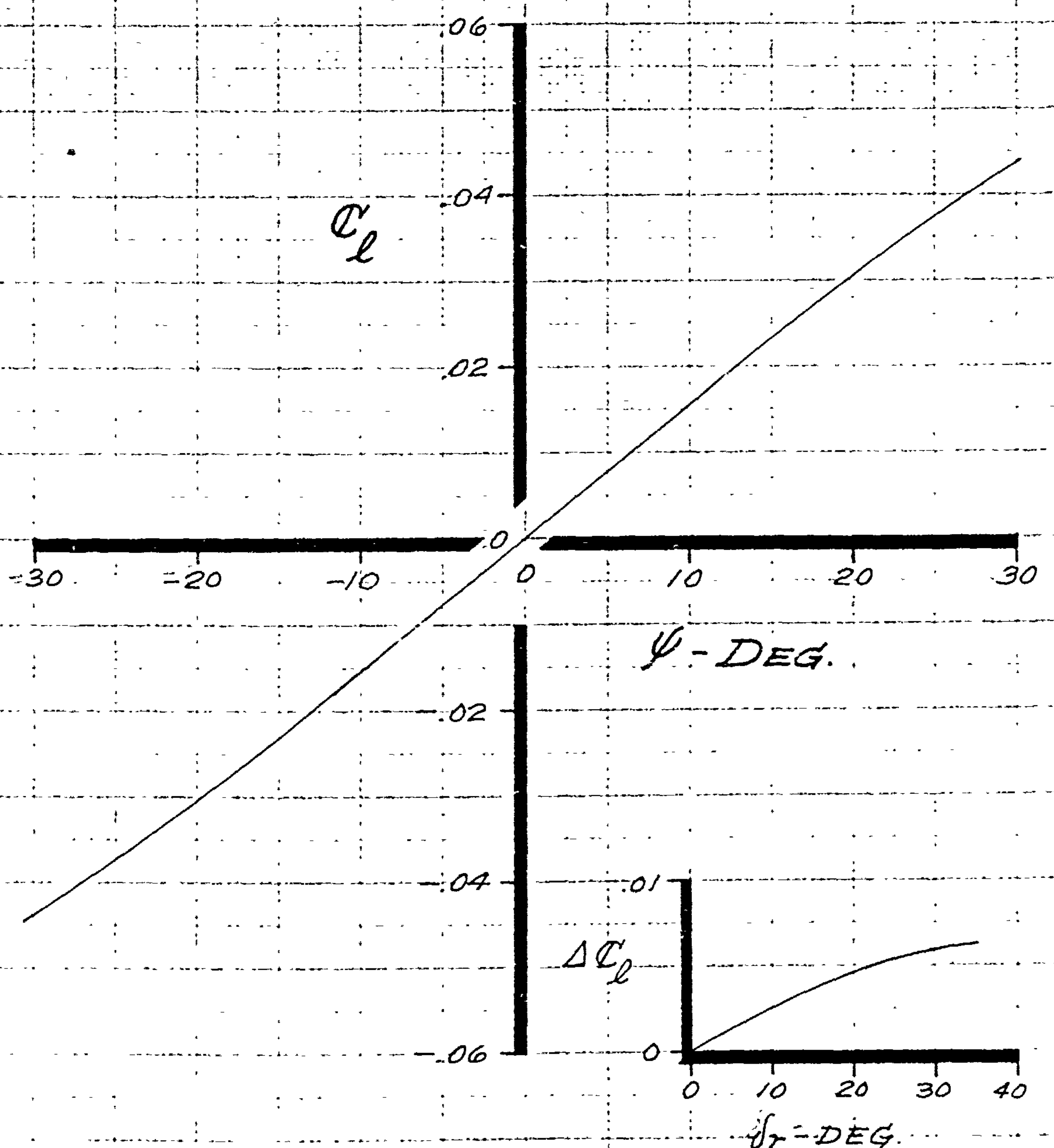

FIG. 50

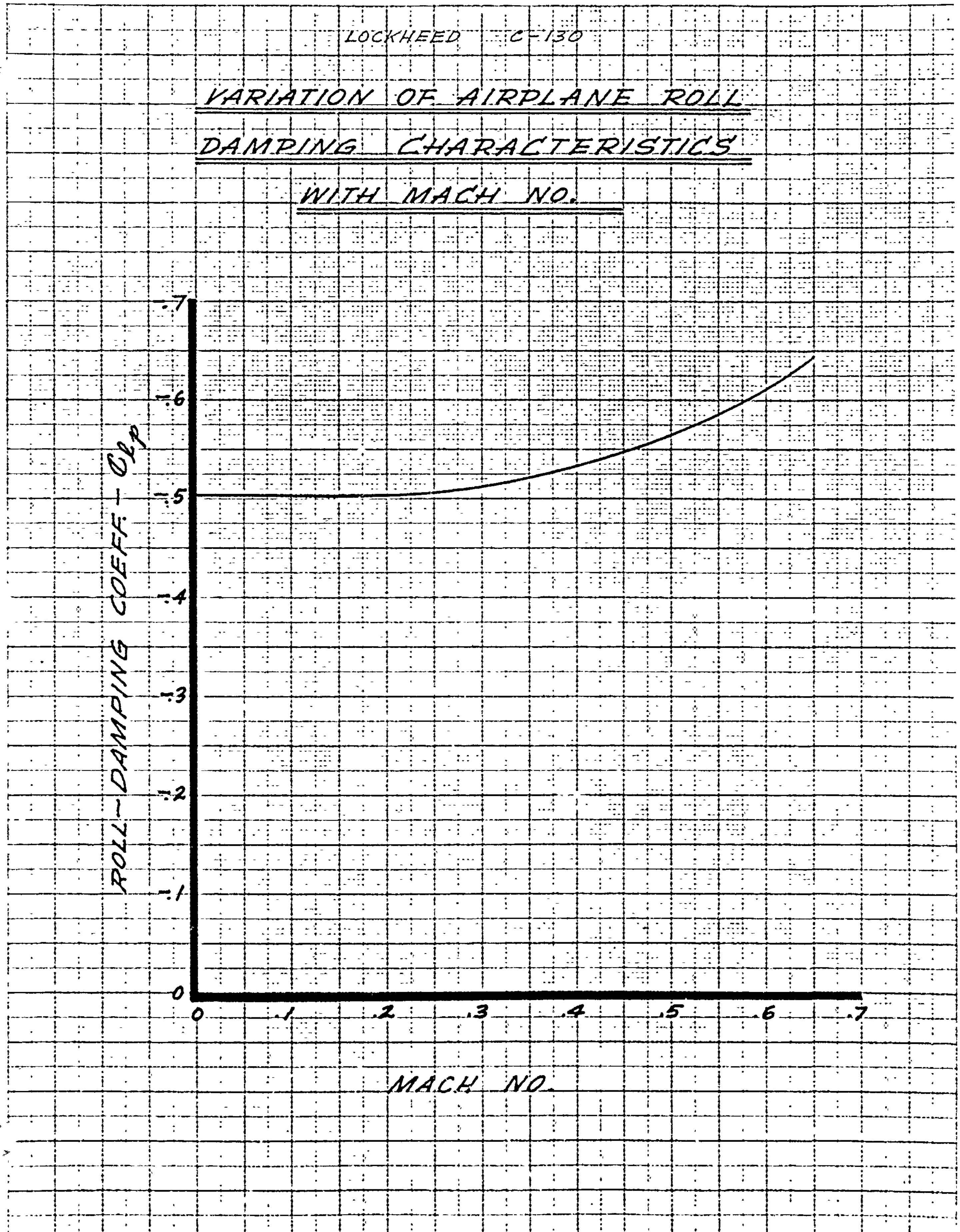
LOCKHEED C-130
VARIATION OF AIRPLANE ROLL DAMPING CHARACTERISTICS WITH MACH NO.
ROLL-DAMPING COEFF - C_{l_p}
-.7
-.6
-.5
-.4
-.3
-.2
-.1
0
0
.1
.2
.3
.4
.5
.6
.7
MACH NO.

FIG. 51

PREPARED BY
DATE
CHECKED BY

LOCKHEED AIRCRAFT CORPORATION
CALIFORNIA DIVISION

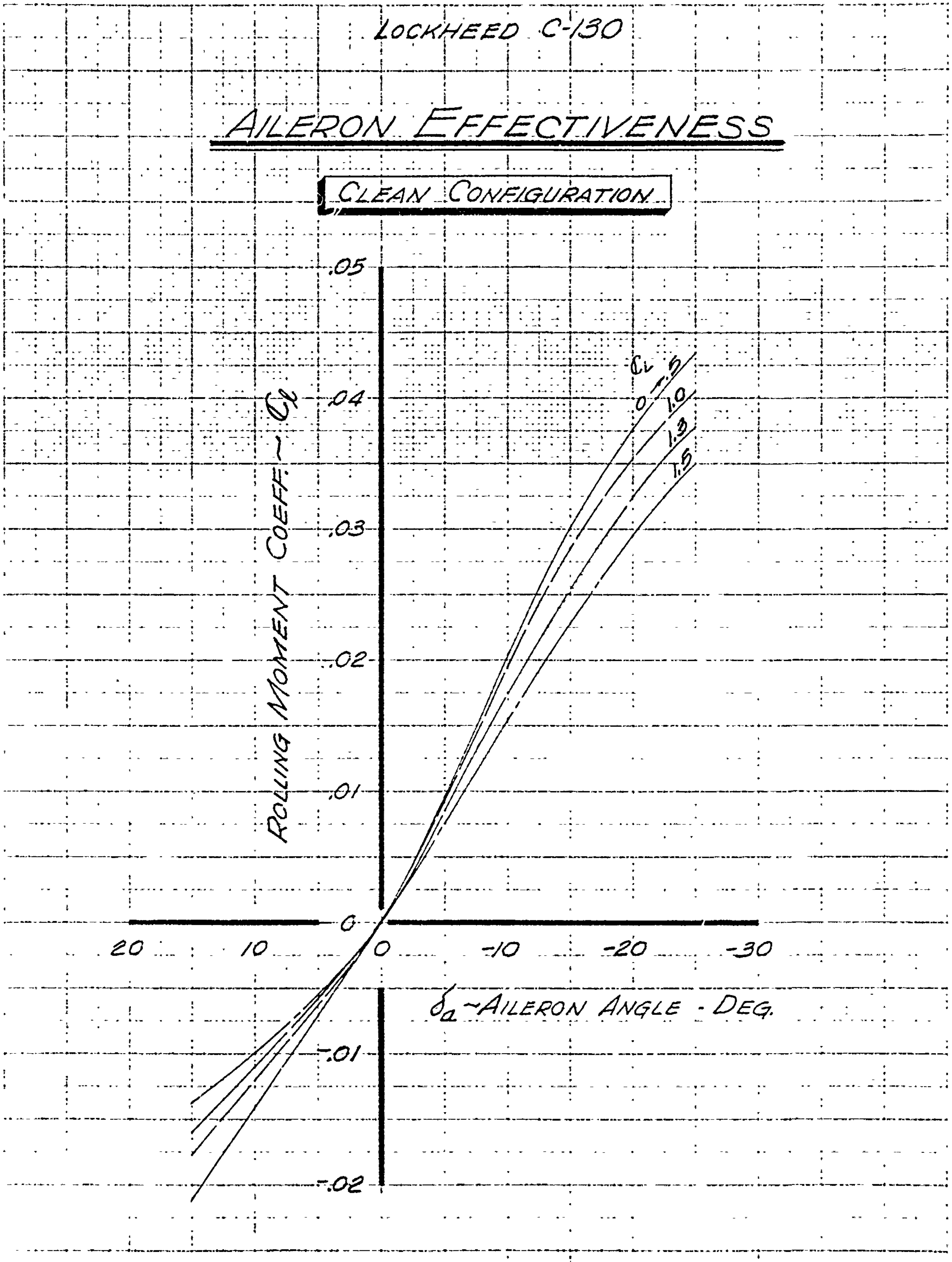

FORM 5278

FIG. 52

LOCKHEED C-130

AILERON EFFECTIVENESS

LANDING CONFIGURATION

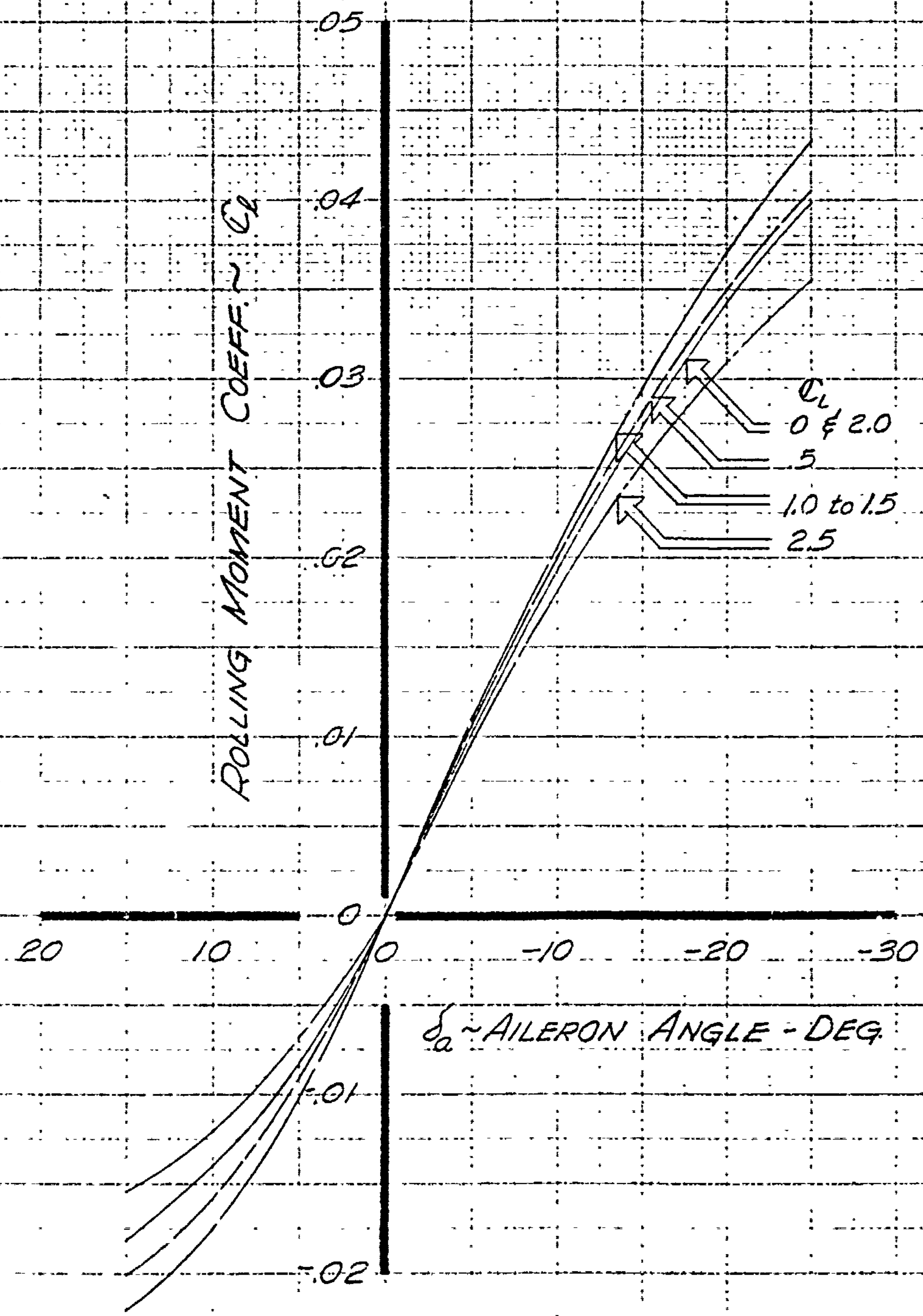

FIG. 53

LOCKHEED C-130

ESTIMATED AILERON HINGE MOMENT CHARACTERISTICS

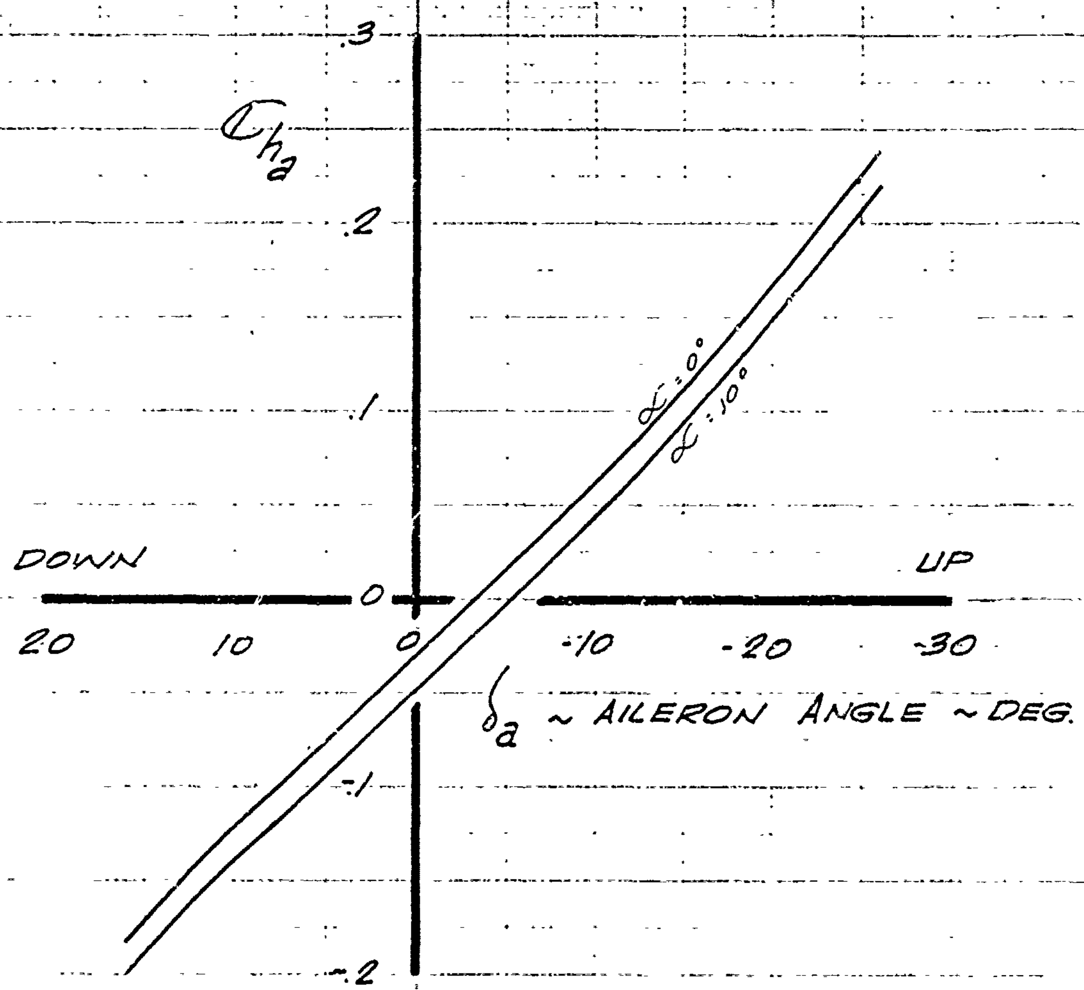

FIG. 54

CHORDWISE PRESSURE DISTRIBUTIONS

All chordwise pressure distributions except that over the wing with Fowler flaps extended have been determined from the methods and data of refs. 8, 10 and 24. The curves for the wing section with Fowler flaps extended are obtained from unpublished wind tunnel test data on the Lockheed XP2V-1 and from flight test pressure measurements on the Lockheed Constellation airplane.

WING

Chordwise pressure distributions are presented for upper and lower surfaces at several lift coefficients for the inboard wing airfoil section, for a typical section in the outboard panel and for the wing tip section in figs. 55, 56, 58, 59 and 61. In addition, net unit and basic pressure distributions are shown for the inboard and typical outboard sections in figs. 57 and 60. The pressure distribution over the wing airfoil section ahead of the extended Fowler flap is presented in fig. 63. Flap load coefficients are shown in fig. 70 and discussed on page 88.

Net pressure distribution increment due to deflection of the aileron is given in fig. 62, determined from the data of ref. 25, using the section pitching moment data of fig. 11.

EMPENNAGE

The horizontal tail surface embodies an inverted NACA 23012 airfoil section. Chordwise pressure distributions are presented in figs. 64, 65 and 66 for the inverted airfoil (the normally lower surface now becoming the upper, and vice versa), for both surface pressures and the net unit and basic distributions. Fig. 67 shows the added net distribution due to elevator deflection. If necessary to determine local surface pressures with elevator deflected, this net distribution may be considered to apply approximately half to each surface. Figures 68 and 69 show the pressure distributions for the vertical tail and the added net contribution due to deflection of the rudder.

LOCKHEED C-130

CHORDWISE PRESSURE DISTRIBUTION OVER INBOARD WING SECTION

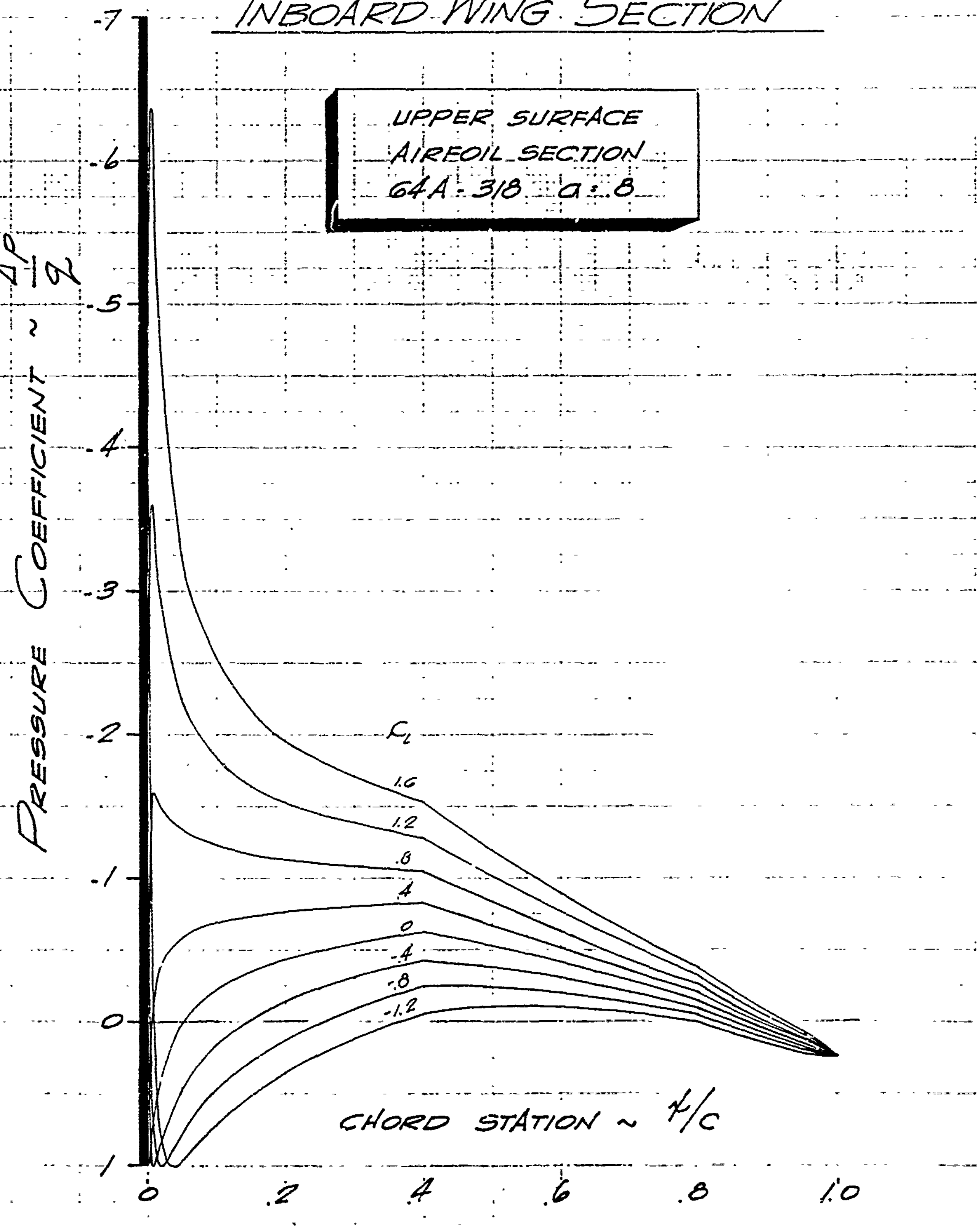

TR 824 & 903

FIG. 55

LOCKHEED C-130

CHORDWISE PRESSURE DISTRIBUTION OVER INBOARD WING SECTION

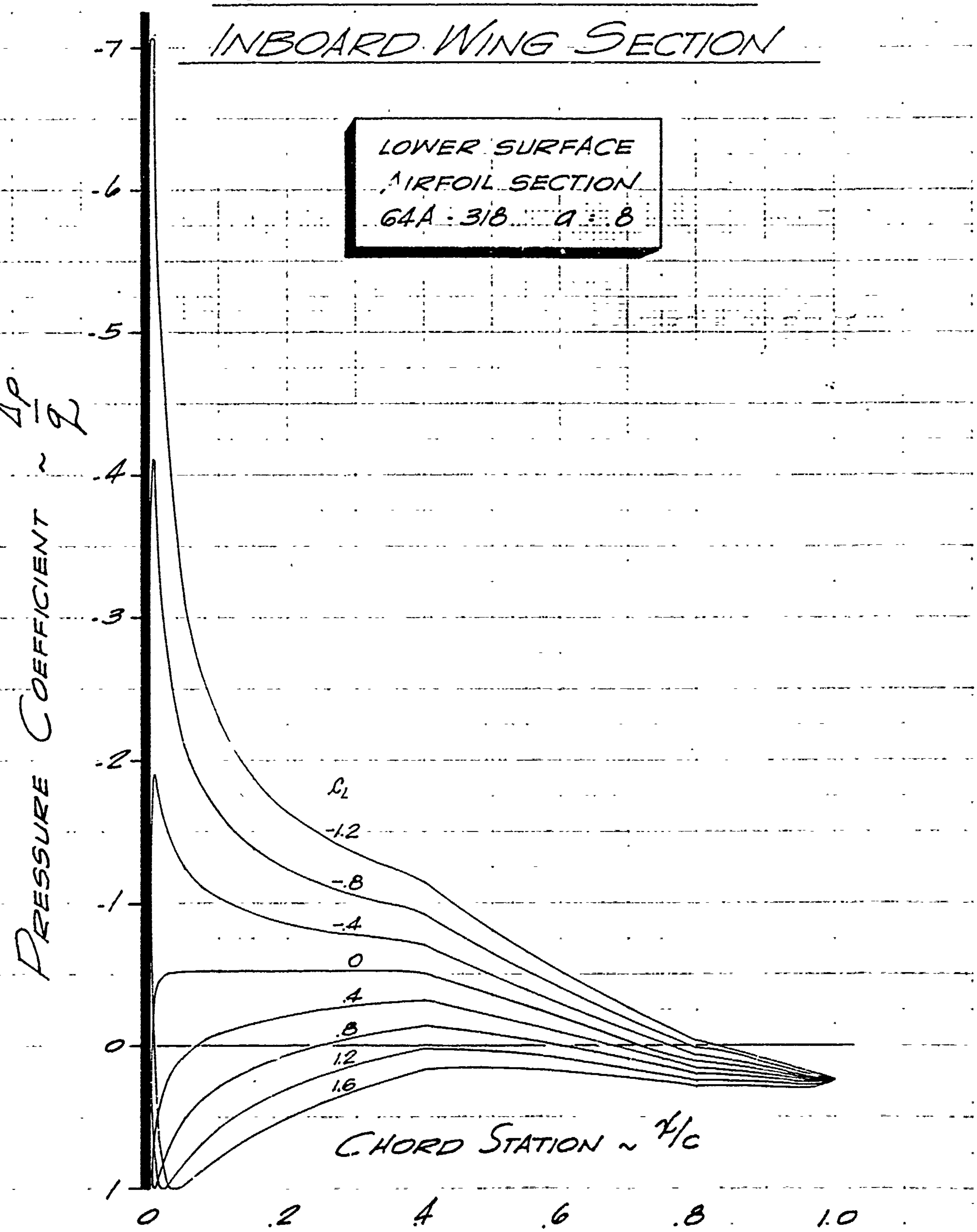

FIG. 56

LOCKHEED C-130

NET CHORDWISE PRESSURE DISTRIBUTION OVER INBOARD WING SECTION

AIRFOIL SECTION
64A-318 a=.8

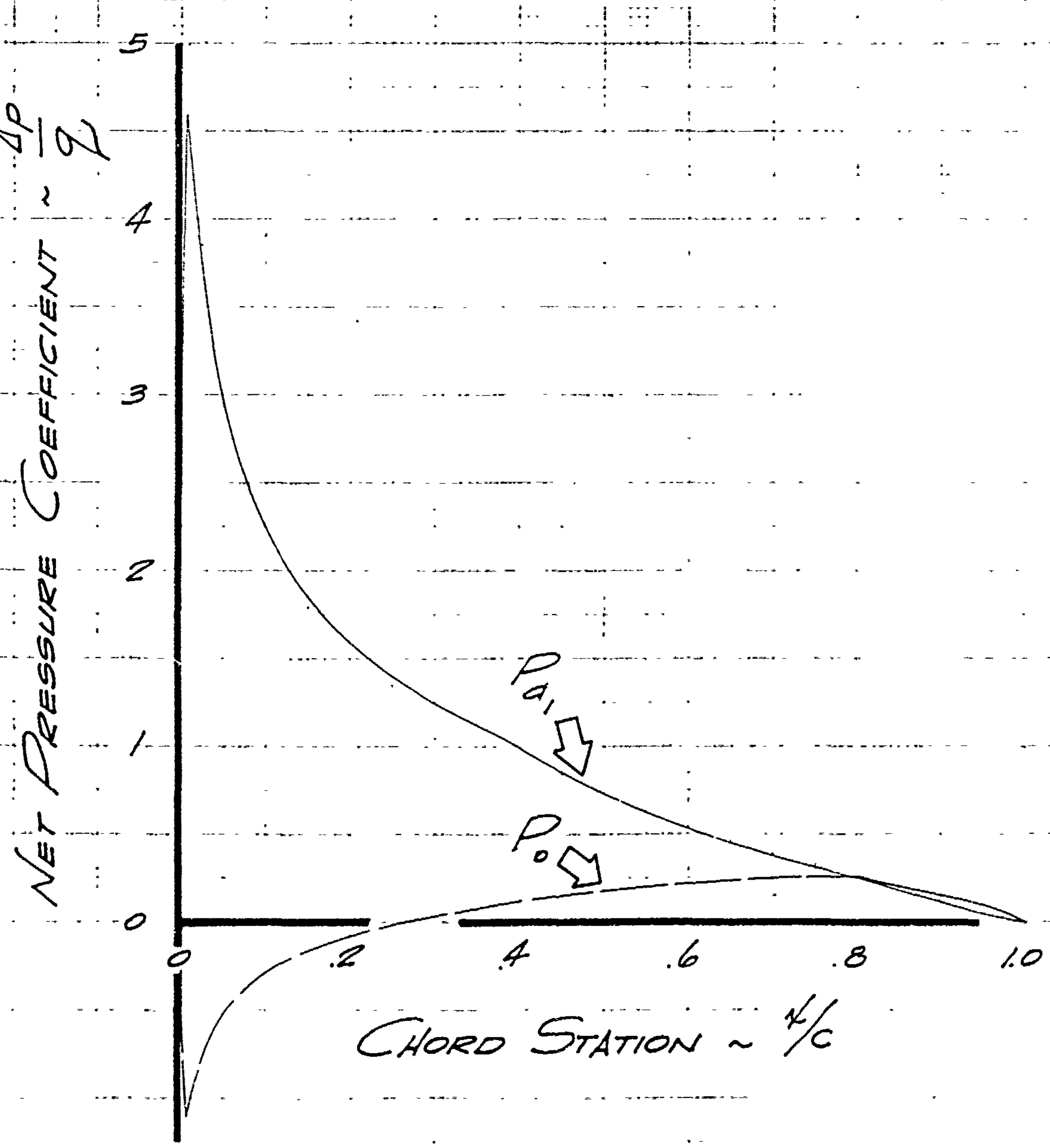

FIG. 57

LOCKHEED C-130

CHORDWISE PRESSURE DISTRIBUTION OVER OUTBOARD WING SECTION

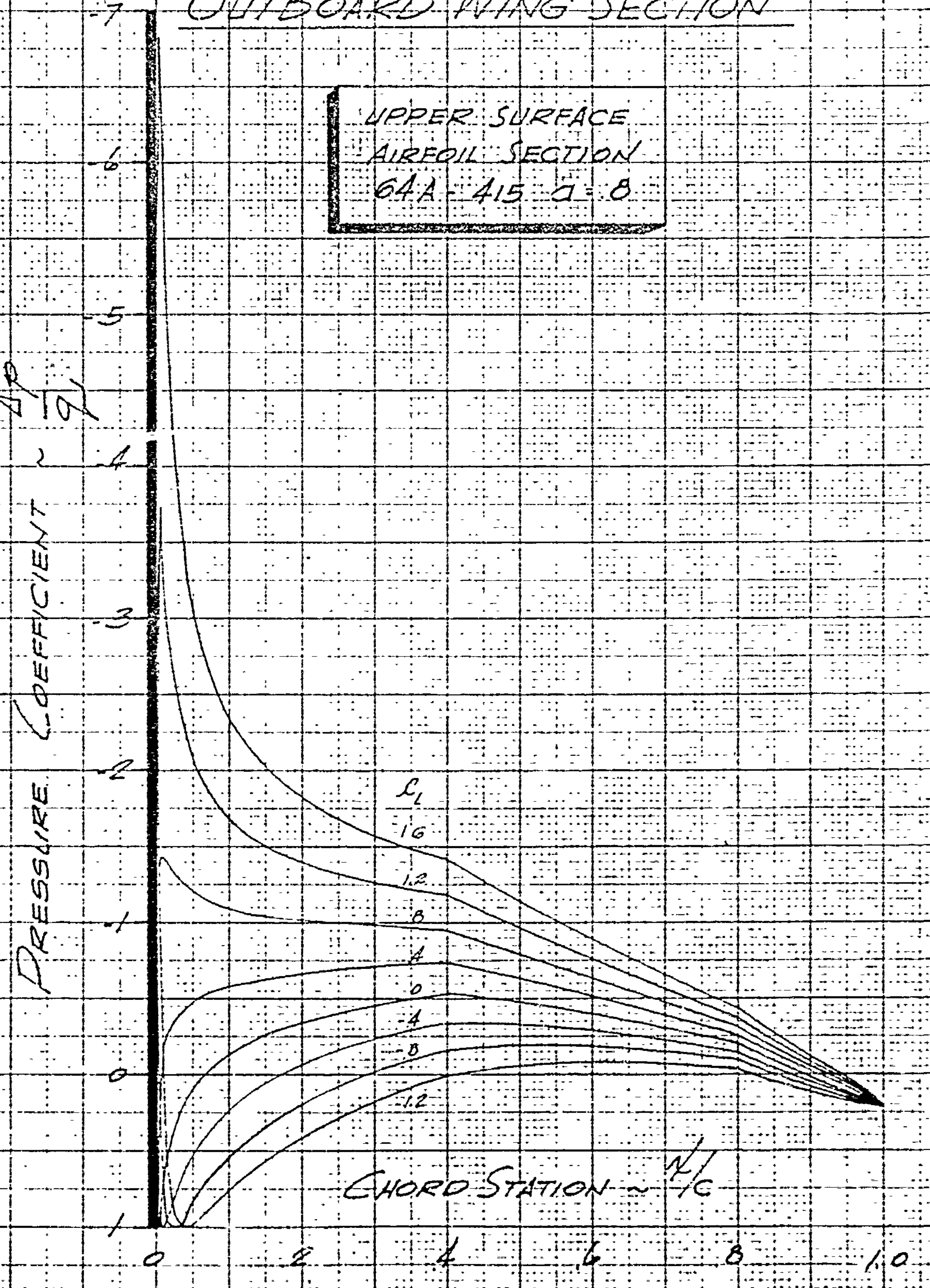

FIG. 58

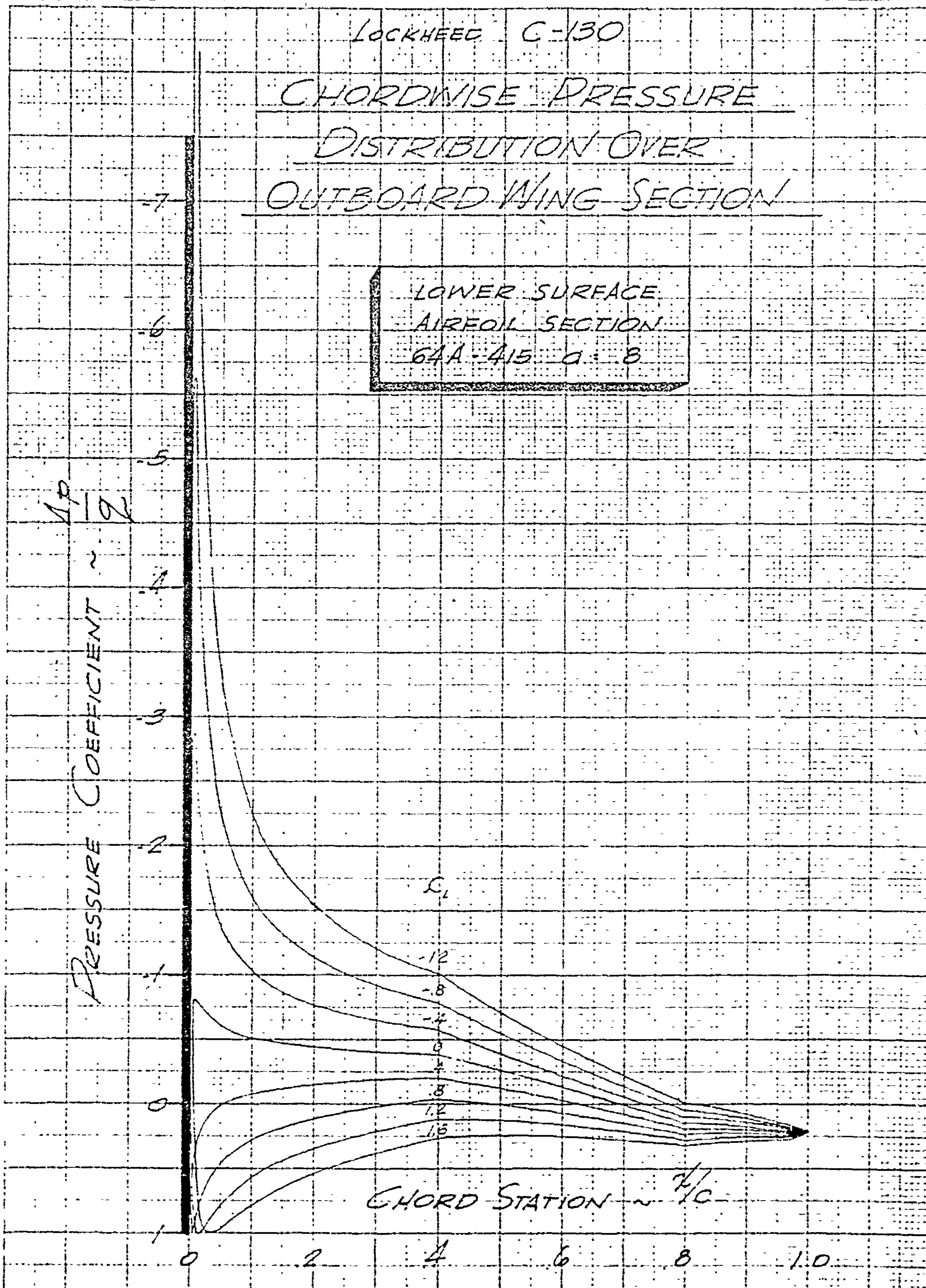
LOCKHEED C-130
CHORDWISE PRESSURE
DISTRIBUTION OVER
OUTBOARD WING SECTION
LOWER SURFACE
AIRFOIL SECTION
64A-415 a=.8
PRESSURE COEFFICIENT ~ Δp/q
-7
-6
-5
-4
-3
-2
-1
0
1
C_L
-1.2
-.8
-.4
0
.4
.8
1.2
1.6
CHORD STATION ~ x/c
0
.2
.4
.6
.8
1.0

Fig. 59

LOCKHEED C-130

NET CHORDWISE PRESSURE DISTRIBUTION OVER OUTBOARD WING SECTION

AIRFOIL SECTION
64A-415 α = 8

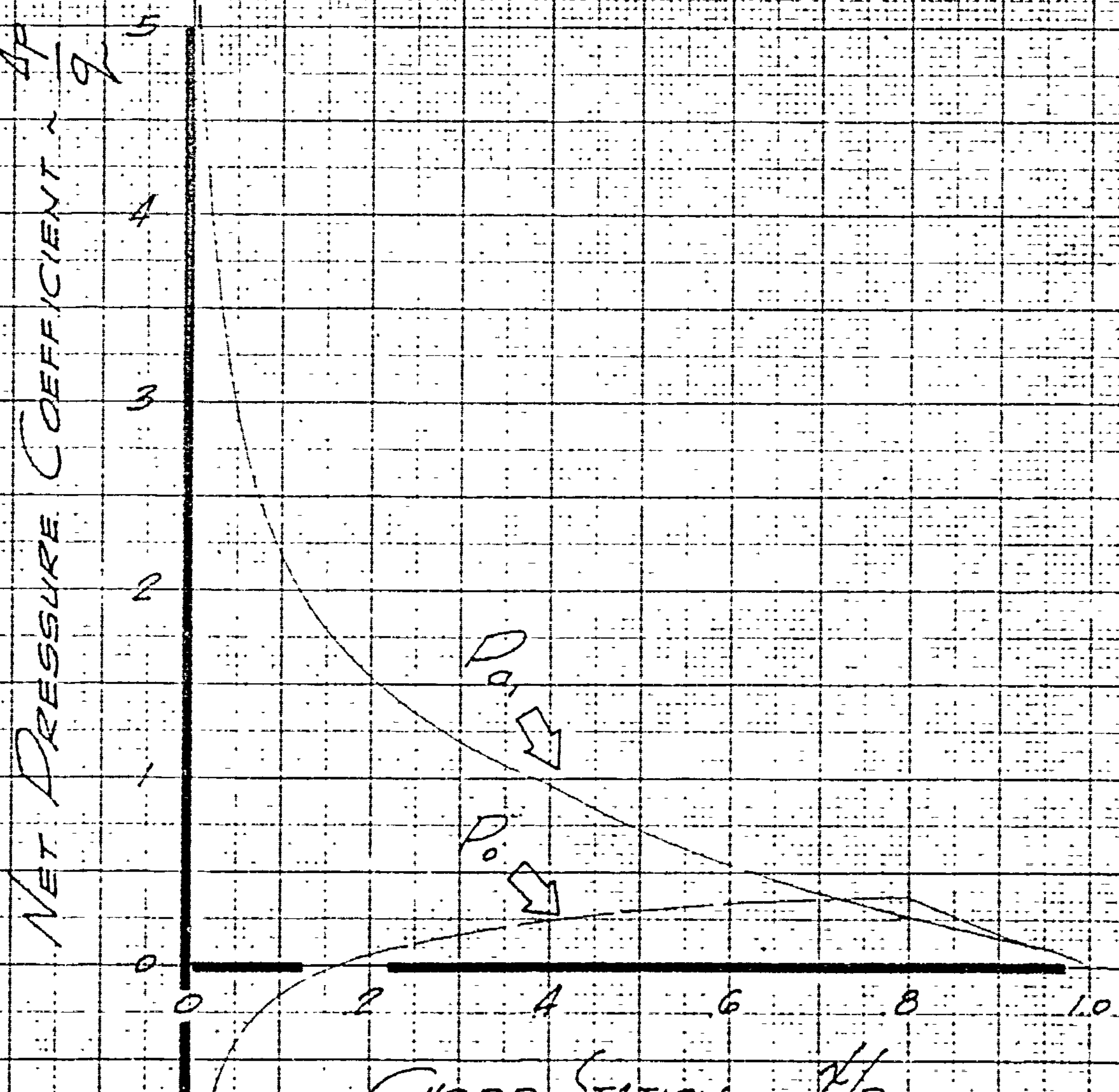

FIG. 60

LOCKHEED C-130

CHORDWISE PRESSURE DISTRIBUTION OVER WING TIP SECTION

AIRFOIL SECTION 64A-412 a=0.8

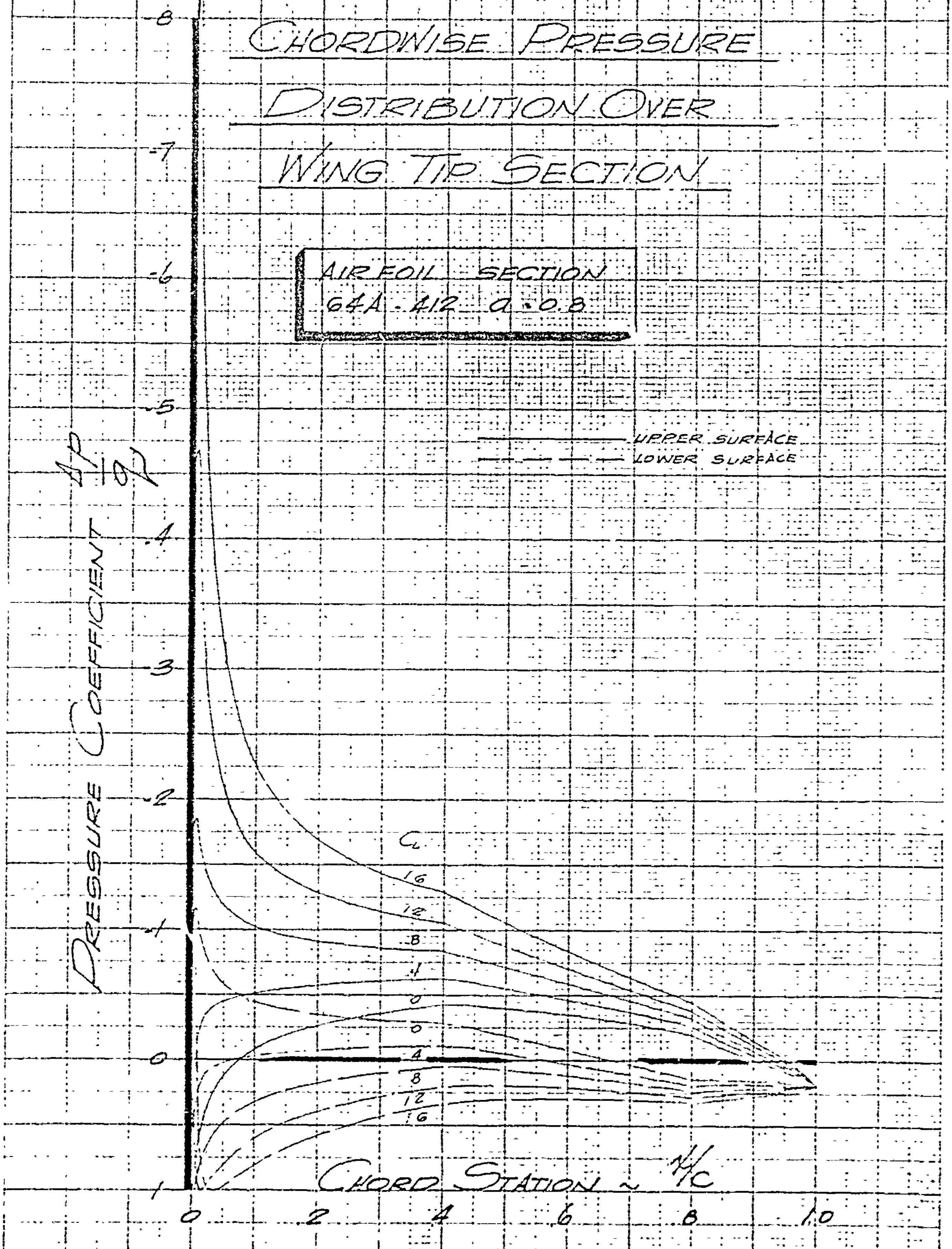

Fig. 61

LOCKHEED C-130

NET PRESSURE DISTRIBUTION INCREMENT DUE TO AILERON DEFLECTION

LOW SPEED

FOR LOCAL SURFACE PRESSURES, DIVIDE THESE NET PRESSURES BY 2.0 AND APPLY TO EACH SURFACE, ADDING BY PRINCIPLE OF SUPERPOSITION.

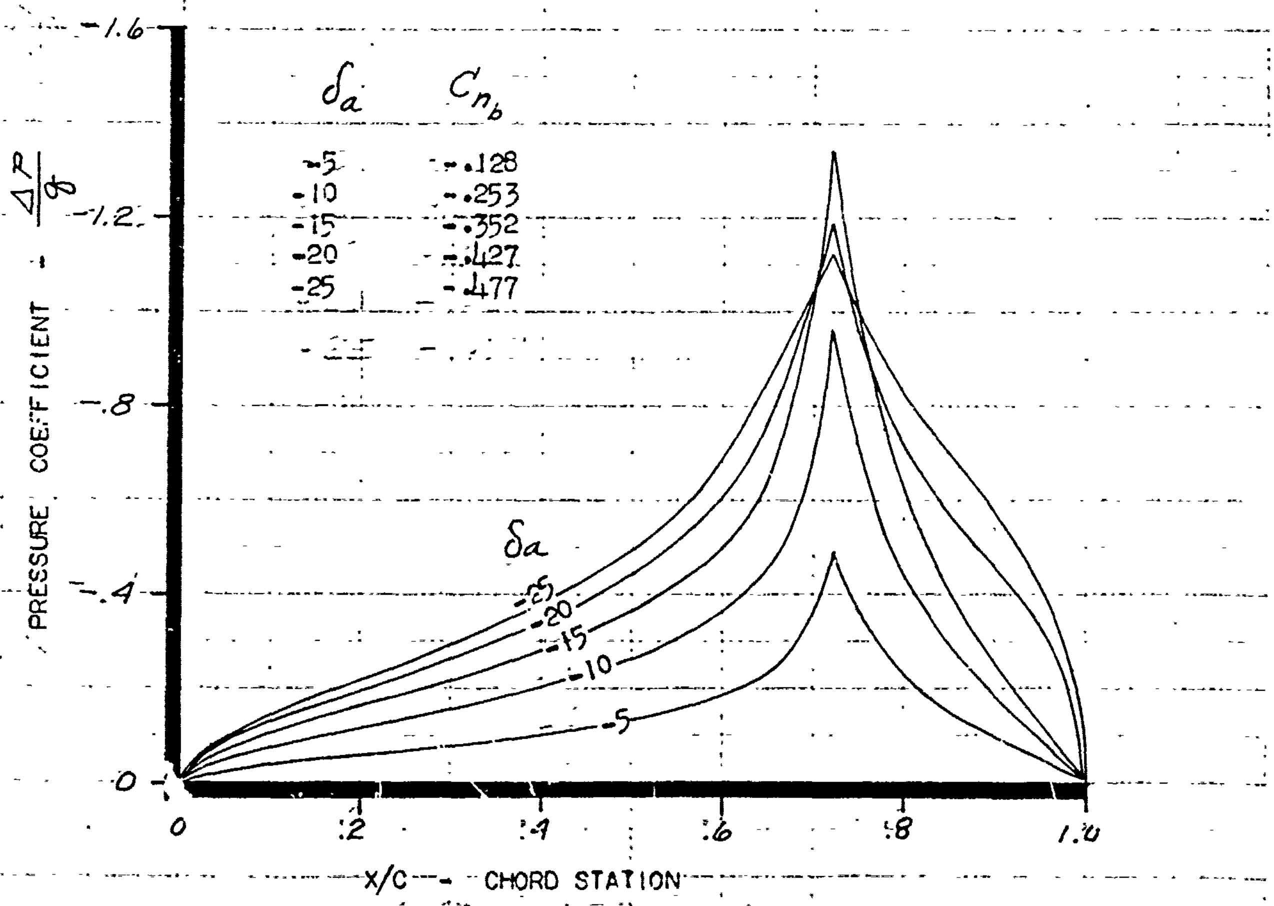

FIG. 62

PREPARED BY
DATE
CHECKED BY

LOCKHEED AIRCRAFT CORPORATION

PAGE 01
MODEL C-130
REPORT NO 9062

LOCKHEED C-130

WING CHORDWISE PRESSURE DISTRIBUTION WITH FOWLER FLAP EXTENDED

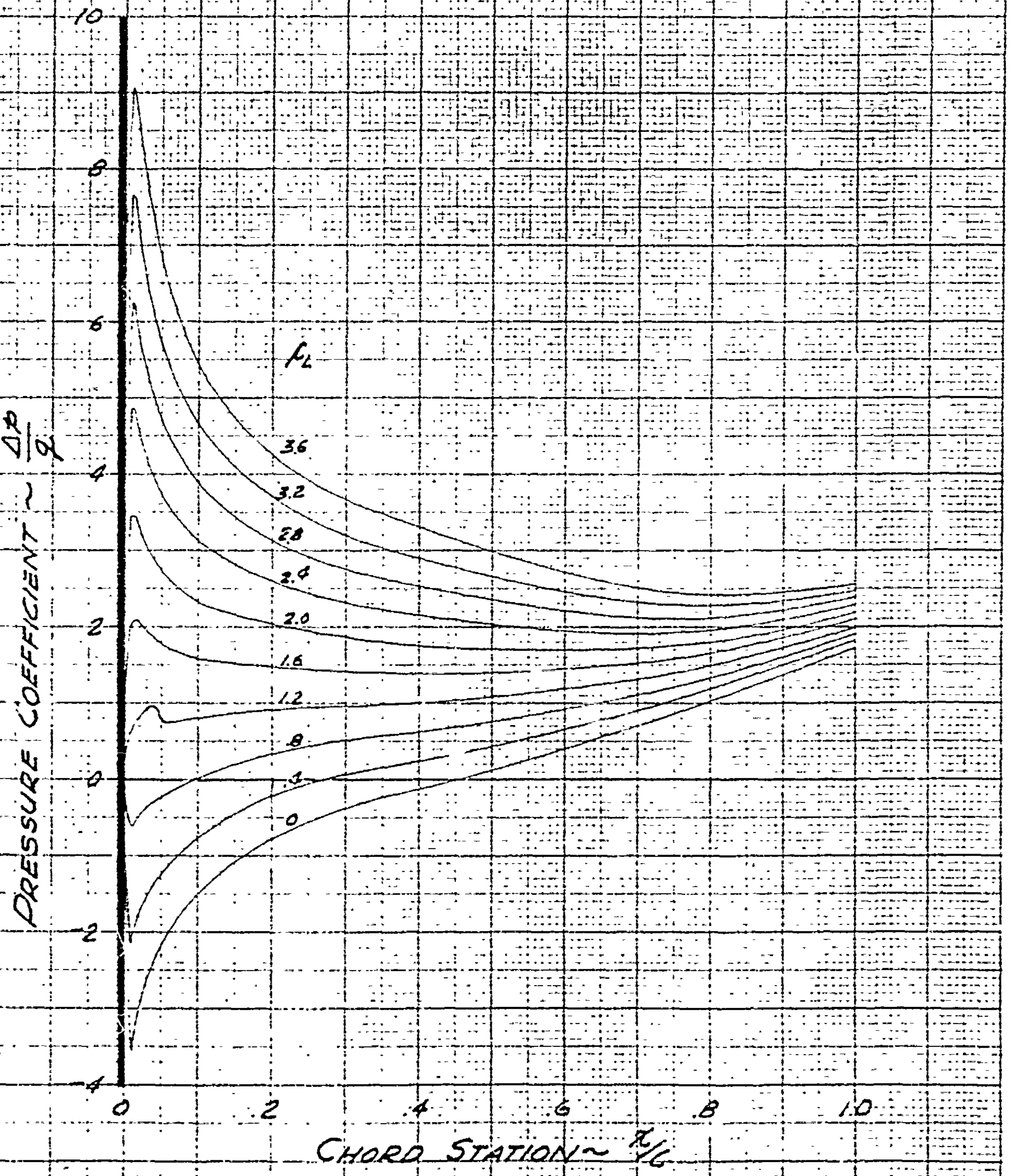

FORM 3278

FIG. 63

LOCKHEED C-130

HORIZONTAL TAIL CHORDWISE PRESSURE DISTRIBUTION

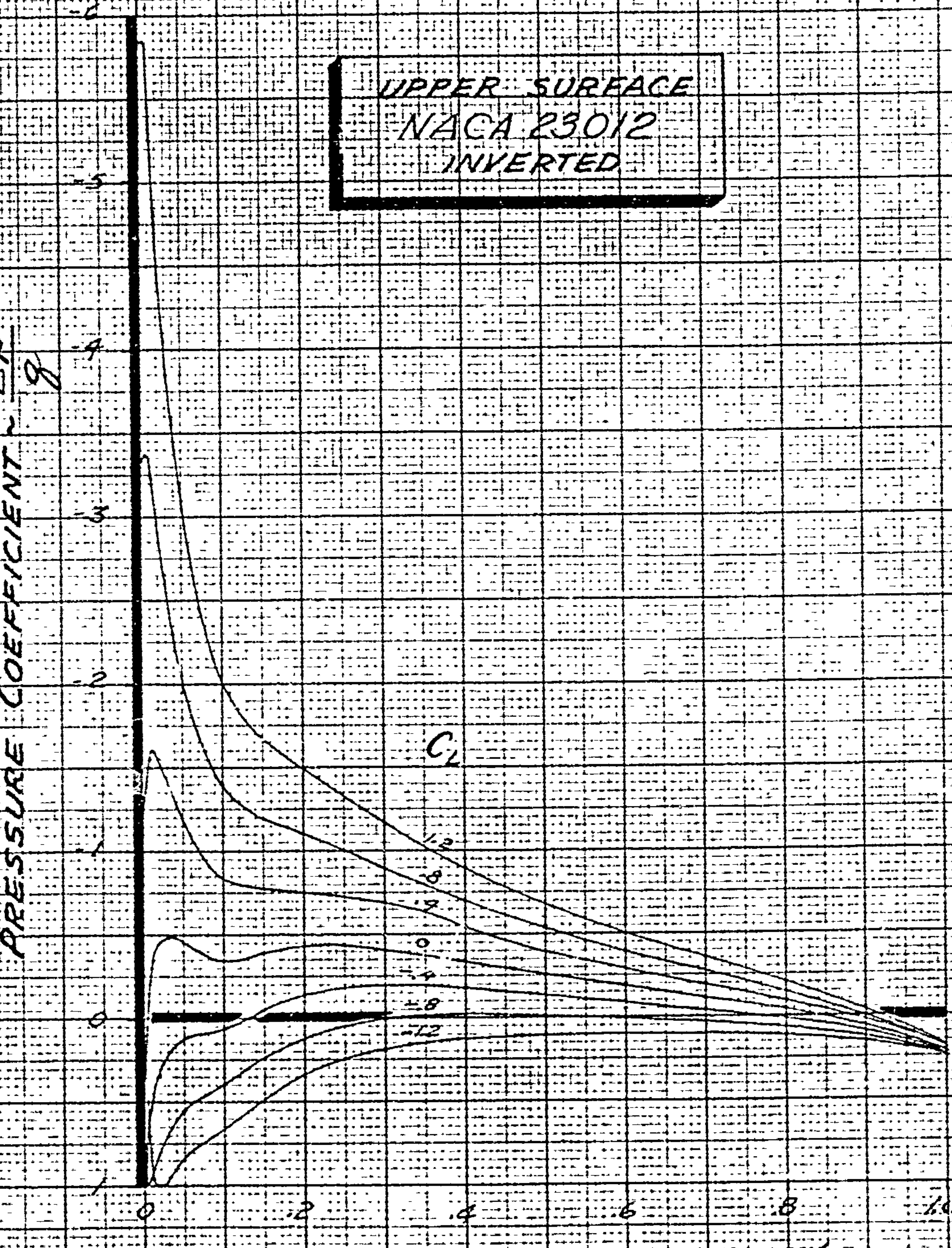

FIG. 64

LOCKHEED C-130

HORIZONTAL TAIL CHORDWISE PRESSURE DISTRIBUTIONS

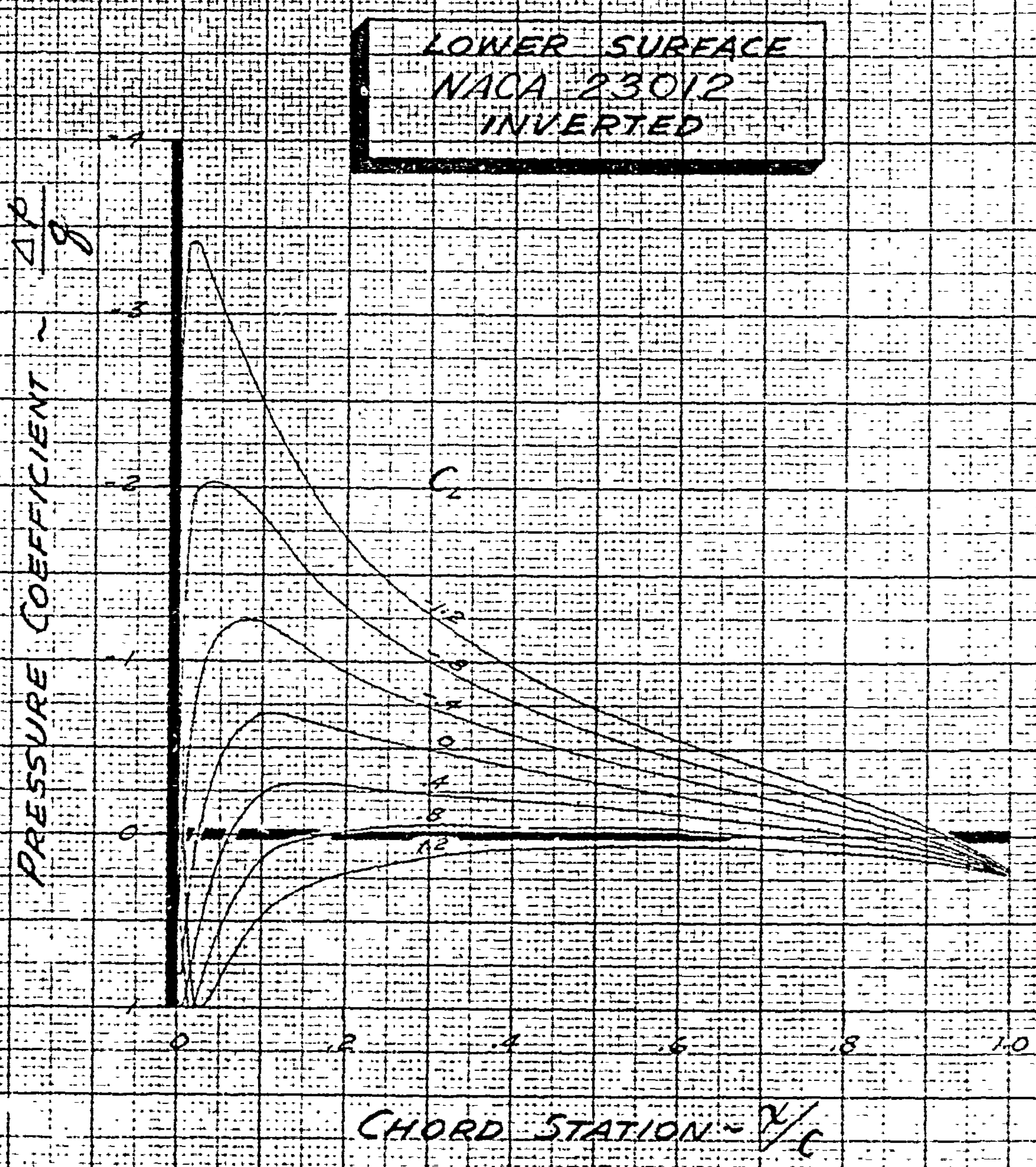

FIG. 65

LOCKHEED C-130

HORIZONTAL TAIL NET CHORDWISE PRESSURE DISTRIBUTION

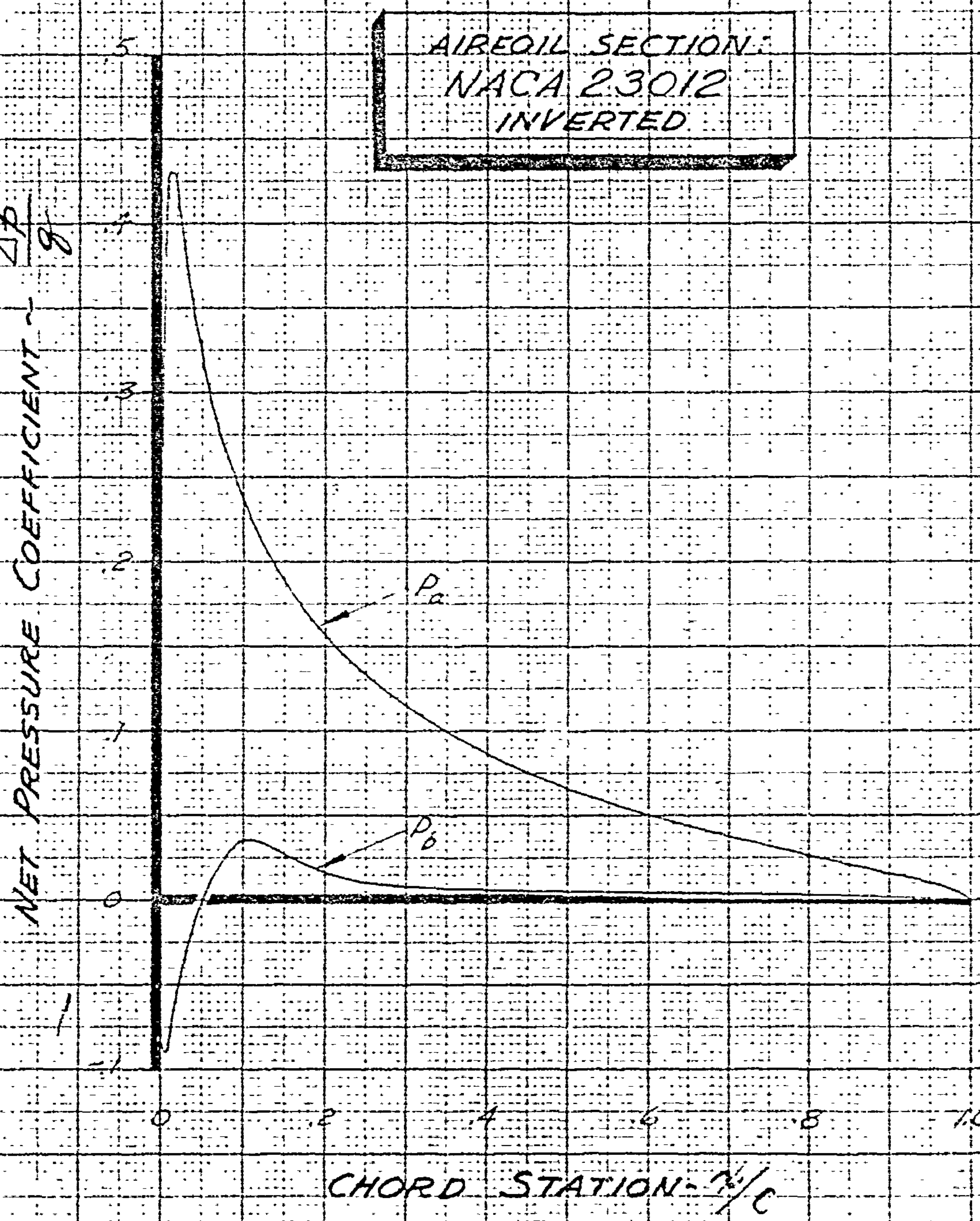

FIG. 66

LOCKHEED C-130

HORIZONTAL TAIL NET CHORDWISE PRESSURE DISTRIBUTION DUE TO ELEVATOR DEFLECTION

LOW SPEED

FOR LOCAL SURFACE PRESSURES, DIVIDE THESE NET PRESSURES BY 2 AND APPLY TO EACH SURFACE, ADDING BY PRINCIPLE OF SUPERPOSITION TO PRESSURES DUE TO ANGLE OF ATTACK.

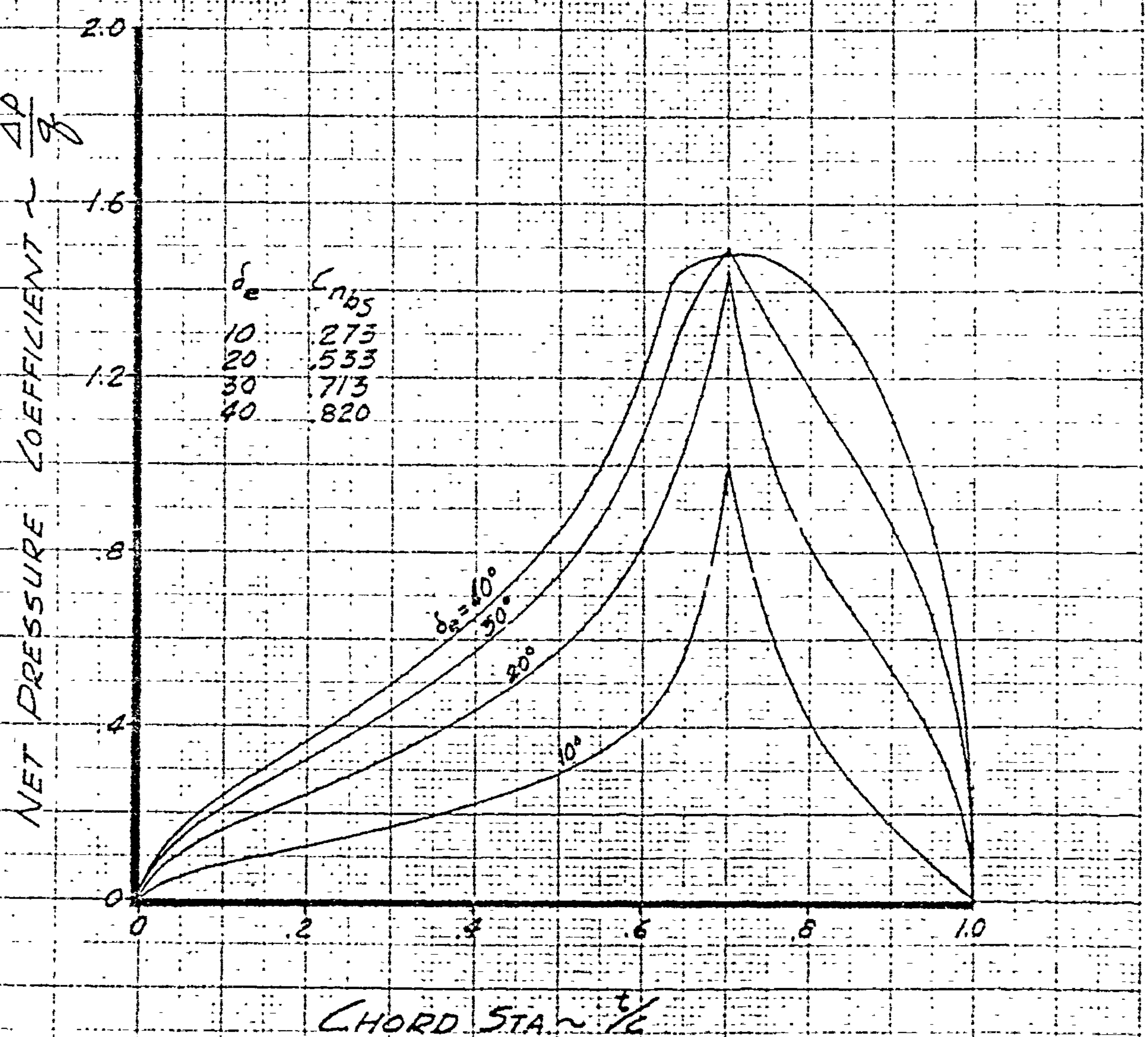

FIG. 67

LOCKHEED C-130

VERTICAL TAIL CHORDWISE PRESSURE DISTRIBUTION

ELEVATOR NEUTRAL

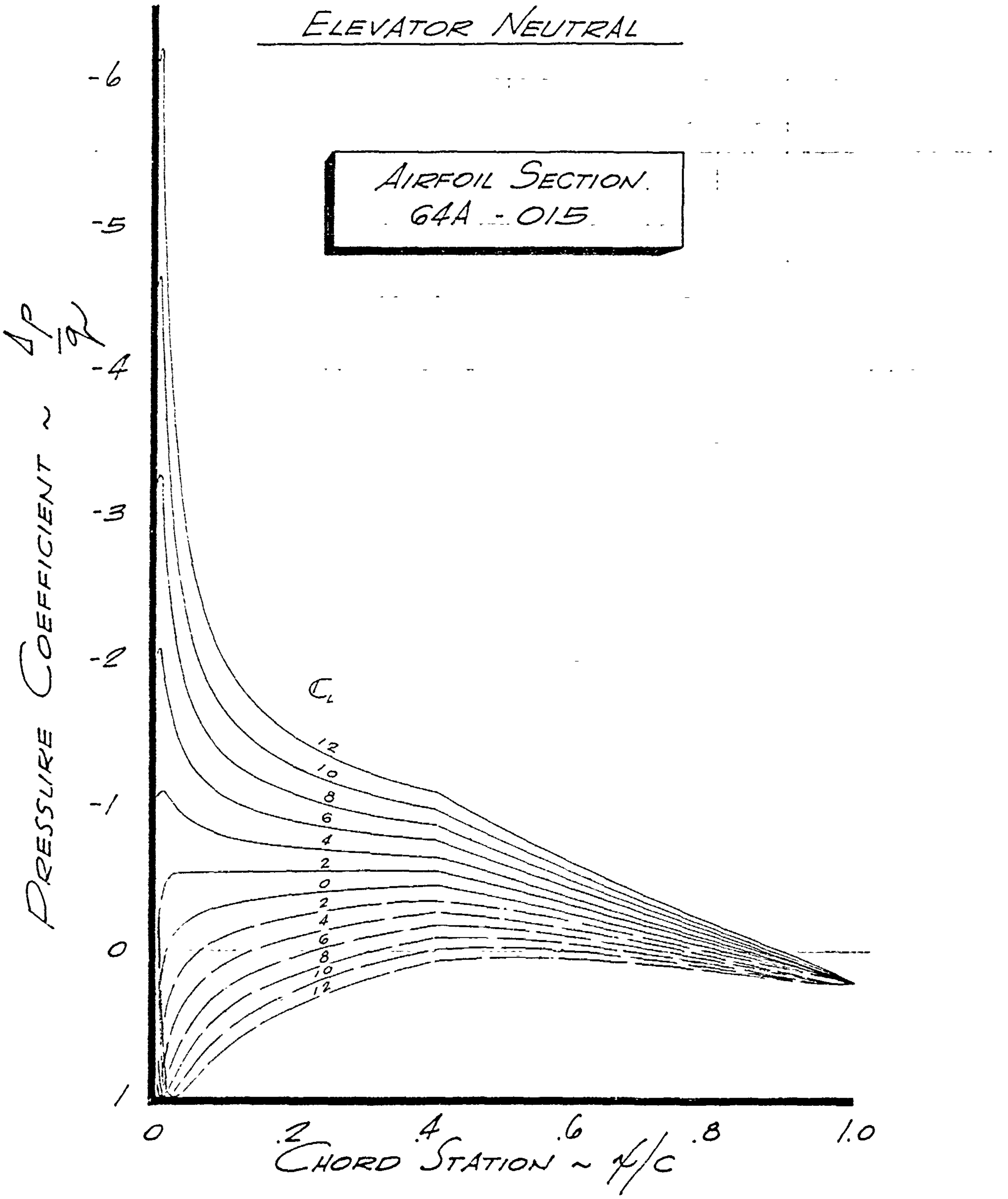

Fig. 68

LOCKHEED C-130

VERTICAL TAIL NET CHORDWISE PRESSURE DISTRIBUTION DUE TO RUDDER DEFLECTION

LOW SPEED

FOR LOCAL SURFACE PRESSURES, DIVIDE THESE NET PRESSURES BY 2 AND APPLY TO EACH SURFACE, ADDING BY PRINCIPLE OF SUPERPOSITION TO PRESSURES DUE TO ANGLE OF ATTACK (YAW)

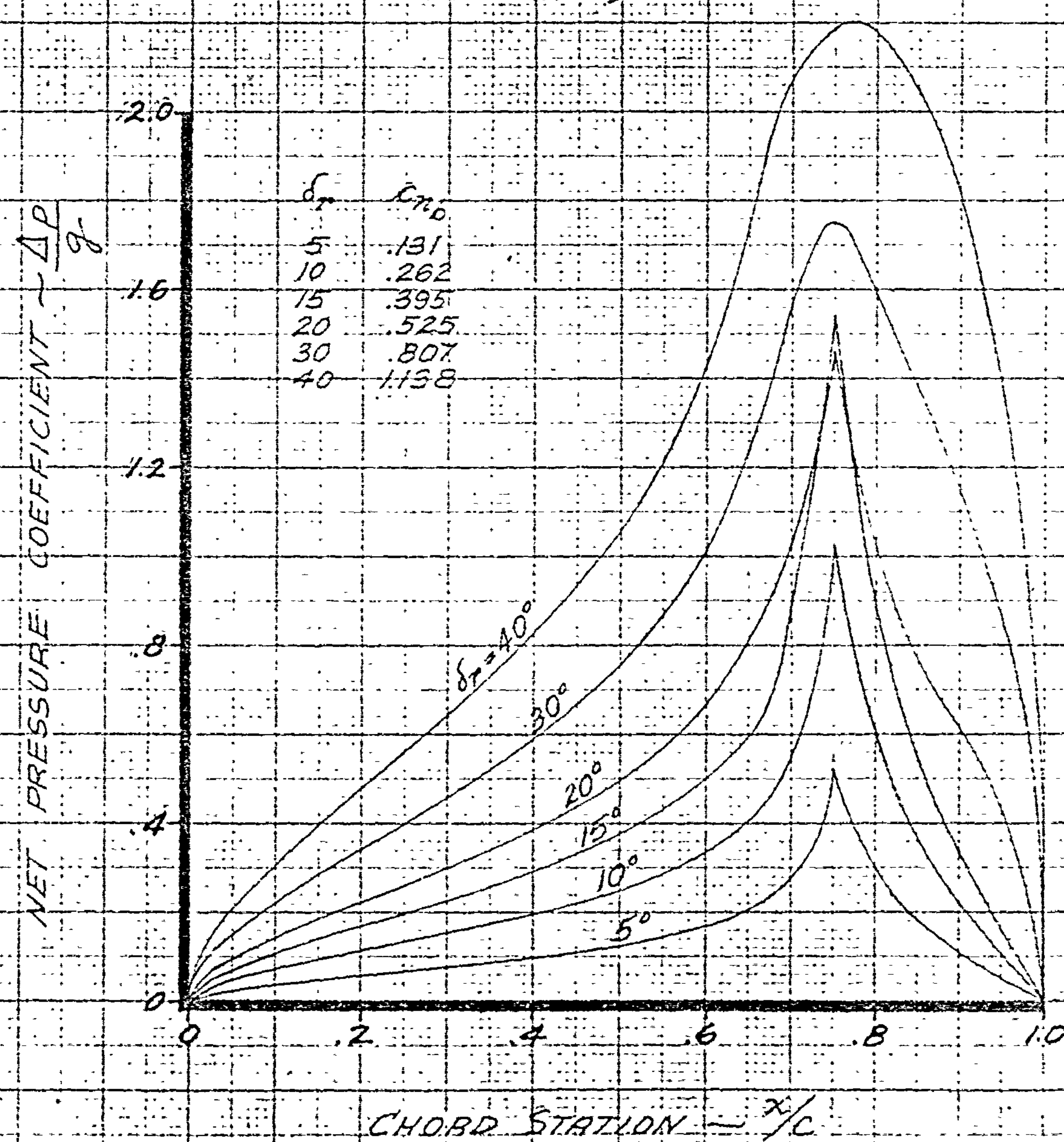

FIG. 69

MISCELLANEOUS AIR LOADS

CARGO DOOR

Hinge moment coefficients for both upper and lower cargo doors are shown in fig. 70 for several different positions of each door. These data were obtained from wind tunnel tests reported in ref. 1.

FOWLER FLAP LOAD COEFFICIENTS

Flap normal and chord force coefficients are presented in fig. 71. These data are determined from extensive two-dimensional wind tunnel tests conducted by Lockheed and summarized in ref. 6. The curves are presented as total force coefficients, although they are developed from pressure distribution measurements and are, therefore, section coefficients. Two curves of chord force coefficient are presented inasmuch as the tests revealed either might be attained, owing largely to gap and condition of the under surface of the wing exposed by extension of the flap. Wing chordwise pressure distributions with the flaps extended are presented in fig. 63.

ENGINE NACELLE PRESSURE DISTRIBUTION

Upper and lower centerline pressures for two airplane angles of attack are presented in fig. 72. These curves are estimated from wind tunnel test data on the nacelle of a Lockheed XP-58 airplane, reported in ref. 24.

PYLON TANK AND STRUT

Aerodynamic characteristics of the pylon tank are presented in fig. 73. These data are estimated from test data of ref. 14 on an isolated body of similar geometry, with the angles of attack modified to account for the effects of wing upwash. Pylon tank strut aerodynamic properties are determined from simple theory, considering it as a swept-forward wing of low aspect ratio with the airplane wing acting as an end-plate and the pylon tank being a partially effective end-plate. Strut characteristics are shown in fig. 74.

PROPELLER SIDE LOADS

Propeller loads may be determined from the Hamilton Standard equation for propeller side force:

$$\frac{F}{\propto q\left(\frac{\pi D^2}{4}\right)} = \frac{.0256}{410}\left[\ AF\ \right]\left[\frac{N}{4}\right]\left[\frac{4}{\pi}\right]\text{Sin}\ (\beta_{.75R} + 10°)$$

where

F = propeller side load, lbs.;

$\propto$ = angle of relative wind with respect to axis of rotation, degrees;

q = dynamic pressure, $\frac{\rho V^2}{2}$ lbs. per sq. ft.;

D = propeller diameter, 15 ft.;

AF = propeller activity factor, 150;

N = number of blades, 3;

$\beta_{.75R}$ = propeller blade angle at .75 radius, fig. 75.

Substituting the known values in the foregoing gives:

$$F = 1.58\ \propto'\ q\ \sin\ (\beta_{.75R} + 10°)$$

The loads in pitch are computed for an angle of attack, $\propto'$, corrected for upwash induced by the presence of the wing such that

$$\propto' = 1.32\left[\propto_{FRL} + 0.7°\right]$$

For propeller loads in yaw, $\alpha' = \psi$.

PARATROOPER SHIELD DOORS

Paratrooper shield door normal force coefficient variation with door position is presented in fig. 76. A range of values is given to allow for effects of airplane yaw. The curves are estimated from wind tunnel test data on various airplane fuselage dive flaps, principally those of the Lockheed P-80 reported in ref. 5.

NOSE LANDING GEAR DOORS

The nose gear doors include three panels which, when closed, form part of the fuselage contour. The forward door is rectangular in shape and is hinged along its forward edge so that, in its extended position, it is similar to a fuselage dive-flap. The rear doors are also rectangular in shape and are arranged symmetrically on either side of the airplane centerline. Each of these doors operates from a linkage which, in opening, allows it to drop down from the fuselage a short distance, enough to clear and then to move sideways along the fuselage contour to clear the wheel well. In the closed position, the forward door is subject to fuselage pressure distribution, estimated to vary between limits of $\frac{\Delta p}{q} = -0.2$ to $+0.1$, accounting for angle of attack variations. When fully open, the forward door is subject to an airload equivalent to a pressure coefficient of $\frac{\Delta p}{q} = 1.2$ tending to close it. During extension, the loads are assumed to vary linearly between the foregoing values. The external face of the rear doors are subject to a pressure coefficient of $\frac{\Delta p}{q} = -0.2$ to 0 in any position. In addition, a ram pressure coefficient of $\frac{\Delta p}{q} = 0.5$ exists between the side of the fuselage and the inner face of the panel.

MAIN LANDING GEAR DOORS

Air load coefficients for the main gear doors are presented in fig. 77. These data are determined from a survey of past design practice and wind tunnel and flight test results on bomb bay and landing gear doors of several Lockheed airplanes.

LOCKHEED C-130

CARGO DOOR HINGE MOMENTS

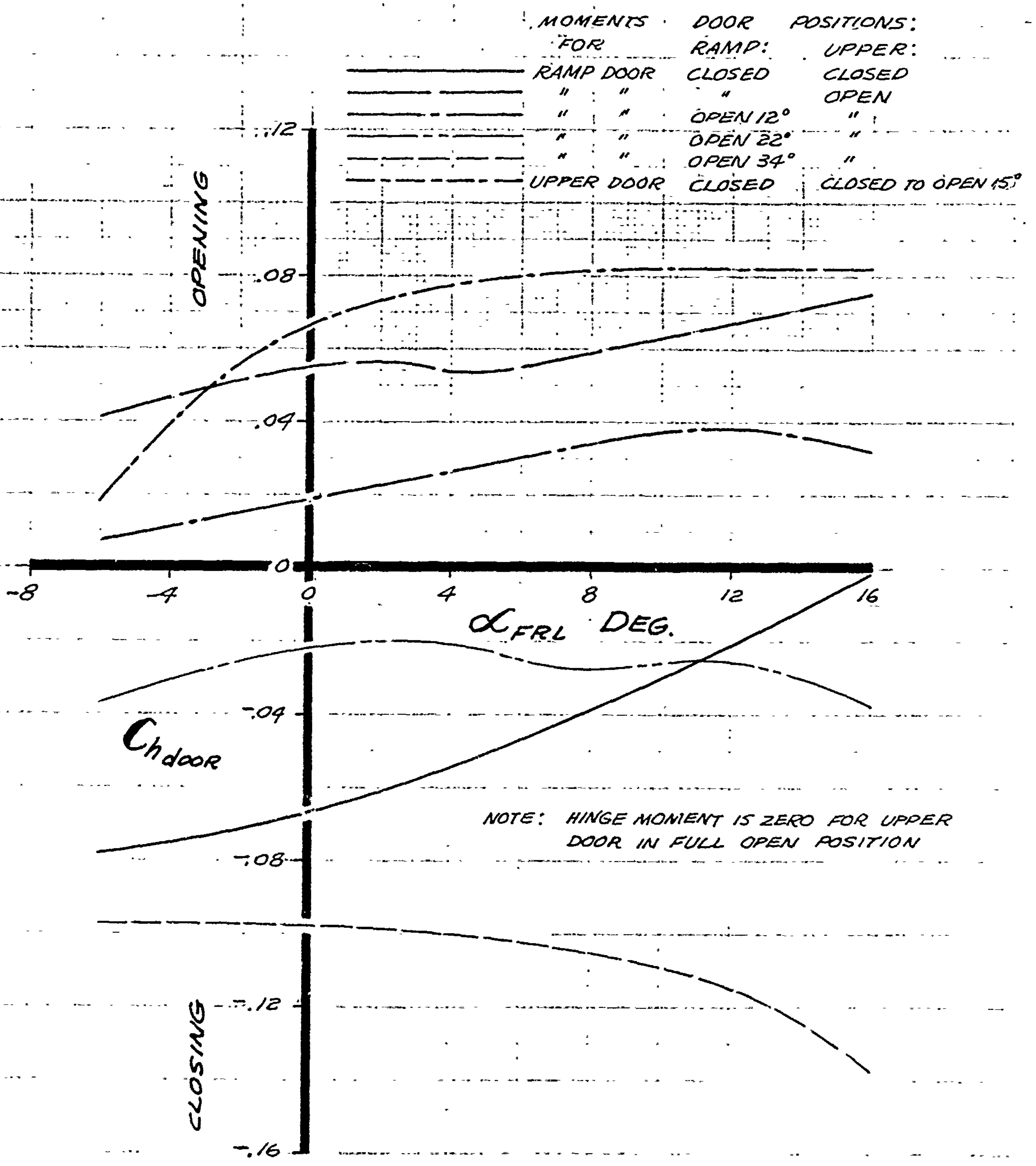

FIG. 70

PREPARED BY R.L.D.
DATE 10-26-51
CHECKED BY

LOCKHEED AIRCRAFT CORPORATION

PAGE 93
MODEL C-130
REPORT NO. 9062

LOCKHEED C-130

FLAP LOAD COEFFICIENTS

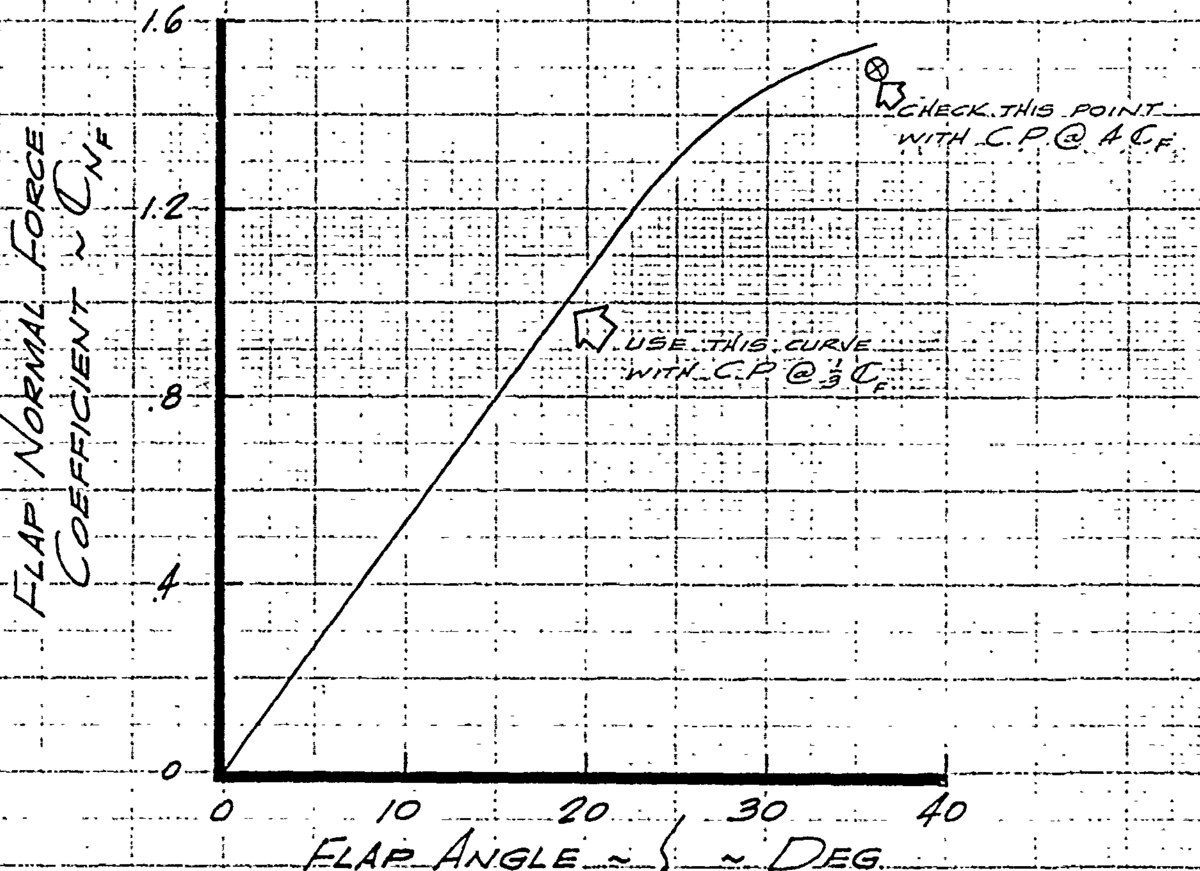

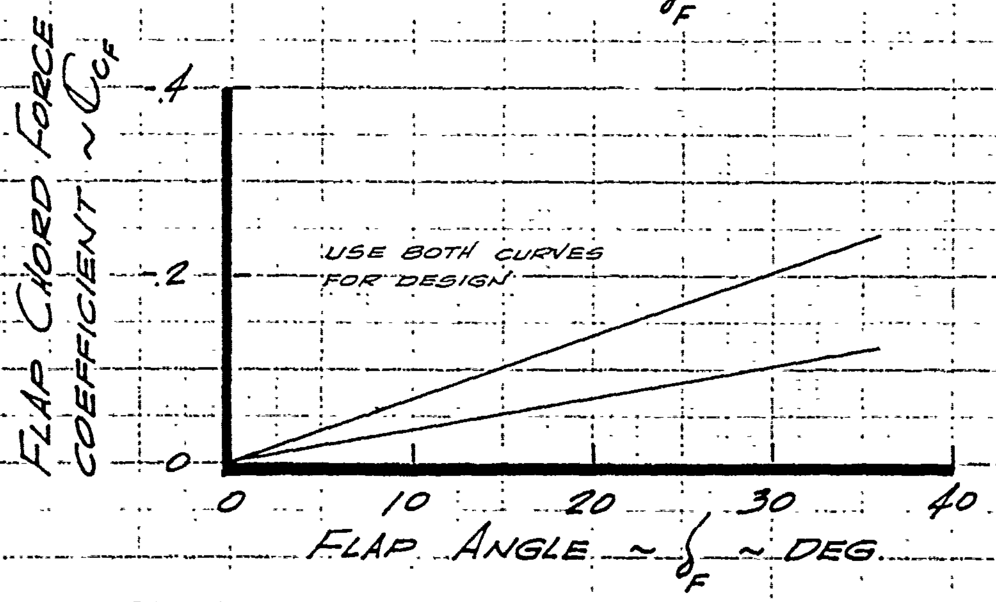

LR 25742

FORM 3278

FIG. 71.

LOCKHEED C-130

ESTIMATED PRESSURE DISTRIBUTION ON NACELLES

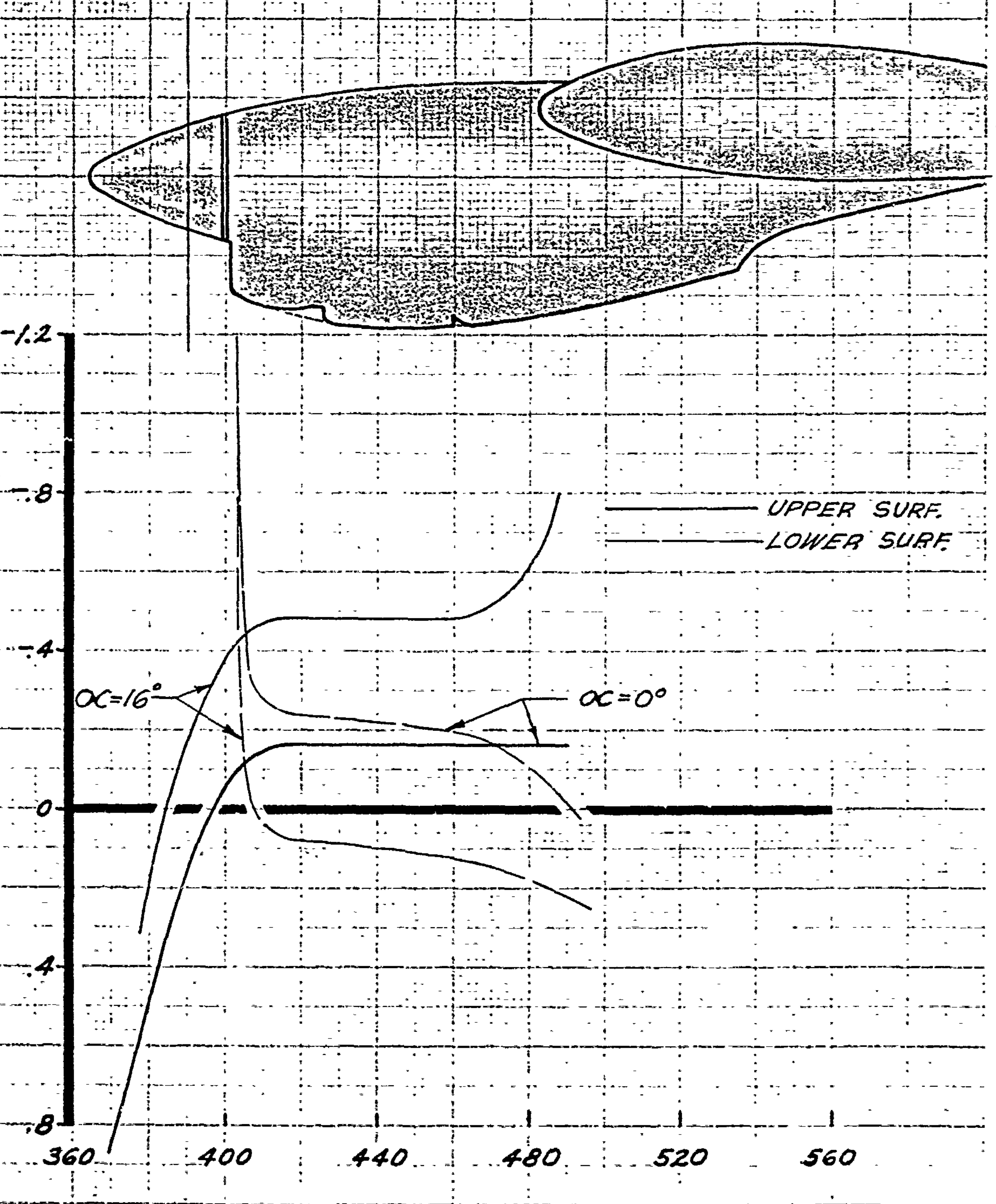

FIG. 72

LOCKHEED C-130

PYLON TANK AERODYNAMIC CHARACTERISTICS

$$C_L, C_D, C_C = \frac{(L, D, C)}{qA}$$

$$C_m, C_n = \frac{(M, N)}{qAL}$$

A = FRONTAL AREA ; L = TANK LENGTH

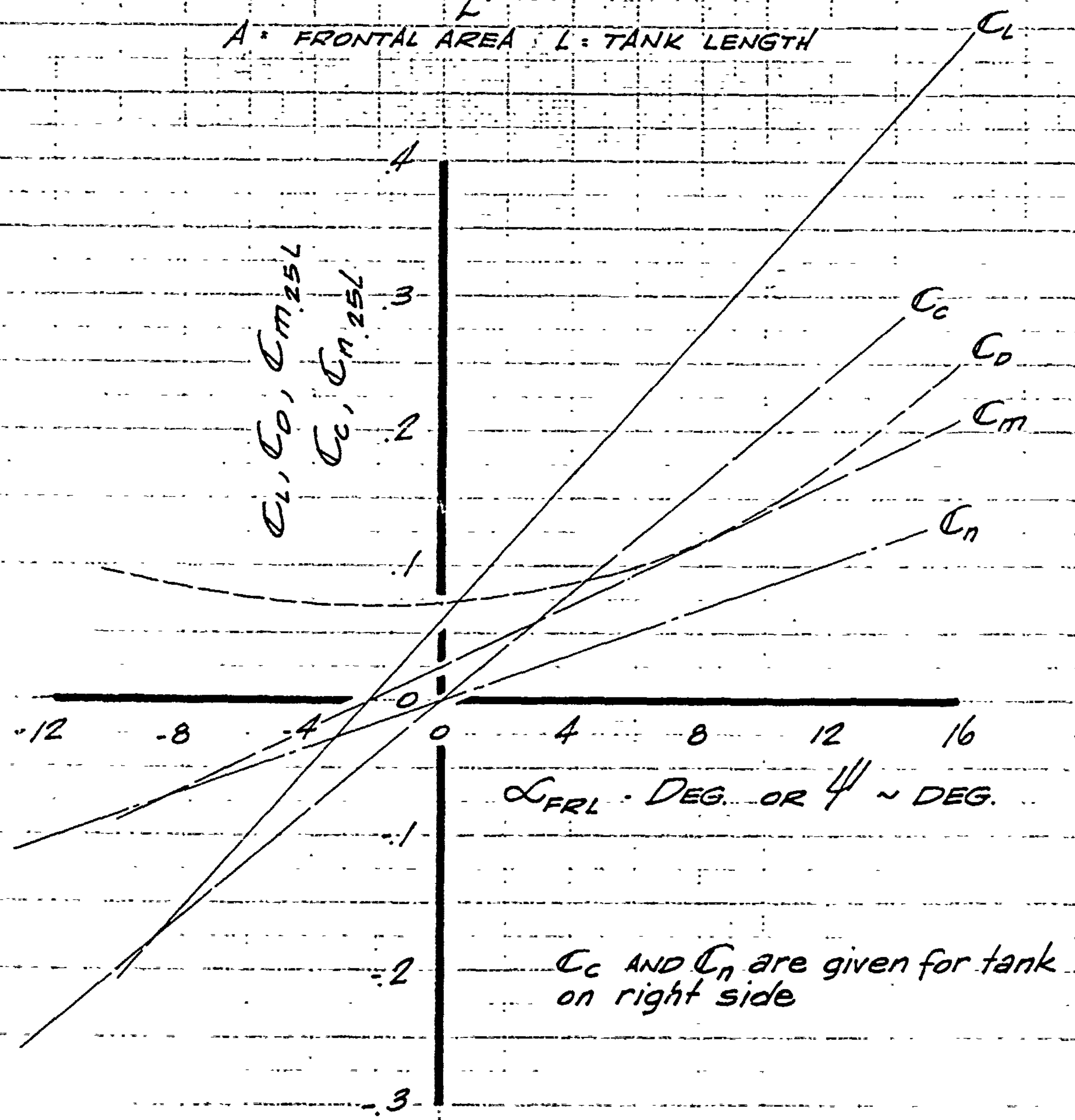

FIG. 73

Lockheed C-130

PYLON TANK STRUT AERODYNAMIC CHARACTERISTICS

coefficients are based on strut area. yawing moment about strut quarter-chord point is zero.

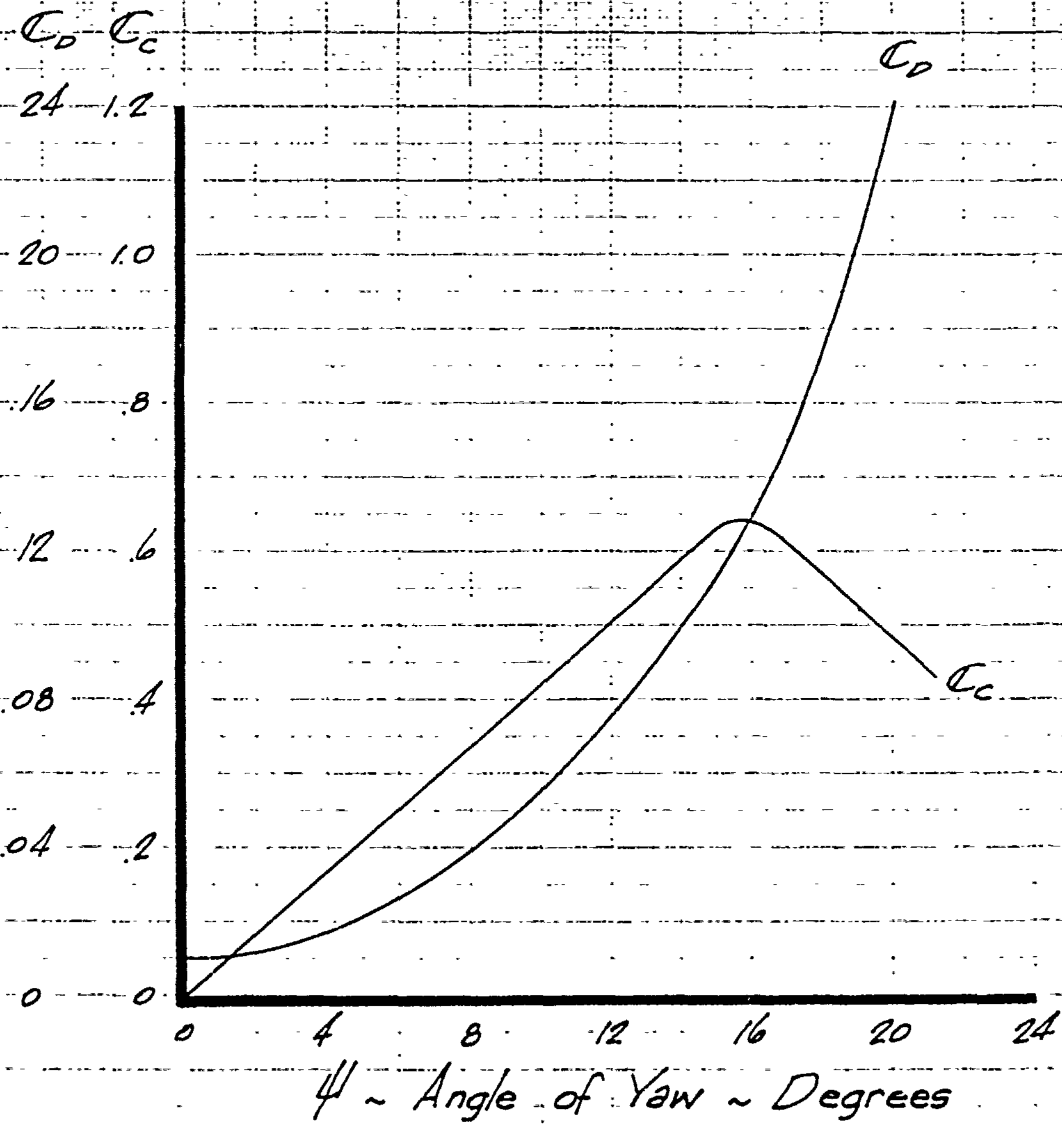

FIG. 74

LOCKHEED C-130

VARIATION OF PROPELLER BLADE ANGLE WITH SPEED

$\beta_{.75R}$ - BLADE ANGLE AT .75 RADIUS

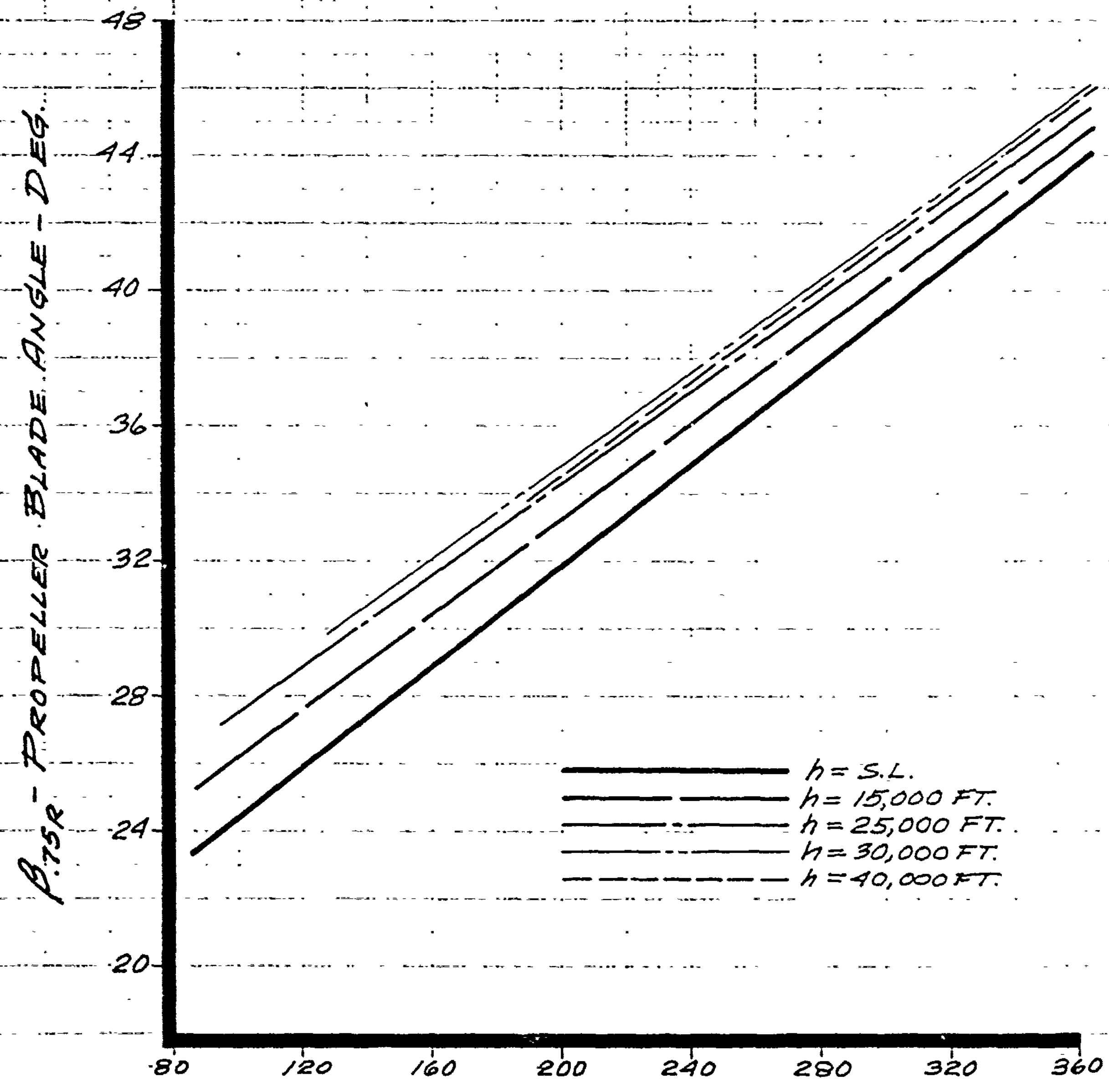

FIG. 75

LOCKHEED C-130

PARATROOPER SHIELD DOOR AIR LOADS

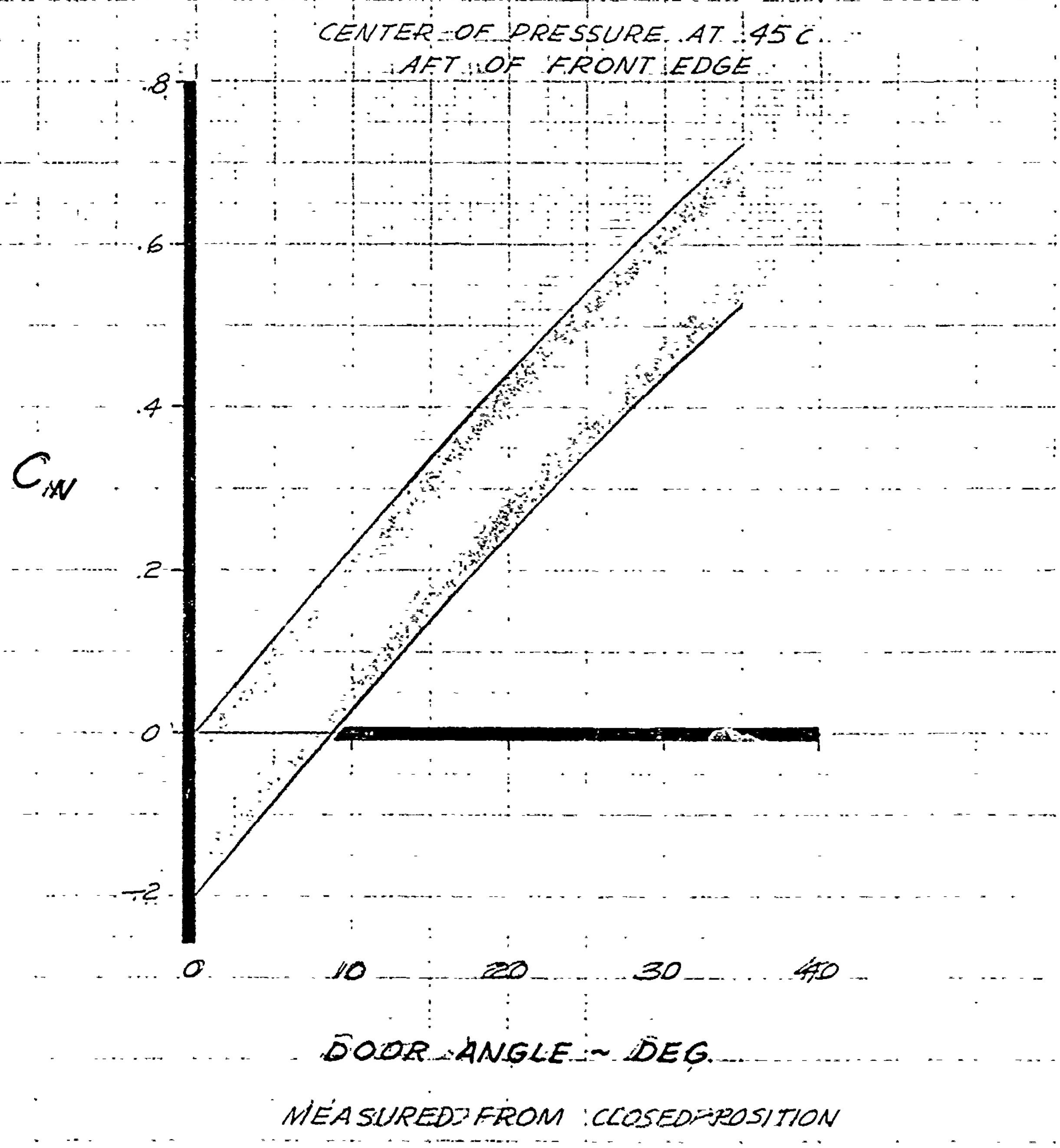

LOCKEED C-130

MAIN GEAR DOOR AIR LOADS

FOR USE WITH FULL DOOR CHORD AND AREA
FOR HINGED SECTION, USE LOADS RESULTING FROM THESE CURVES & ALSO FROM A UNIFORM PRESSURE EQUIVALENT TO $\Delta p/q = 0.10$

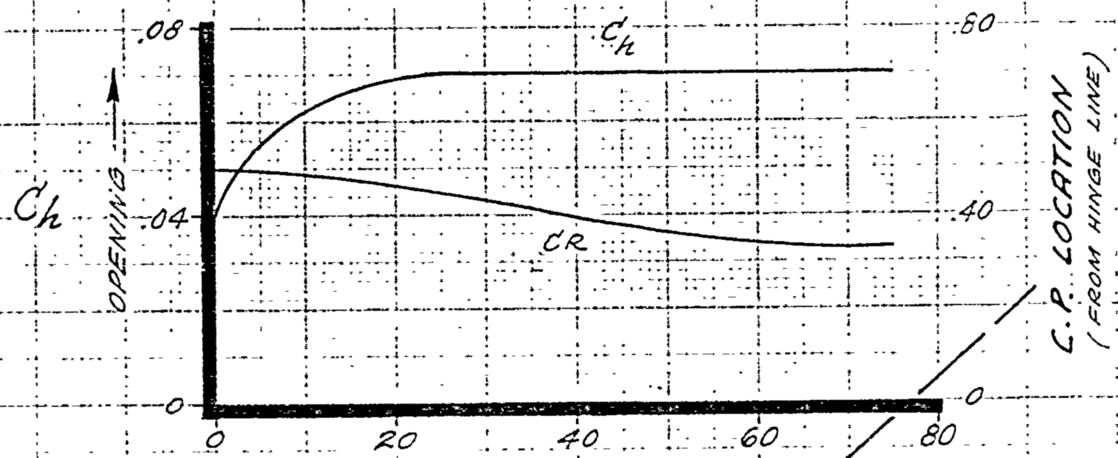

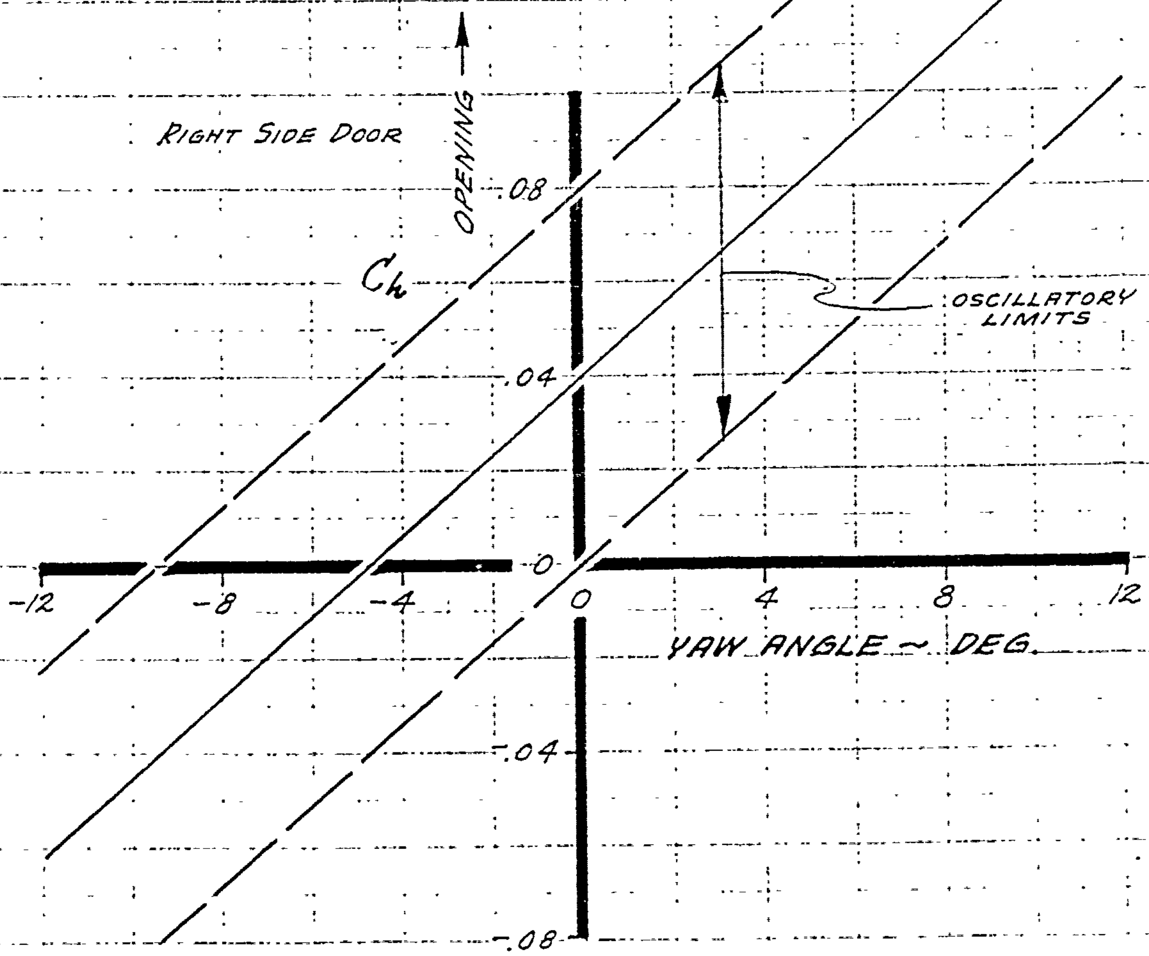

FIG. 77

CONTROL SYSTEM CHARACTERISTICS

All three primary controls are actuated with the aid of hydraulic boosters. In each system, motion of the pilot's control is transmitted through suitable linkages to an arm which operates the booster valve. When this valve is bottomed, which requires only a small fraction of an inch of control movement, further motion is transmitted to the control surface, with the pilot's effort magnified by the action of the boost cylinder. On the prototype airplane, provision has been incorporated in the design for varying the boost ratio. Control system characteristics based on nominal settings are presented in the following pages and curves; final setting for both prototype and production airplanes will be determined during flight testing. The effect of changing boost ratio will, for practical purposes, affect only the magnitude of the pilot force at booster cut-off, decreasing it in the same proportion by which the boost ratio is increased and vice-versa. Mechanical advantage between the pilot's control and the control surface remain unchanged and the hinge moment available at booster cut-off is only negligibly affected. The following data summarize the design requirements of the control surfaces, the control systems and the power boosters.

Elevator System

The nominal boost ratio averages approximately 35:1, as shown in Fig. 79, and with the variable feature of the prototype mentioned above, can be adjusted to any value between 27:1 and 80:1. Owing to the mechanical design of the system. the boost ratio and the other characteristics vary somewhat with control surface position; exact values of each are given in Figs. 78 and 79. The hydraulic supply to the cylinders has been made adequate to permit elevator movement rates of 40 degrees per second at one-third of the design hinge moment for short intervals and 10 full cycles per minute for continuous movement at approximately one-half of booster capacity.

The foregoing relationships have been crossplotted in Fig. 80 to show the variation of pilot effort with elevator hinge moment for several elevator angles. This plot illustrates the effectiveness of the boost system in aiding the pilot and shows that, for practical purposes, the hinge moment available at maximum booster output is the designing factor; further effort by the pilot produces only a negligible increase.

Rudder System

As with the elevator, the mechanical advantage of the rudder system is determined from the relation between the desired rudder pedal length and travel and the required rudder deflection. Hinge moment output capacity required has been determined to be critical for the case of an engine failure at take-off. A value of 3,450 ft.-lbs. with full rudder has been set, which allows sufficient margin of control for this case and which determines the design of the booster cylinder and linkage to the rudder. Maximum pilot effort associated with this output is approximately 180 lbs. which, with the other factors, sets the boost ratio. The nominal boost ratio, based on the foregoing, averages approximately 52:1 and, on the prototype, can be adjusted to any value between 26:1 and 78:1 as explained above. This system provides adequate control at low speeds, with vertical tail loads within reasonable limits. At small rudder angles, the system provides over 4,000 ft.-lbs. of hinge moment capacity which, coupled with the hinge moment coefficient and airplane stability characteristics, results in more than sufficient control and unduly large design vertical tail loads in high speed flight. These loads exceed 120 lbs. per sq. ft. of surface, as compared to less than 90 on comparable airplanes. It was ascertained that the penalties associated with the foregoing could be avoided by reducing the hinge moment output of the boost cylinders for all flight with flaps retracted. Thus, for all flight with flaps extended in any amount, the system is as described above while, with flaps retracted, pressure to the boost cylinder is reduced from 3,000 psi to 1,600 psi with a proportionate decrease in hinge moment output. The resulting system provides ample high speed control, and design vertical tail loads are maintained within reasonable limits. Actual values, based on the nominal boost ratio setting, of the several parameters discussed here are given in Figs. 81, 82 and 83. Certain of these relationships have been crossplotted in Fig. 84 to show the variation of rudder pedal force with rudder hinge moment. The effect of the dual output system, dependent on flap position, is clearly demonstrated here. Also, it is readily apparent that pilot effort beyond that for boost limit produces only negligible effects. The hydraulic supply to the boost cylinders has been made adequate to permit rudder movement rates of 40 degrees per second under one-half of the design hinge moment for short intervals and, for continuous movement, 10 full cycles per minute at approximately one-half of design hinge moment.

Aileron System

Design requirements of the aileron system were set to obtain full aileron travel at $V_T \sigma 1/2 = 200$ knots. With the booster designed for this condition, it was found that appreciably greater hinge moments are available at lesser wheel throws, due to the mechanism of the system which produces dissymetry between up and down aileron travel, so the nominal boost ratio of approximately 50:1 was set so that no more than 80 lbs. pilot effort would be required to attain full booster output at any wheel position consistent with the speed range of the airplane. On the prototype airplanes, the boost ratio may be adjusted to any value between 20:1 and 75:1 as found to be desirable during flight testing. The several parameters necessary to determine the relation between aileron hinge moment and wheel force are presented in Figs. 85, 86 and 87. Figs. 88 and 89 show variation of pilot force and aileron hinge moment with wheel angle for several speeds. The hinge moment data of Fig. 54 have been used with the control and boost system characteristics to determine these plots. The hydraulic supply to the cylinders has been made adequate to permit aileron movement ratio of 40 degrees per second at one-quarter of the design hinge moment for short intervals and 15 full cycles per minute for continuous movement at approximately one-half of design hinge moment.

Control Surfaces Tabs

All tabs are electrically driven and are used to trim pilot forces. Design loads are presented in the table below for conditions determined to be critical. These hinge moments may be regarded to result from a triangular pressure distribution with its peak at the tab hinge line. Tab hinge moment coefficients used are plotted in Fig. 90.

	Rudder	Aileron (One Side)	Elevator (Each Side)
Tab Area, Sq. Ft.	5.0	2.9	7.64
Tab. Chord, In.	10.0	6.5	11.0
Max. Tab Angle, Deg.	±25	±20	±30
Max. Control Surface Angle, Deg.	±35	+15, -25	+15, -40
Limit Design HM, $_{max}$ V_H, In.-Lbs.	3140	1120	5750
Normal Operating HM, $= 10°$ V_H, In.-Lbs.	1430	700	2400
Minimum Operating Rate, Deg./Sec.	3.5	3.5	3.5

LOCKHEED C-130

ELEVATOR CONTROL SYSTEM
MECHANICAL ADVANTAGE

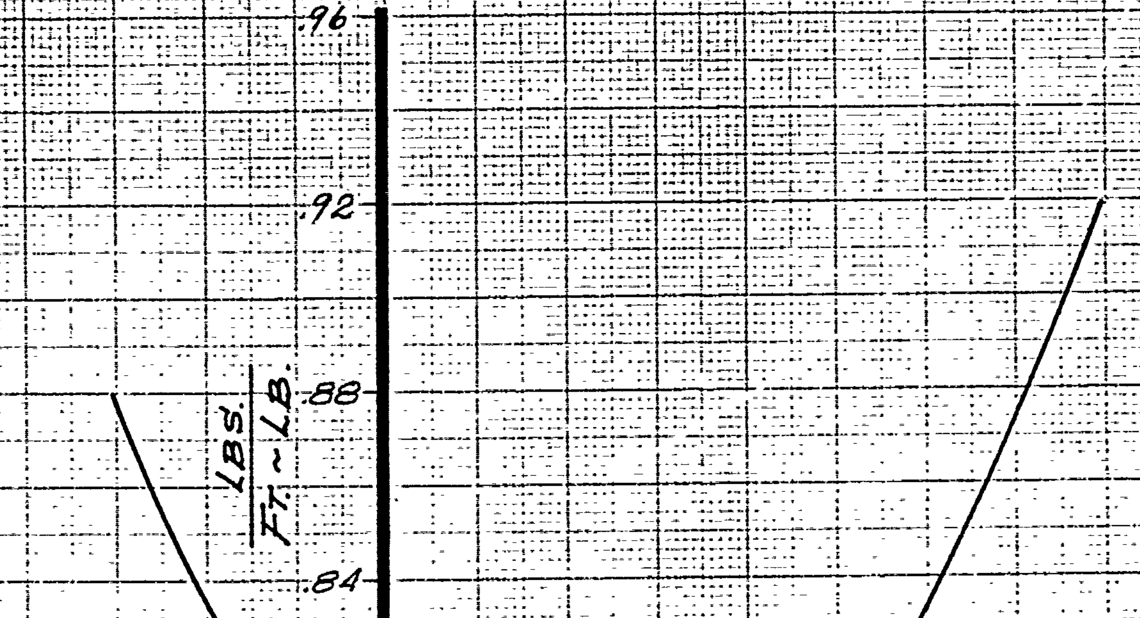

FIG. 78

LOCKHEED C-130

ELEVATOR BOOST SYSTEM CHARACTERISTICS

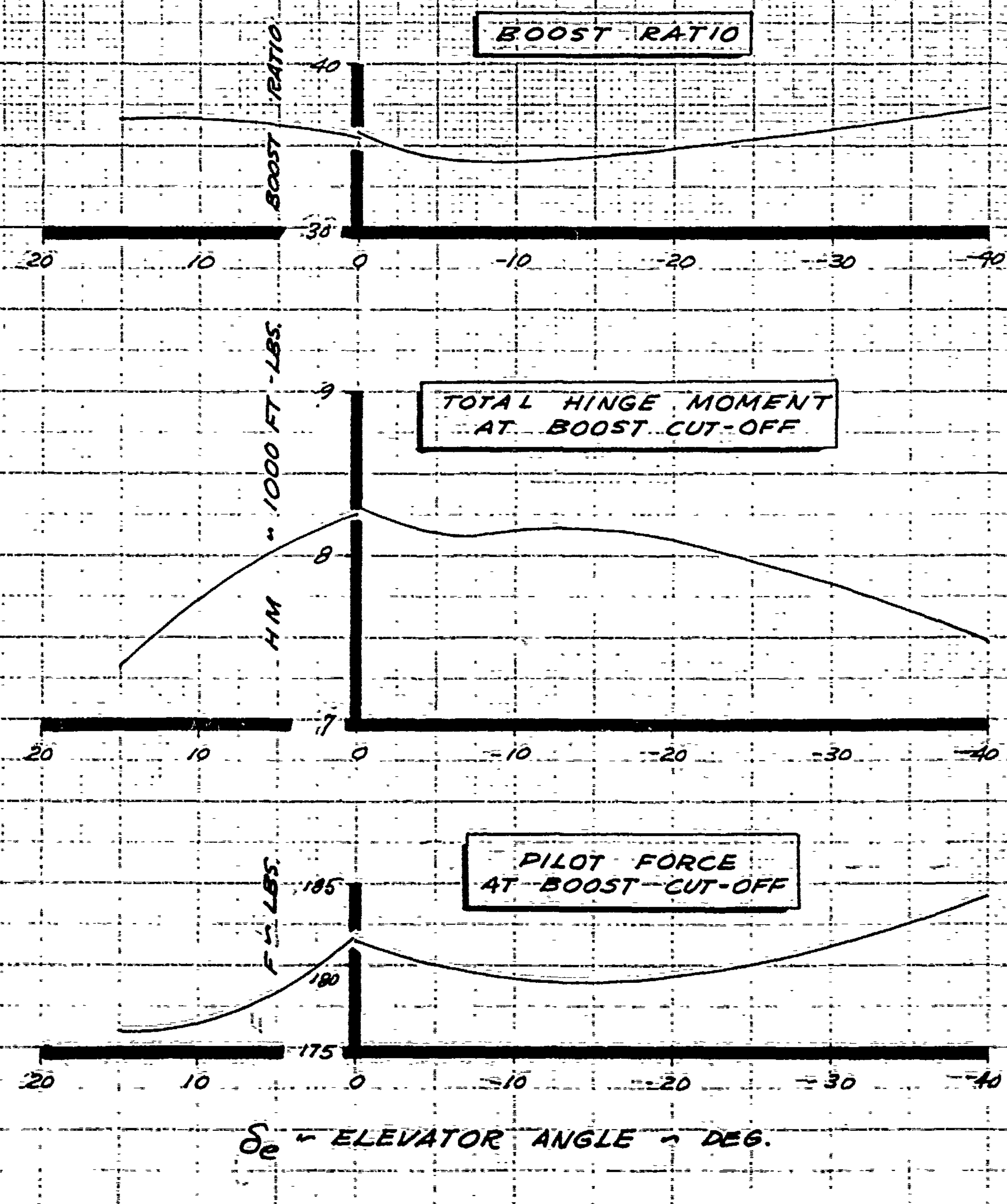

Fig. 79

LOCKHEED C-130

VARIATION OF PILOT FORCE WITH ELEVATOR HINGE MOMENT

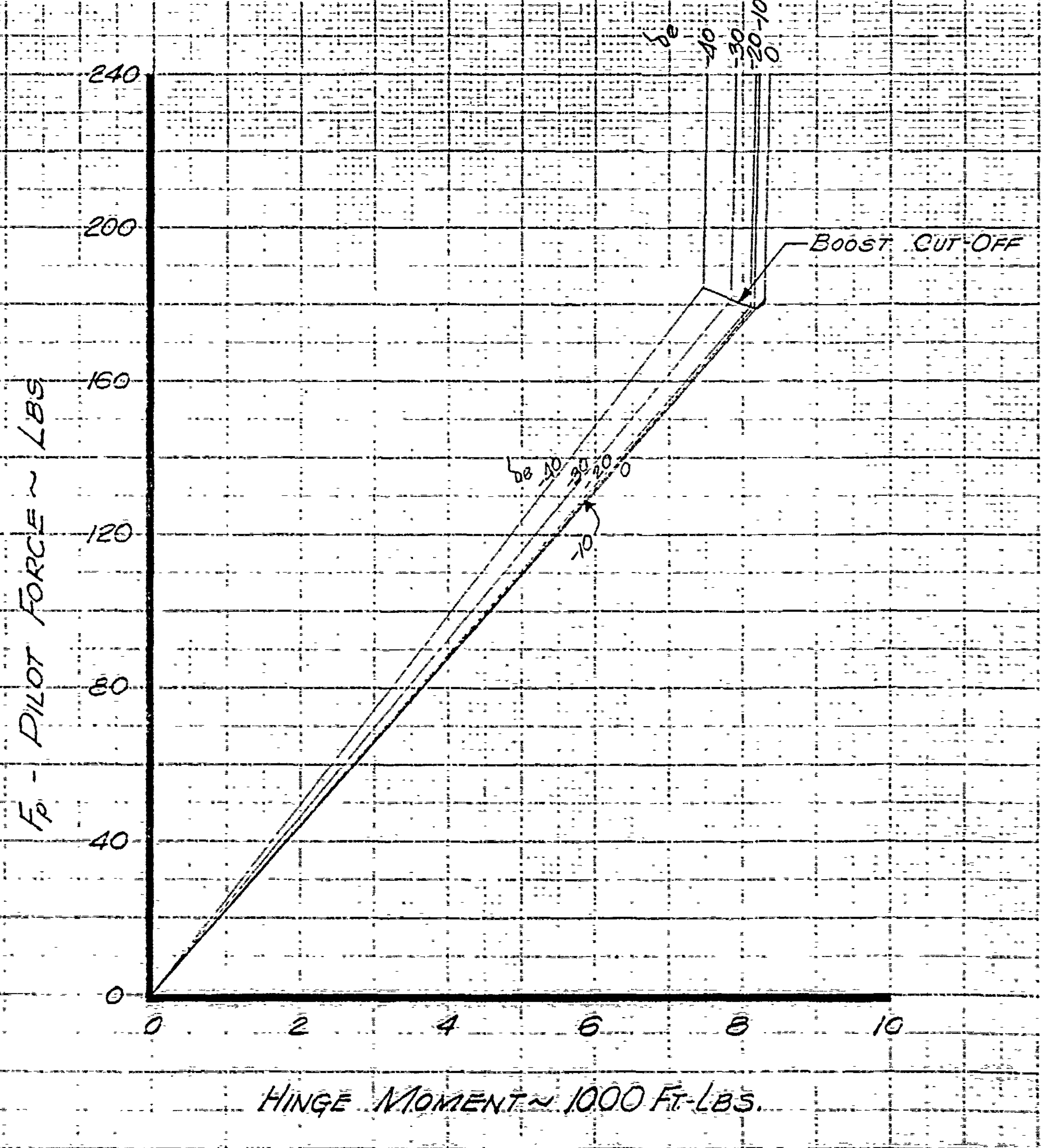

FIG. 80

LOCKHEED C-130

RUDDER SYSTEM CHARACTERISTICS

A. ~ MECHANICAL ADVANTAGE

B. ~ BOOST RATIO

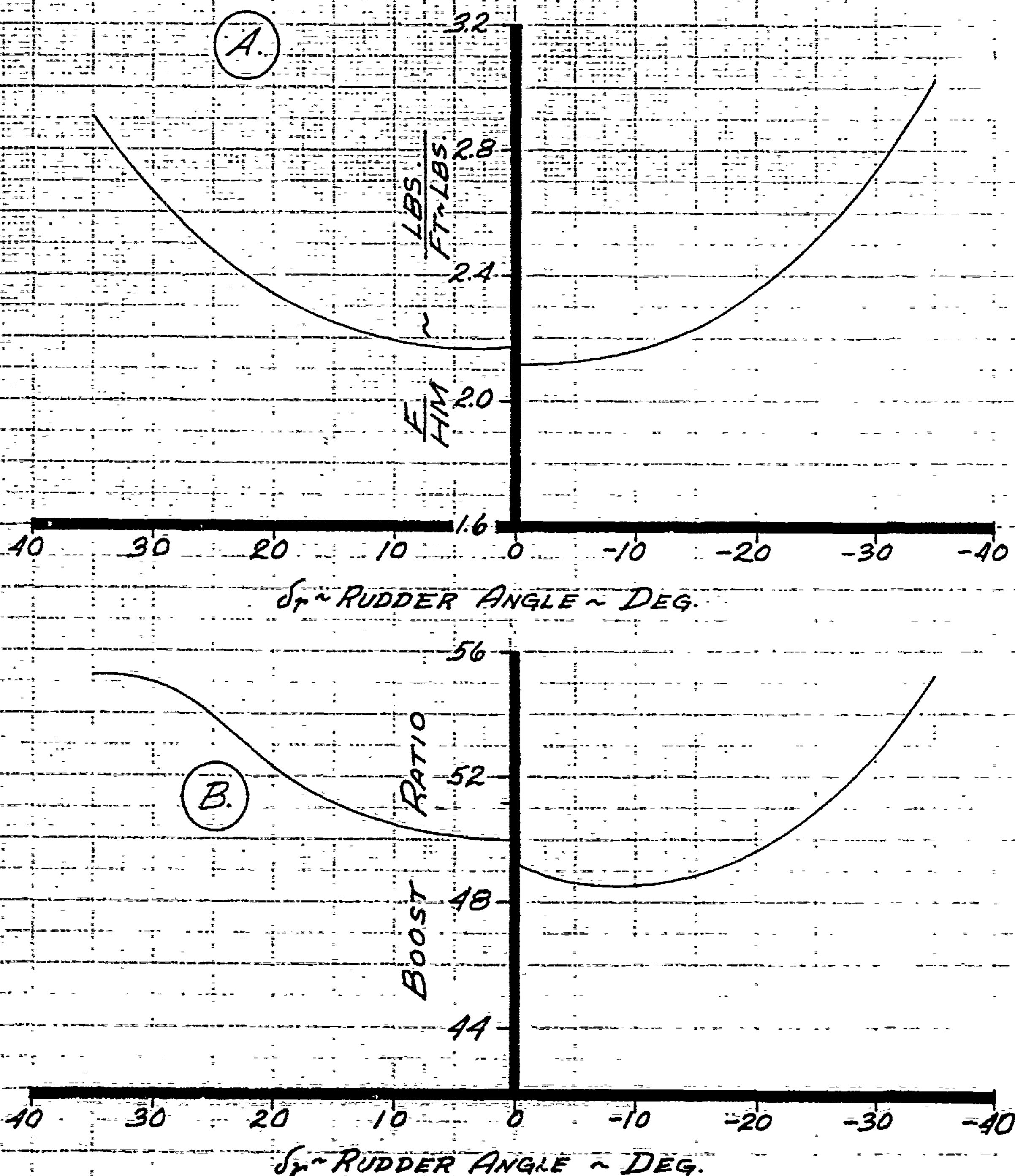

FIG. 81

PREPARED BY
DATE
CHECKED BY

LOCKHEED AIRCRAFT CORPORATION

PAGE 109
MODEL C-130
REPORT NO. 9062

LOCKHEED C-130

PEDAL FORCE AT RUDDER BOOST CUT-OFF

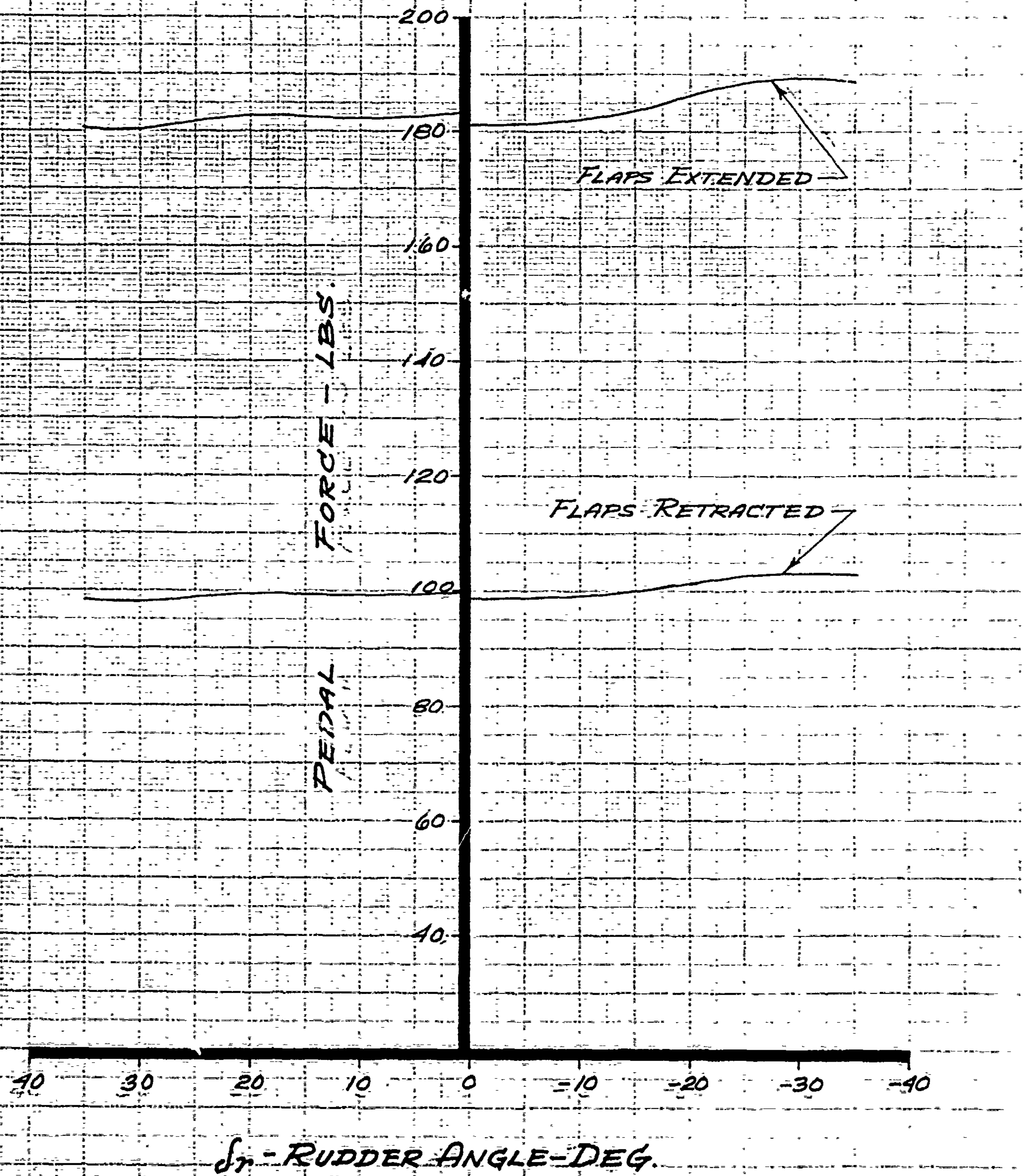

FORM 3278A

FIG. 82

LOCKHEED C-130

RUDDER HINGE MOMENT AT BOOST CUT-OFF

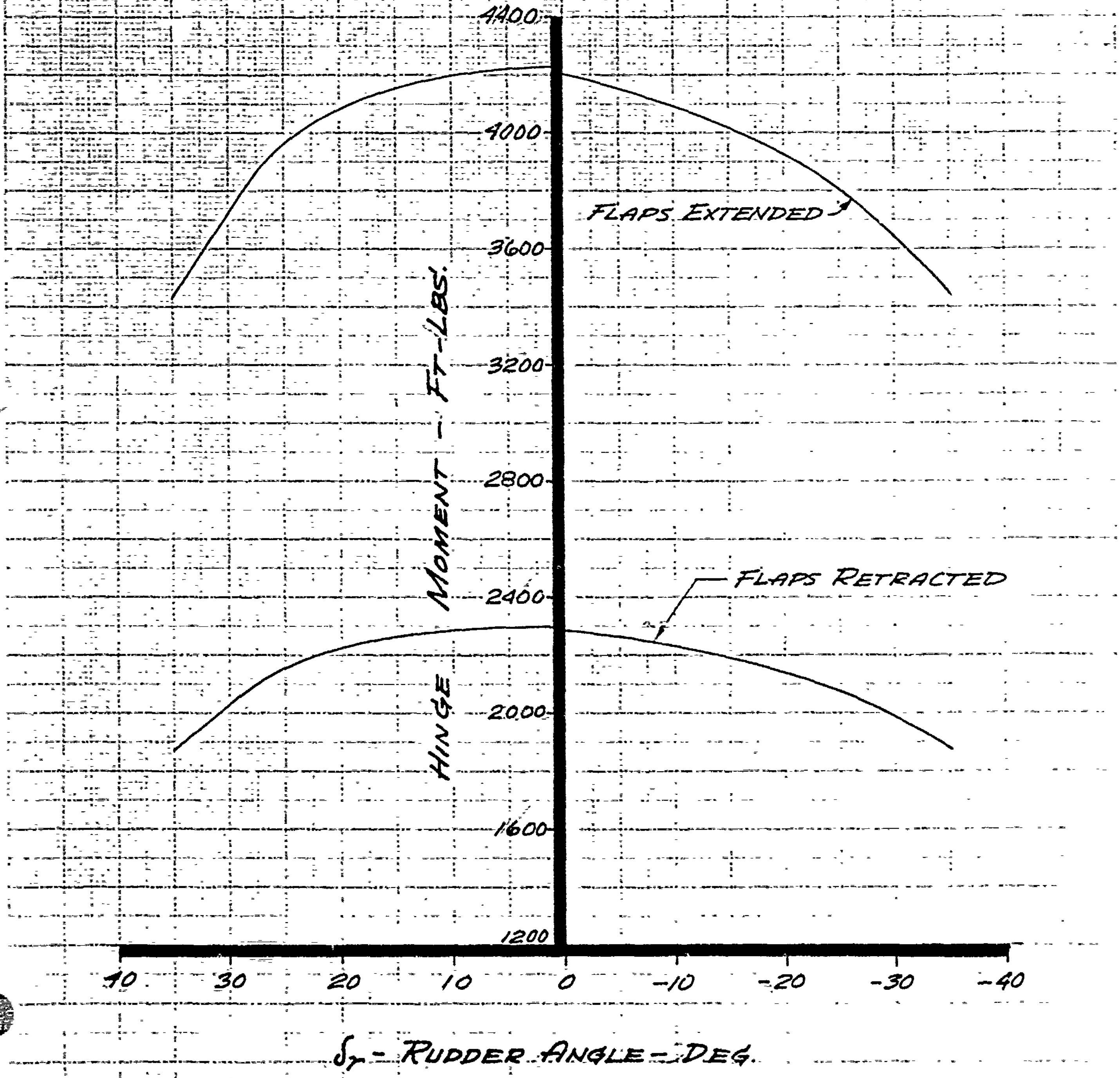

FORM 3276A

FIG. 83

LOCKHEED C-130

VARIATION OF PEDAL FORCE WITH RUDDER HINGE MOMENT

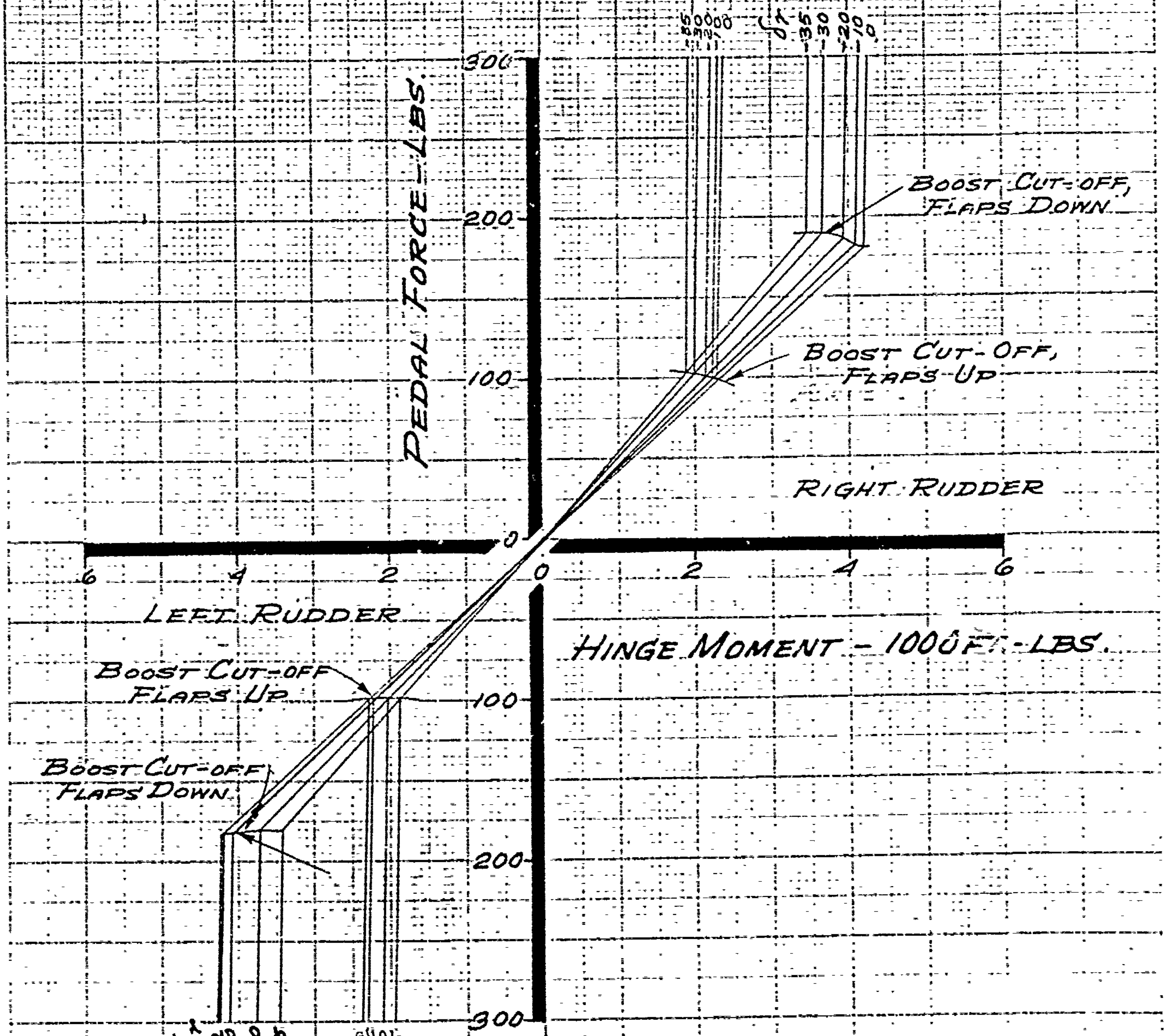

FIG. 84

PREPARED BY R.L.D.
DATE 9-16-52
CHECKED BY

LOCKHEED AIRCRAFT CORPORATION

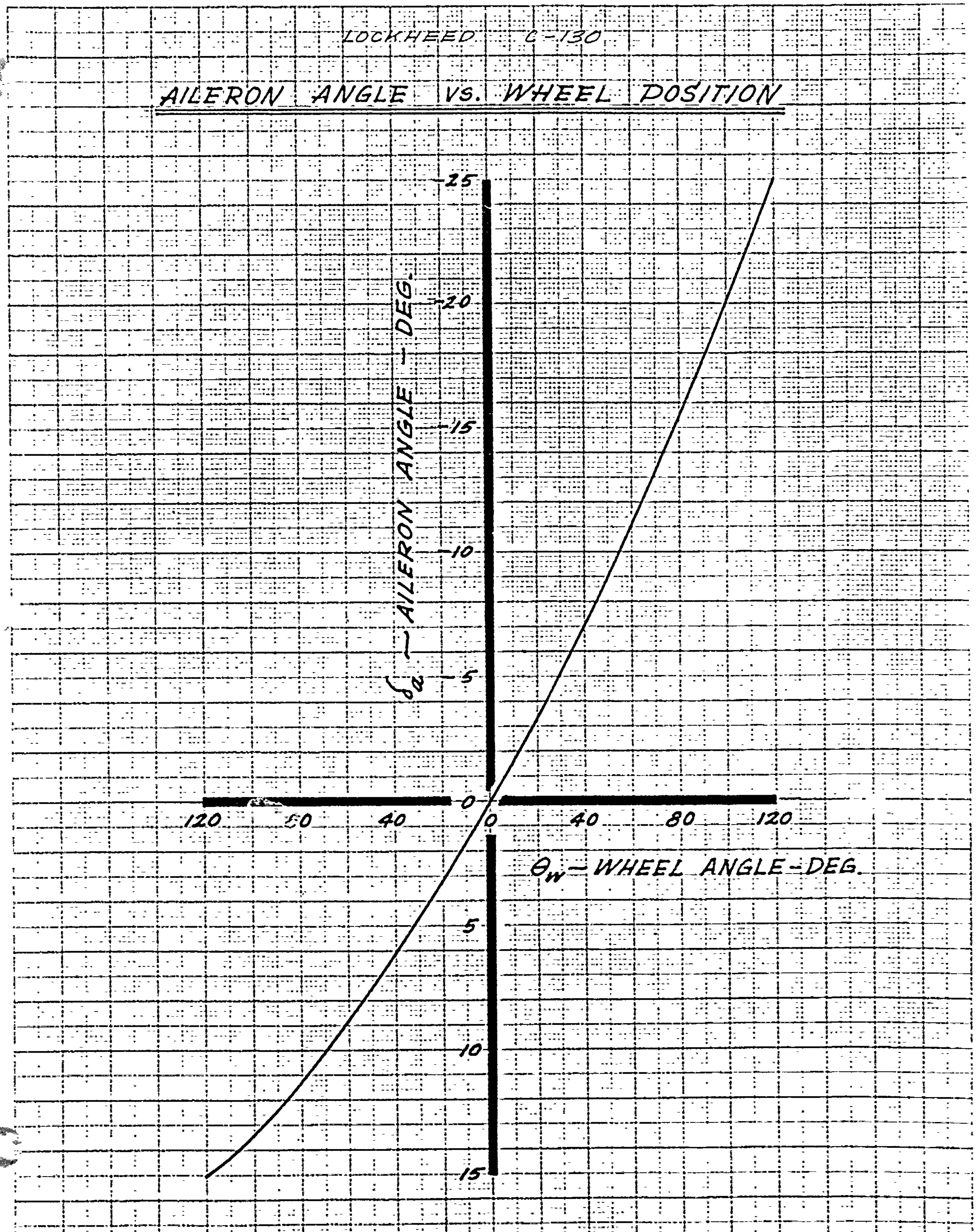

FIG. 85

PREPARED BY
DATE
CHECKED BY

LOCKHEED AIRCRAFT CORPORATION
CALIFORNIA DIVISION

PAGE 113
MODEL C-130
REPORT NO. 9062

LOCKHEED C-130

AILERON CONTROL SYSTEM

CHARACTERISTICS

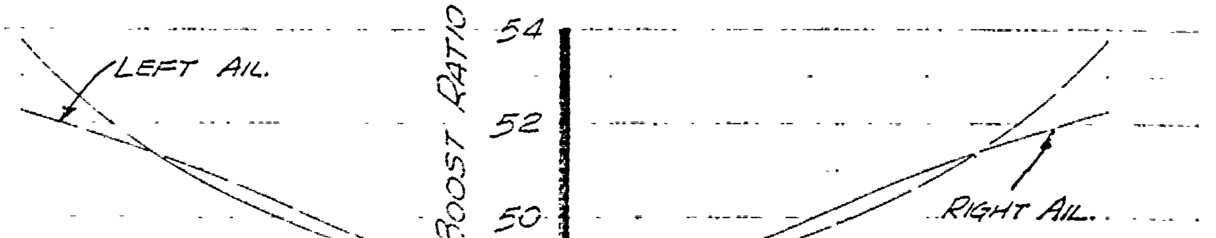

FIG. 86

FORM 5273

LOCKHEED C-130

WHEEL FORCE AT BOOST CUT-OFF

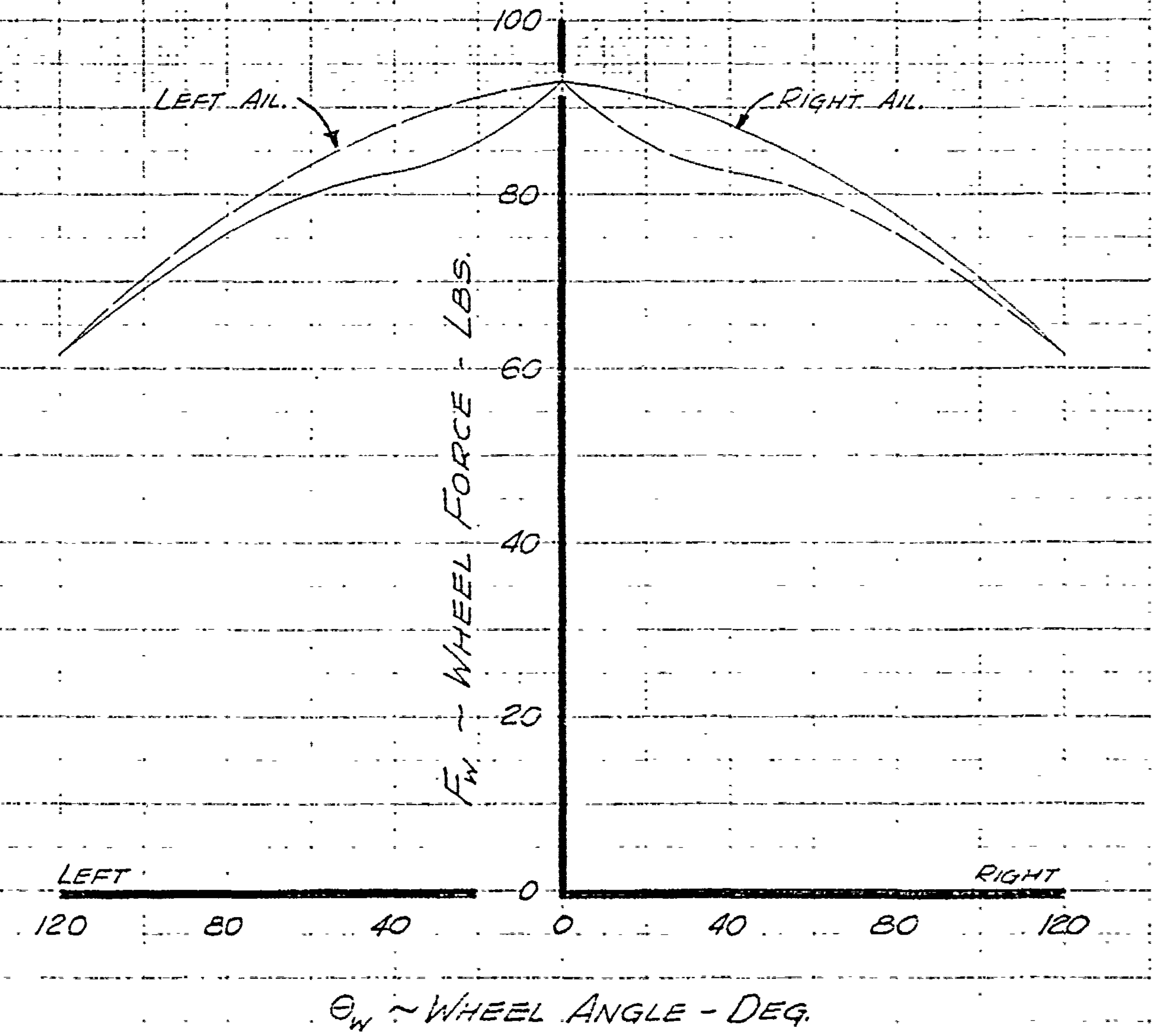

FIG. 87

FORM 5278

LOCKHEED C-130

AILERON HINGE MOMENTS

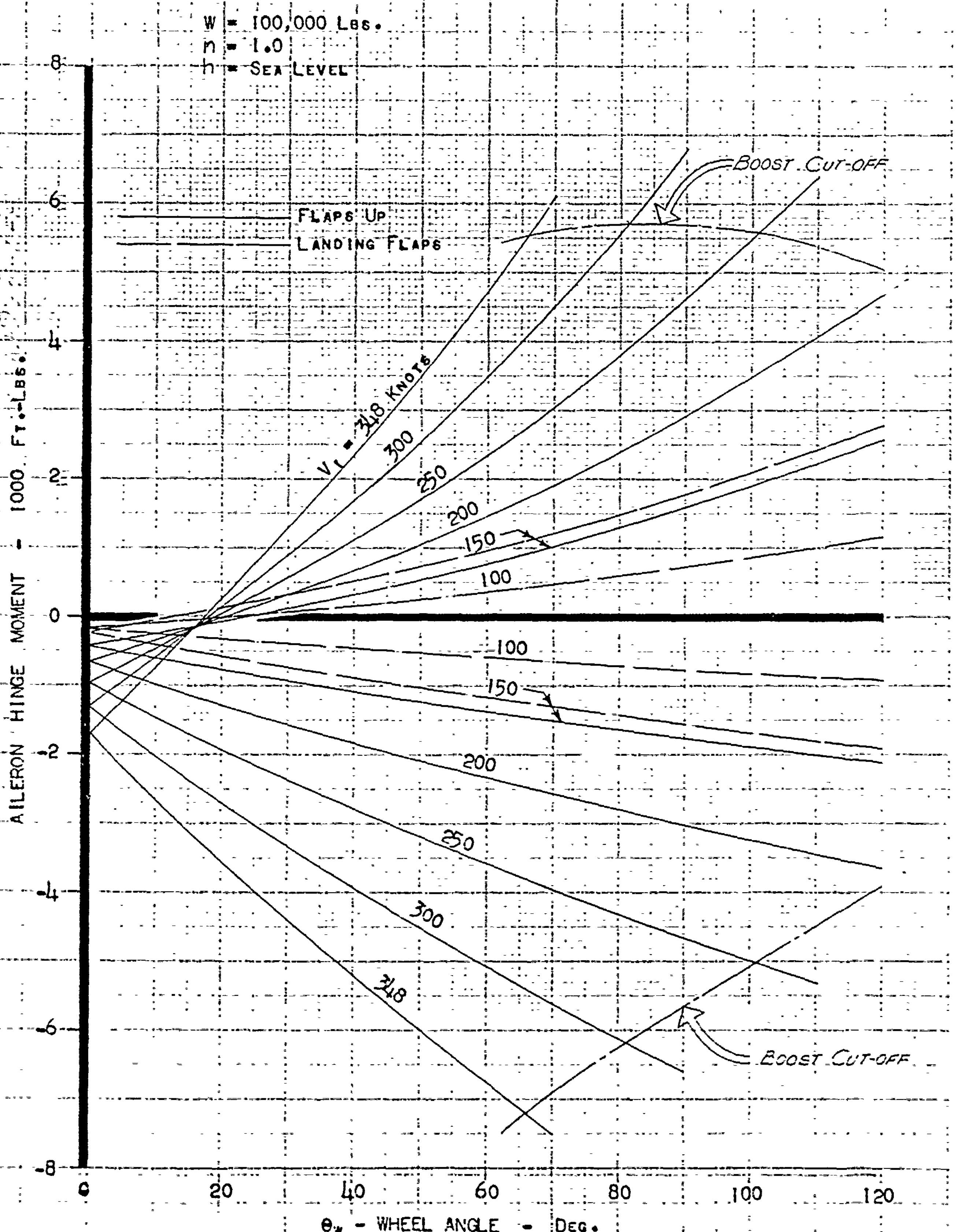

Fig. 88

LOCKHEED C-130

AILERON WHEEL FORCE VS WHEEL POSITION AT SEVERAL AIRSPEEDS

NOTE: THIS CURVE IS BASED ON A NOMINAL SETTING OF THE BOOST RATIO ADJUSTMENT AS DETERMINED BY CONTROL REQUIREMENTS.

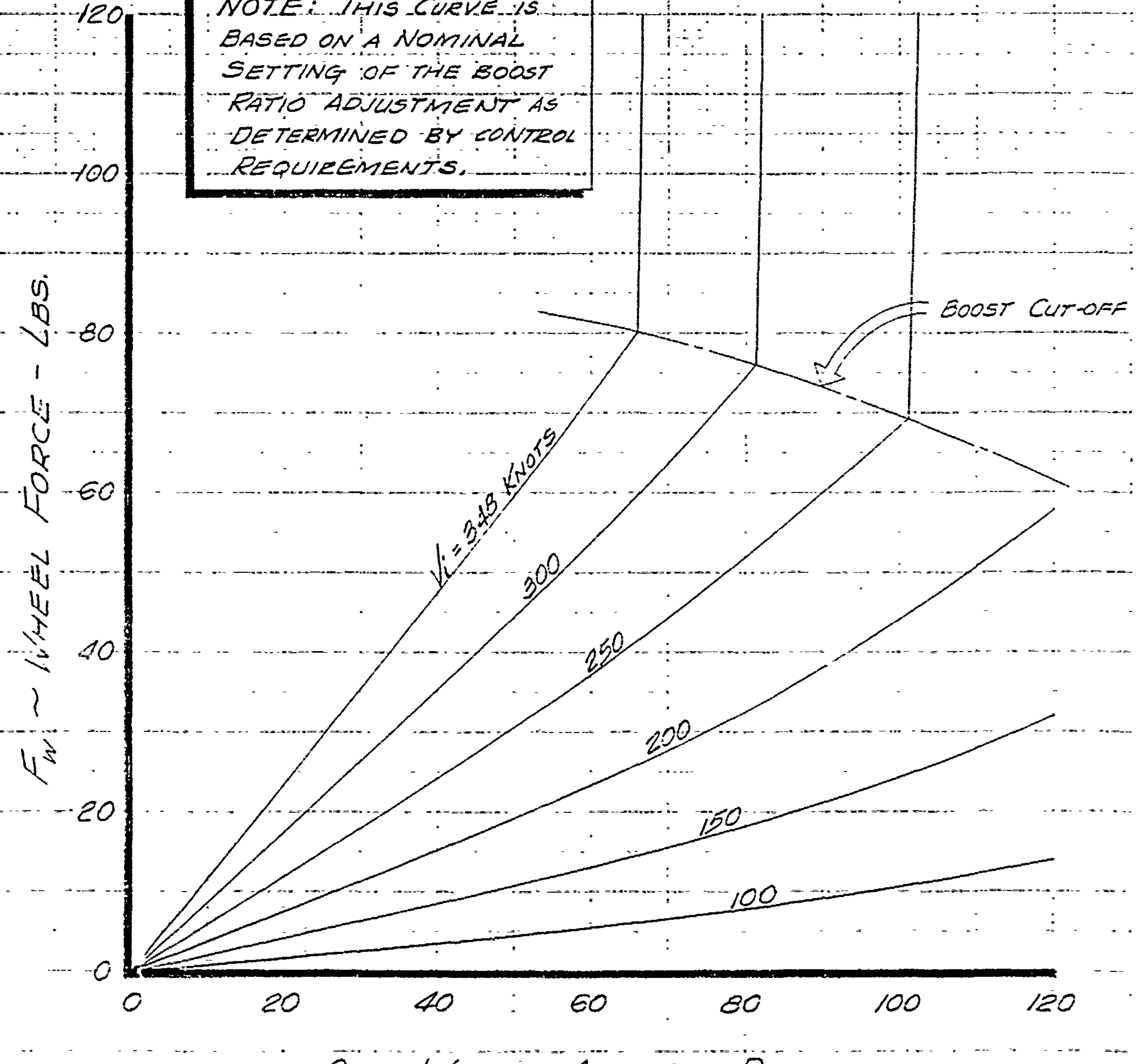

FIG. 89

LOCKHEED C-130

CONTROL SURFACE TAB

HINGE MOMENTS

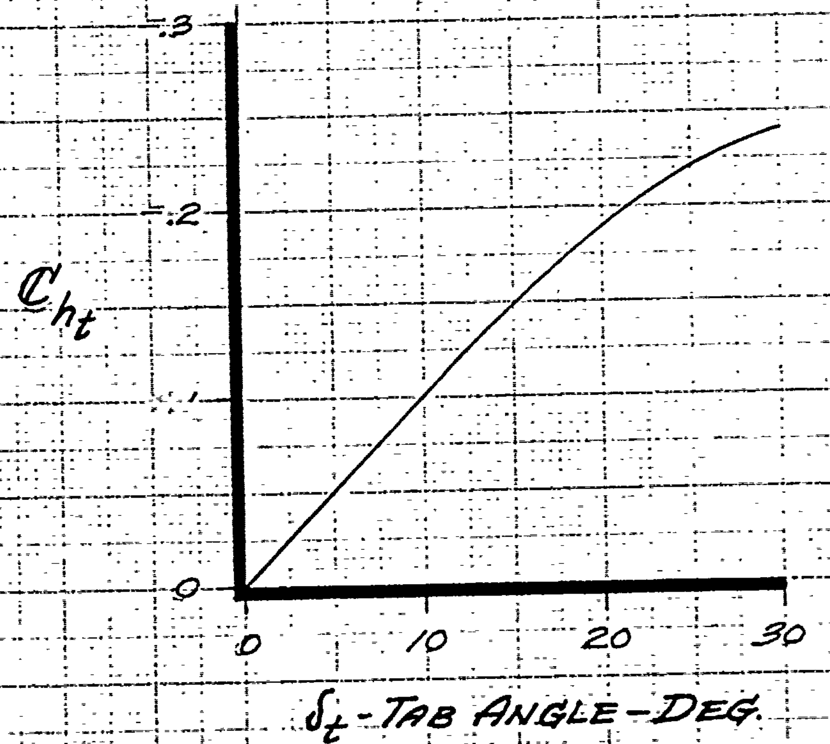

FIG. 90

REFERENCES

Lockheed Publications

1. LAL 201 - Low Speed Wind Tunnel Tests of a 1/15-Scale Model of the YC-130 Airplane.
2. LAL 205 - High Speed Wind Tunnel Tests of a 1/15-Scale Model of the XC-130 Airplane.
3. LAL 216 - High Speed Wind Tunnel Tests of a 1/15-Scale Model of the 082 Airplane (XC-130).
4. LAL 35 - Wind Tunnel Tests of a 20th Scale Powered Model of the Lockheed C-89 Airplane.
5. LAL 140 - Wind Tunnel Tests of 1/6-Scale XF-90 Model.
6. LR 2576 - Aerodynamic Structural Data Handbook.
7. LR 4710 - Aerodynamic Handbook.

NACA Publications

8. TR 620 - Pressure Distribution over Airfoils with Fowler Flaps, by Carl J. Wenzinger and Walter B. Anderson.
9. TR 824 - Summary of Airfoil Data by Ira H. Abbott, Albert E. Von Doenhoff, and Louis S. Stivers, Jr.
10. TR 868 - Summary of Lateral - Control Research, by Thomas A. Toll.
11. TR 903 - Theoretical and Experimental Data for a Number of 6A-Series Airfoil Sections, by Laurence K. Loftin, Jr.

REFERENCES (Continued)

12. TN 419 - Wind Tunnel Tests of the Fowler Variable - Area Wing, by Fred E. Weick and Robert C. Platt.

13. TN 763 - Wind Tunnel Investigation of Two Airfoils with 25-Percent-Chord Gwinn and Plain Flaps, by Milton B. Ames, Jr.

14. TM 1194 - Force and Pressure Distribution Measurements on Eight Fuselages, by G. Lange.

15. RM L7C05a - Tuft Studies of the Flow Over a Wing at Four Angles of Sweep, by Gerald Hiesser (Lockheed RM 200).

16. RM A8B11 - Wind Tunnel Investigation of Horizontal Tails.
II - Unswept and 35° Swept-Back Plan Forms of Aspect Ratio 4.5, by Jules B. Dods, Jr. (Lockheed RM 290).

17. RM A8H30 - Wind Tunnel Investigation of Horizontal Tails.
III - Unswept and 35° Swept-Back Plan Forms of Aspect Ratio 6, by Jules B. Dods, Jr. (Lockheed RM 401).

18. RM A51C12a- Influence of Airfoil Trailing-Edge Angle and Trailing-Edge Thickness Variation on the Effectiveness of a Plain Flap at High Subsonic Mach Numbers, by Albert H. Hemenover and Donald J. Graham (Lockheed RM 638).

19. RR - Wind Tunnel Investigation of Control-Surface Characteristics. I - Effect of Gap on the Aerodynamic Characteristics of an NACA 0009 Airfoil with a 30-Percent-Chord Plain Flap, by Richard I. Sears (Lockheed RR 103).

UNCLASSIFIED

UNCLASSIFIED

REFERENCES (Continued)

20. RR - Wind Tunnel Investigation of Control-Surface Characteristics - III - A small Aerodynamic Balance of Various Nose Shapes Used with a 30-Percent-Chord Flap on an NACA 0009 Airfoil by Milton B. Ames, Jr. (Lockheed RR 111).

21. RR - Wind Tunnel Investigation of Control Surface Characteristics. VI - A 30-Percent-Chord Plain Flap on the NACA 0015 Airfoil by Richard I. Sears and Robert B. Liddell (Lockheed RR 174).

22. ARR L4112a-Notes on the Propeller and Slipstream in Relation to Stability, by Herbert S. Ribner (Lockheed RR 455).

23. MR - Lift and Drag Tests of Three Airfoil Models with Fowler Flap, by Ira H. Abbott and Harold R. Turner, Jr. (Lockheed CM 153).

MISCELLANEOUS

24. University of Washington Aeronautical Laboratory Report No. 153, Wind Tunnel Tests of a 1/4 Scale Model of the Lockheed XP-58 Airplane Boom.

25. ANC-1(2) - Chordwise Air-Load Distribution.

UNCLASSIFIED

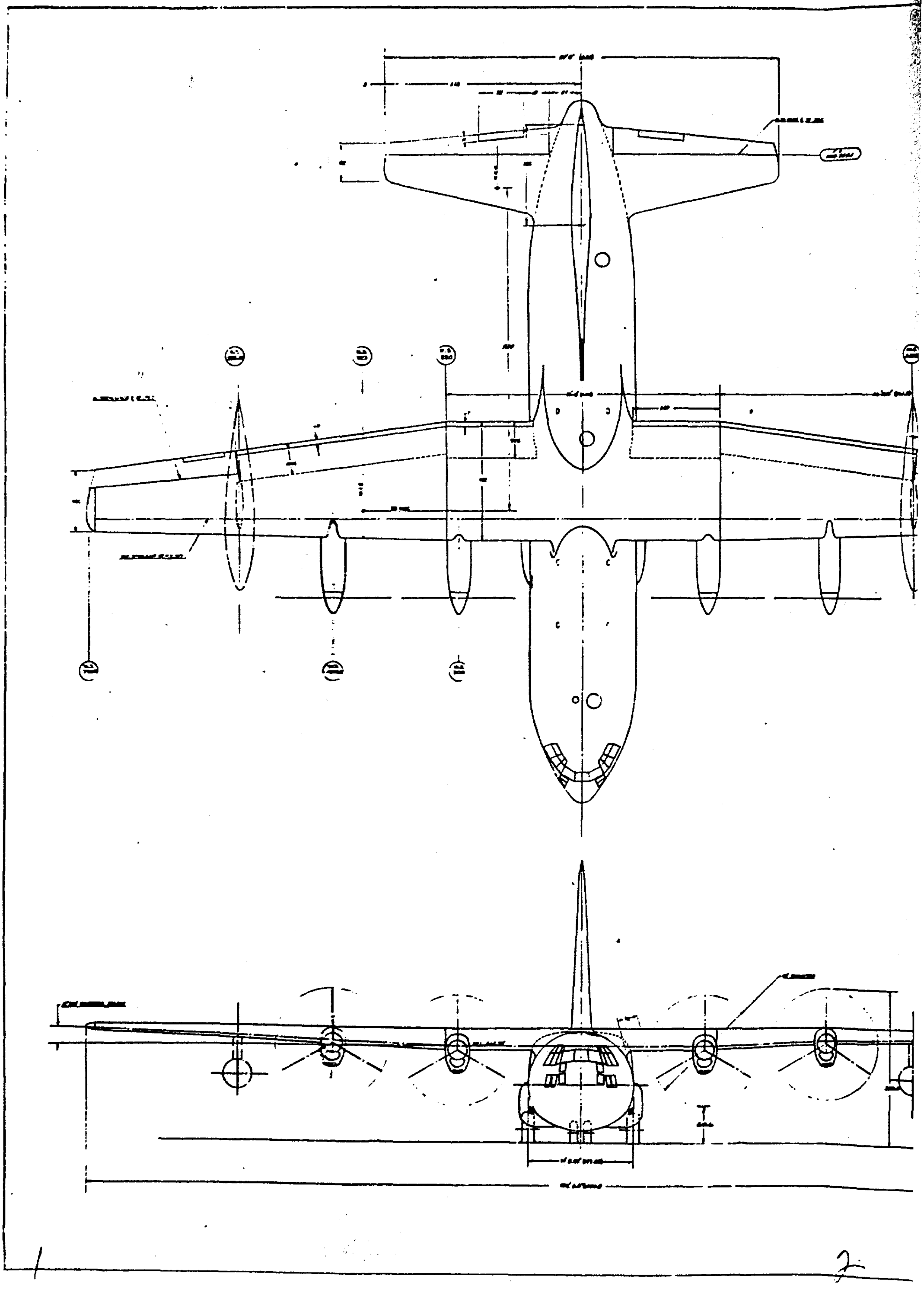

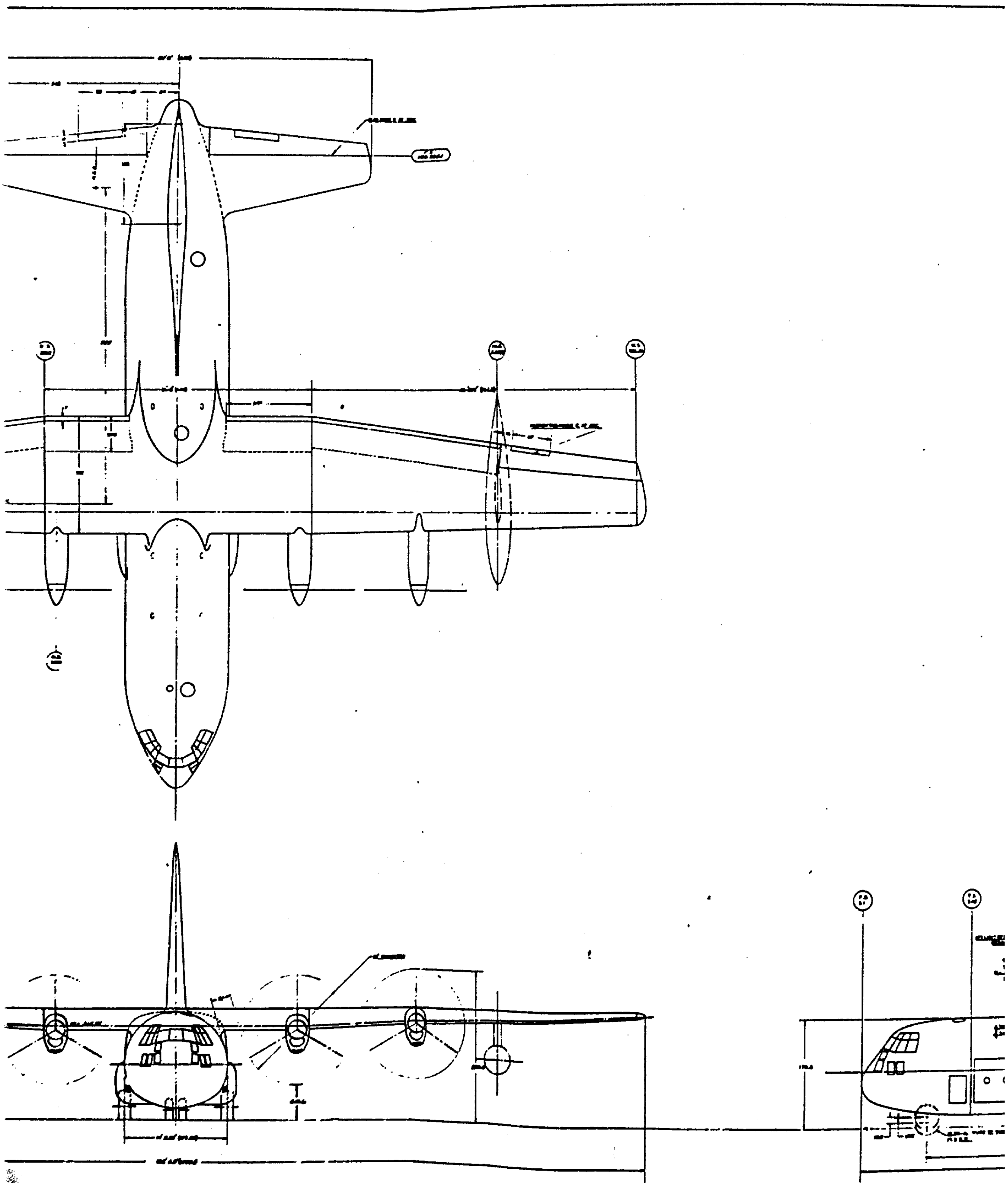

L R

AIRFOIL SECTION AND DATA
WING: NACA [illegible] ROOT
NACA [illegible] TIP
MAC [illegible]
HORIZONTAL STABILIZER
NACA [illegible]
VERTICAL STABILIZER
NACA [illegible]

TOTAL SURFACE AREAS AND ANGULAR MOVEMENTS

WING AREA	174[illegible] SQ. FT. ASPECT RATIO [illegible]
AILERON AREA (2)	110 SQ. FT. [illegible]
AILERON TAB AREA (2)	5.6 SQ. FT. [illegible]
FLAP AREA (4)	342 SQ. FT. 45°
HORIZONTAL TAIL	[illegible] SQ. FT.
ELEVATOR (2)	[illegible] SQ. FT. [illegible]
ELEVATOR TABS (2)	[illegible] SQ. FT.
VERTICAL TAIL	302 SQ. FT.
RUDDER	75 SQ. FT. [illegible]
RUDDER TAB	5.0 SQ. FT. [illegible]

NOTE:
+ INDICATES DOWN MOVEMENT
- INDICATES UP MOVEMENT

WEIGHT DATA

EQUIPPED WEIGHT EMPTY	[illegible] LBS.
DESIGN USEFUL LOAD	[illegible] LBS.
DESIGN GROSS WEIGHT	[illegible] LBS.

ENGINES
4 ALLISON [illegible] GAS TURBINES
([illegible]
ALLISON MODEL NO. 501-D2)

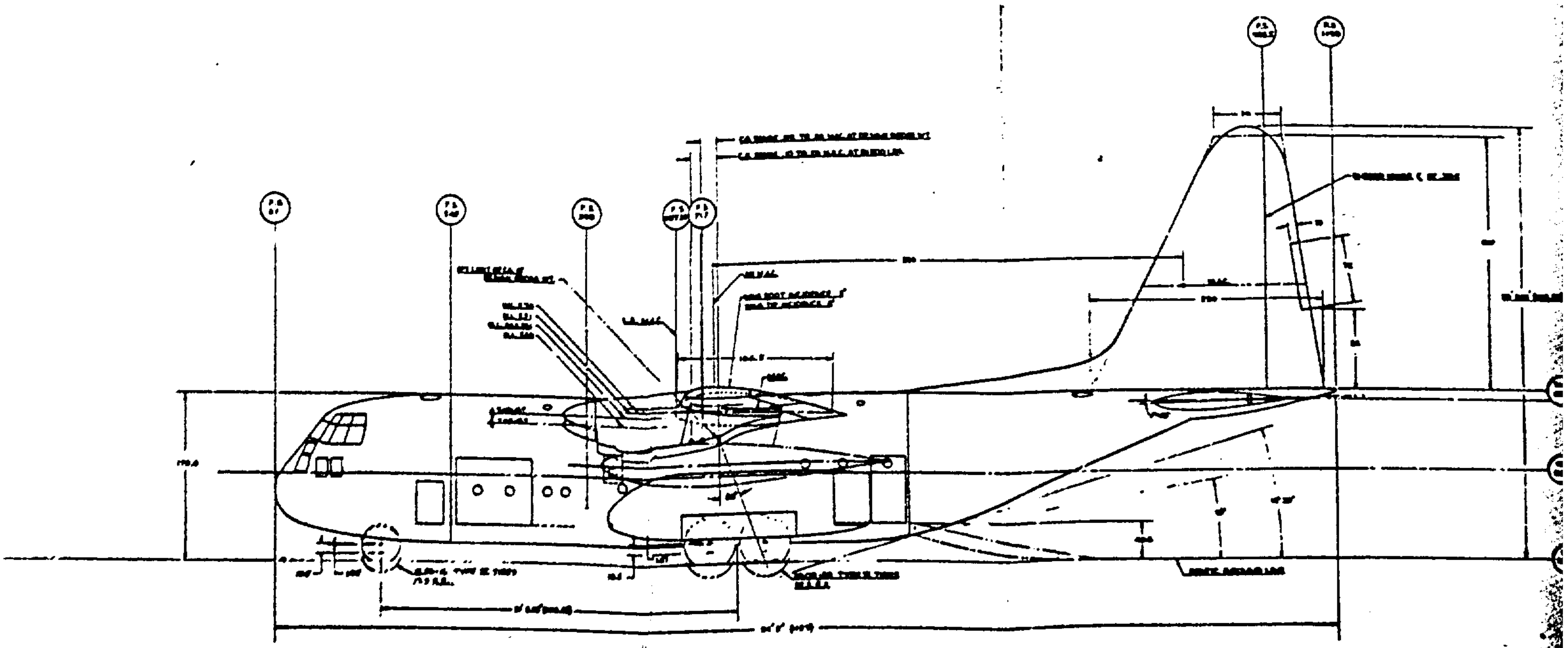

LR 9062

[redacted]

FIG. 1

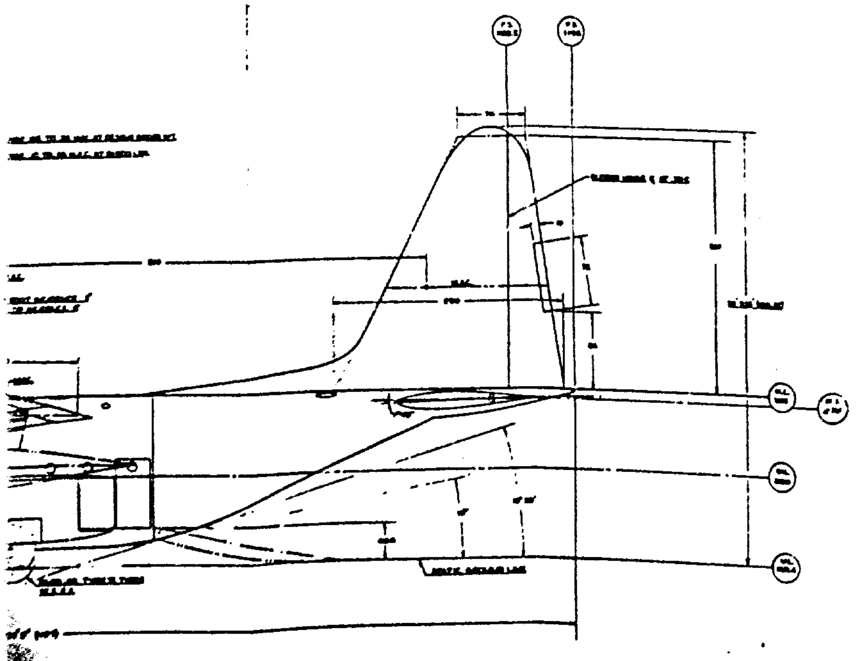

[redacted]

1/30

337000 4

337000